REHABILITATION OF CONTINUOUS COMPOSITE GIRDERS UTILIZING CFRP

BY

ALA'A HUSAM AHMAD GHAITH

A Thesis Presented to the

DEANSHIP OF GRADUATE STUDIES

KING FAHD UNIVERSITY OF PETROLEUM & MINERALS

DHAHRAN, SAUDI ARABIA

In Partial Fulfillment of the

Requirements for the Degree of

MASTER OF SCIENCE

In

CIVIL ENGINEERING

MAY, 2015

KING FAHD UNIVERSITY OF PETROLEUM & MINERALS

DHAHRAN- 31261, SAUDI ARABIA

DEANSHIP OF GRADUATE STUDIES

This thesis, written by **Ala'a Husam Ahmad Ghaith** under the direction of his thesis advisor and approved by his thesis committee, has been presented and accepted by the Dean of Graduate Studies, in partial fulfillment of the requirements for the degree of **MASTER OF SCIENCE IN CIVIL ENGINEERING.**

Dr. ALFARABI SHARIF
(Advisor)

Dr. Mohammed Ba-Shammakh
Summer Chairman Term 143

Dr. MUHAMMED BALUCH
(Member)

Dr. Salam A. Zummo
Dean of Graduate Studies

Dr. ALI AL GADHIB
(Member)

16/6/15
DATE

عمادة الدراسات العليا
DEANSHIP OF GRADUATE STUDIES

To my beloved family

ACKNOWLEDGMENTS

Praise for Allah for granting me with knowledge, patience, opportunity and health to complete my master degree and thesis.

I am thankful for my parents, siblings and all my family for their devoted love and support. I am grateful for their prayers, moral and emotional support throughout my study. Words fail to express my gratitude towards them.

I would like to express my gratitude to King Fahd University of Petroleum and Minerals for the support provided to complete this research through the outstanding facilities and providing me the chance to complete my master degree graduate study.

I highly appreciate the inspiration and wonderful encouragement and assistance provided by my thesis advisor Professor Sharif Alfarabi. His helpful recommendations made this journey exciting and a wonderful educational experience. I am indebted to the members of my committee, Prof. Mohammad Baluch and Dr. Ali Al Gadhib, to their continuous support and encouragement.

I would like to acknowledge my friends at King Fahd University of Petroleum and Minerals, Saudi Arabia, Jordan, and everywhere for their support and love.

TABLE OF CONTENTS

LIST OF TABLES

LIST OF FIGURES

ENGLISH ABSTRACT

FULL NAME :ALA'A HUSAM AHMAD GHAITH

THESIS TITLE :REHABILITATION OF CONTINUOUS COMPOSITE GIRDERS UTILIZING CFRP

Major field :CIVIL ENGINEERING

Date of degree :MAY 2015

Composite girders are used widely in structures. Due to cost effectiveness and high efficiency, steel-concrete girders are used in many applications where long span length is needed. However for continuous composite girders at the negative moment region, loss of composite action occurs which leads to a reduction in the stiffness and strength of the girder. At the negative moment region, the concrete slab develops flexural cracks due to being under tension and consequently becomes ineffective to maintain the composite action with the steel girder.

The aim of this project was to study strengthening distressed concrete slabs for continuous girders at the negative moment region by using carbon fiber reinforced polymer. A CFRP sheet was bonded along the top of the concrete slab at the distressed region to restore its function. An experimental testing was conducted to determine the feasibility of using CFRP laminates to strengthen distressed concrete slab for continuous composite girders. Four girders were tested to determine the ability of CFRP to restore the capacity of the distressed girders. Two out of the four girders were distressed to 40% and 60% of the ultimate load. CFRP sheets showed improvements in the behavior of the continuous composite girders. Increase of both strength and stiffness were achieved. The

yield capacity of the distressed girders increased up to 9%. Whereas stiffness have increased up to 50% compared to non-strengthened girder. Two failure modes developed in the study. The first was crushing of concrete at the positive moment zone. The other was CFRP debonding at the negative moment zone. Furthermore, the girder capacity was evaluated analytically using plastic analysis – virtual work method. Strain compatibility approach was used to determine the section capacity. Finally, a simplified design approach was developed for strengthening distressed concrete slab for continuous composite girders utilizing CFRP.

ARABIC ABSTRACT

ملخص الرسالة

الاسم الكامل: علاء حسام أحمد غيث

عنوان الرسالة: إعادة تأهيل الكمرات المركبة المستمرة باستخدام بوليمر مدعم بألياف الكربون

التخصص: الهندسة المدنية الإنشائية

تاريخ الدرجة العلمية: شعبان ١٤٣٦ هـ الموافق (مايو ٢٠١٥ م)

تستخدم الكمرات المركبة المستمرة من الفولاذ والخرسانة على نطاق واسع في المنشآت. نظرا للفائدة الاقتصادية و والكفاءة العالية، تستخدم الكمرات المركبة المستمرة في العديد من التطبيقات التي تحتاج إلى بحرطويل. ولكن تتعرض الكمرة المركبة المستمرة منطقة العزم السلبي الى فقدان خاصية العمل المركب بين الفولاذ والخرسانة، يؤدي ذلك إلى انخفاض في صلابة وقوة الكمرة المركبة المستمرة. في منطقة العزم السلبي، والبلاطة الخرسانية تتشقق نظرا لكونها تحت قوة الشد، وبالتالي تصبح غير فعالة للحفاظ على خاصية العمل المركب مع الجسرالفولاذي.

الهدف من هذا المشروع هو تدعيم البلاطة الخرسانية في منطقة العزم السلبي باستخدام بوليمر مدعم بألياف الكربون. تم تثبيت صفائح البوليمر المدعم بألياف الكربون على السطح العلوي للخرسانة في منطقة العزم السالب لاستعادة وظيفتها. أجري اختبار تجريبي لتحديد جدوى استخدام بوليمر مدعم بألياف الكربون لتعزيز البلاطة الخرسانية على الكمرة المركبة المستمرة. تم اختبار أربعة كمرات مركبة مستمرة لتحديد مقدرة البوليمر المدعم بألياف الكربون لاستعادة قوة تحمل الكمرات المركبة المستمرة المجهدة. اثنان من الكمرات أربعة اجهدت إلى 40٪ و 60٪ من الحمولة القصوى، أظهرت صفائح البوليمر المدعم بألياف الكربون تحسينات في أداء الكمرات المركبة المستمرة المجهدة. وتحققت زيادة كل من قوة وصلابة. تمت زيادة قوة الكمرات المركبة المستمرة المجهدة ما يصل إلى 9٪ مقارنة بالكمرة الغير مدعمة. في حين زادت الصلابة بنسبة 50٪ مقارنة مع الكمرة الغير مدعمة. نمطين

من الفشل قد لوحظت في هذه الدراسة. نمط الفشل الاول هو فشل الخرسانة في منطقة العزم الموجب. بينما نمط الفشل الاخر هو فشل في تماسك البوليمر مدعم بألياف الكربون مع الخرسانة بمنطقة العزم السالب.

كما حسبت قوة الكمرات المركبة المستمرة المدعمة ببوليمر مدعم بألياف الكربون تحليليا بواسطة طرق التحليل اللدن – التحليل بالشغل الافتراضي. تم حساب قوة المقاطع باستخدام طريقة توافق الاجهاد (المطاوعة). و ختاما، تم تطوير طريقة تصميم لاعادة تأهيل الكمرات المركبة المستمرة المتدهورة باستخدام البوليمر مدعم بألياف الكربون.

CHAPTER 1

INTRODUCTION

1.1 GENERAL

Composite structures (steel/concrete structures) are generally utilized for long spans in buildings and bridges. They are cost efficient and hence they utilize the material properties efficiently. Concrete has a high compressive capacity and a low tensile capacity. On the other hand, steel has a high tensile strength. One advantage of the composite steel-concrete girders is the ability to have long spans due to the increase of the stiffness and reduction of selfweight. The composite girder is composed of concrete slab cast on steel girder (hot rolled or fabricated plates) and the composite action is achieved by the use of welded shear studs to the contact surface of steel (steel girder top flange). Shear studs maintain the composite interaction by preventing the relative slip at the contact zone between the concrete slab and the steel girder.

For continuous composite girders, the moment at internal support region is negative and will create tensile stresses on the concrete slab. These stresses cause the followings:

1. Cracks in concrete slab.
2. Relative slip.

3. Deformations of shear connectors.

As a result, the composite action is lost and consequently strength and stiffness are reduced. According to the American Institute of Steel Construction manual (AISC), the allowable negative flexure strength for the negative moment segment of composite girders shall be determined by the steel section alone. An alternative by AISC, the negative flexure strength shall be determined using the plastic stress distribution of the composite section where the steel reinforcement is considered at the negative moment region (Salomon *et al.* 2009, AISC 2010).

Carbon Fiber Reinforced Polymer (CFRP) is a composite material made of polymer with carbon fibers as the matrix reinforcement. It is characterized in its high strength and light weight fiber materials. The behavior of CFRP depends on the matrix composition; unidirectional composites have very good resistance. Rehabilitation using CFRP is widely used for structures. It is used for seismic retrofitting, repairing of damaged structures and increasing the capacity of old structures. Retrofitting is popular in many cases as the cost of replacing a deficient structure can significantly exceed its CFRP strengthening. Using of CFRP has a large impact on the strength of structure but moderate increase in stiffness. The presence of FRP composites reduces the initiation and propagation rate of cracks. This reflects in increasing of the yield load, stiffness, and strength capacity of the beams. This improvement is valid as long as the bond between concrete or steel with FRP is adequate. When CFRP is bonded to the tension side of the concrete member, it provides an increase in the flexural strength of the structure. The increase in overall flexural strength ranges from 10 to 160%. When taking into account the strengthening limits of for the CFRP (Section 9.2-ACI 440.R-08), serviceability and

ductility limits, a strength increase of up to 40% are reasonable (ACI440.R-08). The rehabilitation of composite girders with the advanced composite materials such as CFRP is a smart resolution for immediate retrofitting and durable rehabilitation. Numerous laboratory conducted studies have shown that CFRP plates can be utilized with high effectiveness in strengthening steel girders.

The retrofitting costs in most cases are much less than the replacement costs. Additionally, CFRP retrofitting usually requires less construction time than replacing the structure, and consequently, reduces service disruption time. Utilization of bolted or welded steel plates to the structure is one of the current methods of retrofitting steel structures. However, this method may present constructability and durability disadvantages. Steel plates add more dead load to the structure and also they are vulnerable to corrosion leading to future maintenance costs. Therefore, utilizing cost effective durable materials to be used for retrofit techniques is evident. Using non metallic materials such as fiber reinforced polymers (FRP) is a possible solution. The superior physical and mechanical properties of FRP plates, show their high potential for repairing and strengthening of structures.

The aim of this project is to study the feasibility of using carbon fiber reinforced polymer to strengthen distressed concrete slabs for continuous composite girders at the negative moment segment. A CFRP sheet will be attached to the top of the concrete slab surface at the distressed segment to restore its function. An experimental testing will be conducted to determine its feasibility. Furthermore, the girder capacity will be evaluated analytically using plastic analysis. Finally, a simplified design approach will be developed for strengthening distressed concrete slab for continuous composite girders.

1.2 NEED FOR THE RESEARCH

Continuous girders are heavily used for bridges and buildings. The capacity of continuous girders is reduced due to deterioration of required steel or distressing due to excessive loading. All previous work for using CFRP on composite girders at the negative moment segment was conducted on non-distressed sections. However, due to the necessity to perform such strengthening methods for existing structures, this project will conduct experimental testing on distressed concrete slab for continuous composite girder at the negative moment segment. For continuous composite girders under negative moment, cracks will be developed due to the weak tensile strength of concrete. These cracks will cause reduction in the structure capacity. The composite action will be lost in the presence of cracks and slip. This will cause the reduction of section stiffness and consequently structure failure.

In this study, the use of Carbon Fiber Reinforced Polymer as a repair material can be a solution to retrieve the loss in capacity and to retrieve the composite action at the negative moment segment for distressed concrete slab in composite girders.

1.3 RESEARCH OBJECTIVES

Distressed composite steel concrete girders will be retrofitted with CFRP at the negative moment segment. The CFRP laminates will be attached to the top of concrete distressed slab at negative moment segment where the concrete will be cracked. The performance of continuous composite girder will be evaluated and compared to control girder and to girders with bonded CFRP before distressing. Consequently, proper method of designing

for retrofitting steel composite girders with CFRP laminates will be developed. The main objectives of this study are:

1. Experimental testing as follows:
    a. Material testing to evaluate their mechanical properties.
    b. Evaluating the behavior of distressed continuous composite girders repaired with bonded CFRP sheets at the negative moment segment (Interior support zone)
2. Analytical evaluation of the capacity of distressed continuous composite girders repaired with CFRP, using plastic analysis – virtual work method, and comparing it with experimental results.
3. Develop a simple design approach to repair distressed continuous composite girders with CFRP.

CHAPTER 2

LITERATURE REVIEW

2.1 UTILIZATION OF CFRP FOR STRENGTHENING CONCRETE BEAMS

(Spadea *et al.* 2001) carried out experimental work on simply supported rectangular reinforced concrete beams strengthening with CFRP. Eleven (plated and un-plated) beams divided into three groups. The groups were with different percentages of longitudinal reinforcement, internal stirrups, and variable location and configuration of external anchorage. The results showed that responses of the original beams (without CFRP) were affected by bonding of the CFRP plates without the external anchorages. However, the beams with end anchorages produced more ductile failures, carrying higher failure load with respect to beams without external anchorage. The bonded CFRP plates increased the capacity and strength of the beams, and decreased their deflection and energy absorption.

(Nguyen *et al.* 2001) performed an experimental work on ten simply supported rectangular reinforcement concrete beams and studied the performance utilizing bonded CFRP plates. Various configurations of CFRP plates (such as: the plate length, steel ratio, and concrete cover thickness) in the study to analyze their effects on the failure modes and ultimate strength capacity. A four point bending test was conducted on the beams to

be tested under. Four failure modes were observed: flexure failure, shear failure, ripping of concrete and combination between shear and ripping. A considerable increase in strength was observed with the CFRP-strengthened beams up to 236%. Beams failed in flexure showed more increase in strength after applying CFRP compared with other beams. The development length bond was found to be almost constant, though the beams were reinforcement with different lengths of CFRP plates.

(Namboorimadathil *et al*. 2002) conducted and experimental study on inverted simply supported RC T-beams. The aim of the study was to investigate the increase in capacity after using CFRP as strengthening material for both flexure (along the flanges) and shear (U-warp), see Figure 1. Three beams were tested one for control, one strengthened for flexure, and the last one for both flexure and shear. The result of the study that bonded CFRP laminates were found to be very efficient in increasing the member capacity, for both flexural and shear. The strength increase for Beams B1 and B2 were noted to be 41 and 39%, respectively.

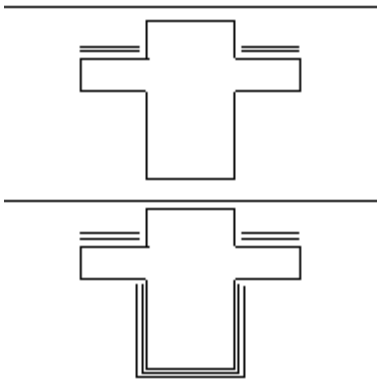

Figure 1: Strengthening scheme

(Dong *et al.* 2002) studied the flexural behavior of simply supported rectangular reinforced concrete beams with CFRP plates attached externally. The test was carried out

under 4-point loading. One reference beam and another 6 beams strengthened with CFRP were tested. The failure modes, such as the peeling of concrete cover and the debonding between the CFRP fabric and concrete occurred in the specimens. It was found that both of peeling and debonding failures are more difficult to illustrate than flexure. Different parameters affect the mode of failure such as epoxy thickness, concrete preparation, and sensitivity to motion along member. The result of this study, attaching CFRP plates to the surface where tensile stresses governs of either un-cracked or cracked beams increased the carrying capacity up to 95% for the strengthened beams.

(Higgins *et al.* 2006) studied the performance of CFRP for repairing damaged girders in diagonal cracking (shear). Laboratory experiments were conducted on full size T-beam and inverted T-beam with diagonal cracks, strengthened with CFRP to investigate the improvement. The CFRP was applied as a U-warp around the web to increase the shear capacity of the section as well as longitudinal sheets was used to increase flexural strength. The study showed that Strengthening with CFRP strips provided a significant increase in load capacity and stiffness compared to unrepaired beams. The study emphases that the CFRP strips shall be placed in the critical areas, which controlled by the shear capacity instead of across the entire length.

(Aidoo *et al.* 2006) conducted an experiment on 8 decommissioned bridge simply supported girders and retrofitted with 3 systems of CFRP: Conventional adhesive application, Near-surface mounted, and Powder actuated fasteners. Specimens were subjected to monotonic loading till it failed. For monotonically loaded beams, the observations indicated that CFRP debonding was the dominant failure mode. However,

retrofitting has increased the girders capacity to resist the increase in design loads despite the decrease in strength for steel reinforcement.

2.2 UTILIZATION OF CFRP FOR STRENGTHENING COMPOSITE GIRDERS

(Al-Saidy *et al.* 2007) has experimented the behavior of simply supported steel–concrete composite girders strengthened using CFRP plates. CFRP plates were attached at two locations in the girder: the web and the bottom flange. Two types of CFRP plates were utilized based on their tensile modulus of elasticity. Shear stress distribution along the bond line between CFRP plates and steel was recorded and reported. The results showed that using lightweight CFRP plates improved the strength capacity and stiffness of steel–concrete composite girders up to 45% of their original strength.

(Schnerch *et al.* 2007) suggested a design procedure for strengthening composite girders. The paper emphased on the use of High Modulus carbon fiber rinforecment polymers. The guide lines declared that the allowable gain of load for a composite girder strengthened with High Modulus carbon fiber reinforecment polymers should be chosen to satisfy the following criteria:

1. The flexural yield strength of the retrofitted girder should be more than the one of the unstrengthened girder.
2. The retrroffitted girder shall maintain is elastic behavior under the increasing load effect. This is accomplished by assuring that the total service load should not exceed 60% of the calculated new yield capacity of the retrofitted girder.

3. To satisfy the ultimate capacity requirements, the factored loads should not exceed the ultimate capacity of the retrroffitted girder after applying a suitable strength reduction factor.
4. To ensure that the safety of the structure in the case of a possible loss of the strengthening system such as debondong of the CFRP sheets, the total applied load should not exceed the capacity of the unstrengthened beam.

(El-Hacha and Ragab 2006) investigated experimentally the static behavior of simply supported steel-concrete composite girders strengthened with Different strengthening materials bonded to the bottom of steel section (tension flange). Different strengthening materials were used in this investigation such: unidirectional intermediate and high modulus Carbon Fiber Reinforced Polymer (CFRP) plates, unidirectional CFRP sheets and the newly developed unidirectional Steel Reinforced Polymer (SRP) sheets. The research objective was to analyze the flexural behavior of the girders and to study the effectiveness of the different strengthening materials. Table 1 shows a summary of the specimens:

Table 1 : Test matrix for the composite girder specimens

Beam #	Strengthening System
B1	Control beam without strengthening
B2	Beam strengthened using 2 layers of 82mm wide SRP sheets
B3	Beam strengthened using 1 layer of 80 mm wide CFRP plate
B4	Beam strengthened using 5 layers of 98 mm wide CFRP sheets
B5	Beam strengthened using 1 layer of 25 mm wide HM-CFRP plate

The results were as follow: “beams B2 and B3 the increase in strength was 29%, and 35%, respectively, except for beam B4 the increase in strength was 23% because the

applied area of CFRP sheets of 187mm2 CFRP plate resulted in the highest stiffness increase. Beam (B5) strengthened with HM-CFRP plate demonstrated strength increases up to 49%. All strengthened beams had minimal losses in ductility compared to the control beam".

(Schnerch *et al.* 2005) instigated experimentally strengthening of composite girders with CFRP. Two groups of flexural testing have been performed. First group of beams, three 6400 mm long beams have been strengthened with CFRP with an elastic modulus of either 640 GPa or 440 GPa. The second groups of five 3050 mm long beams were studied in detail. Strain distribution of the strengthened beams was compared to an unstrengthened beam. The results of the investigation showed an increase of strength and stiffness up to 45% and 36%.

(Miller *et al.* 2001) studied the use of CFRP plates for repairing losses of bridge girders. The study confirmed that CFRP restored the strength in distressed repaired bridge girders for reasonable limits. The CFRP were bonded to the bottom flange of the steel section. "10-37% increasing in stiffness achieved for the bridge girders damaged by corrosion. The development length was found to be on the order of 100 mm. The results indicated an 11.6% increase in flexural stiffness due to the retrofit". The values found by using the transformed sections also have shown similar results found by testing.

(Sen *et al.* 2001) investigated experimentally the feasibility of using (CFRP) as a repair material for steel composite bridge members. A total of six specimens, made of 6.1 m long W8x24 A36 steel beam with a composite cast reinforced concrete slab 0.114 m thick by 0.71 m wide on top of the beam, were firstly loaded till the tension flanges reached

above their yield to simulate the severe service distress. CFRP laminates were used then to repair the damaged specimens. 3.65 m CFRP plates were bonded to the tension flanges and different thickness of 2 or 5 mm plates were used. The beams were loaded till failure. A significant increase in the strength capacity of steel composite bridge members was observed after strengthening by CFRP laminates from 9% to 52%. Strengthening steel composite members with CFRP laminates is feasible as the study has showed.

2.3 MAINTAINING THE COMPOSITE ACTION AT THE NEGATIVE MOMENT SEGMENT FOR CONTINUOUS COMPOSITE GIRDERS

(Prodyot *et al.* 1987) performed an analytic study on the behavior of composite steel concrete beams pre-stressed at the negative moment region. The study evaluated prestress tendons effects on concrete cracks at the negative moment segment. Also, it was found that the load carrying capacity increased by 20%. This can cause a reduction in the section size if prestressing cost is less than the cost of utilized materials. A reduction in the primary prestressing moment at the support is an effect of the secondary prestressing moment.

(Basu *et al.* 1987) studied the behavior of two-span composite beams (concrete slab cast on top of steel beam and prestressed at the central support region). The two spans beam was of 18 ft. The results were compared with predicted values (Prodyot *et al.* 1987). The summary of the results, as follows: the experimental results were found to be in correspondence with the predicted linear and nonlinear response of the two-span partially

prestressed composite beam up to collapse. The nonlinearity turned into more prominent behavior near the central support with the beginning of the local buckling at the bottom flange.

(Samaaneh 2012) performed a study to maintain the composite action of continuous fully composite steel-concrete girders at the negative moment region. CFRP sheets were utilized by bonding them to the top of concrete slab along the negative moment segment. FEM was used to study the girder behavior, and to investigate the effect of partial reinforcement of CFRP on the capacity using ANSYS software. Different parameters were studied on the girders such as the fibers length and thickness and their effects on the ultimate girder capacity. At the negative moment segment, the ultimate load capacity has improved by 39% by using a 0.25 mm layer CFRP. Both of strength and stiffness increased because of the capabilities of carbon fibers to the composite action at the negative moment section.

(Sharif and Samaaneh 2014) evaluated the feasibility retaining the composite action for a continuous composite girder utilizing (CFRP) plates to the top of concrete slab at the negative moment section. FEM was used to calculate the behavior of the continuous composite girder with carbon fibers while loading it. Also, the ultimate capacity of the girder is evaluated analytically using virtual work method which is plastic analysis. The paper confirmed that the stiffness and strength have improved due to CFRP. The increase in girder strength depends on the CFRP thickness.

All previous work for using CFRP on composite girders at the negative moment segment was conducted on non-distressed sections. However, due to the necessity to perform such

strengthening methods for existing structures, this project will conduct experimental testing on distressed concrete slab for continuous composite girder at the negative moment segment. Utilizing CFRP as retrofit material was shown to be cost efficient for existing structures. In this project distressed concrete slab for composite girders due to negative moment segment will be retrofitted with CFRP. The CFRP laminates will be bonded to the top of the concrete distressed slab at negative moment segment where the slab is cracked. The Performance of continuous composite girder will be evaluated and compared to control girder and to members with bonded CFRP before deterioration of the memebr. Analytical solution will be performed to evaluate the girder capacity. Consequently, proper method tp design for retroffiting steel composite girder with CFRP will be developed.

CHAPTER 3

EXPERIMENTAL PROGRAM

3.1 INTRODUCTION

This chapter discusses the experimental testing program. Initially, evaluation of material properties was conducted in accordance to ASTM standards. Later, full scale testing of continuous composite girders was conducted to evaluate their behavior and the retrofitting capabilities of CFRP at the negative moment zone.

3.2 MATERIAL TESTING

In this section, ASTM standards were used to evaluate concrete, steel reinforcement and structural steel properties. CFRP bond strength was also evaluated using the single shear test (Bilotta 2010). Finally push-out test was performed to evaluate the composite action between concrete slab and steel girder (Topkaya *et al.* 2004).

3.2.1 CONCRETE TESTING

Concrete samples were tested after 28 days of curing to determine the compressive, tensile and flexural strengths. The following standards: (ASTM-C39M 2003), (ASTM-C496M 2004), and (ASTM-C293 2002) were used to evaluate the compressive strength,

tensile strength, and flexural strength, respectively. All tests were conducted in Civil engineering laboratories at KFUPM.

3.2.1.1 Concrete Compressive Strength

Three cylindrical concrete samples were cast to evaluate compressive strength. The dimensions of the cylinders are 75x150 mm, as shown in Figure 2.

Figure 2: Cylindrical samples of concrete

For the compressive test, the specimens were capped with sulfur. Strain gauges were installed to evaluate the behavior of the concrete, see Figure 3.

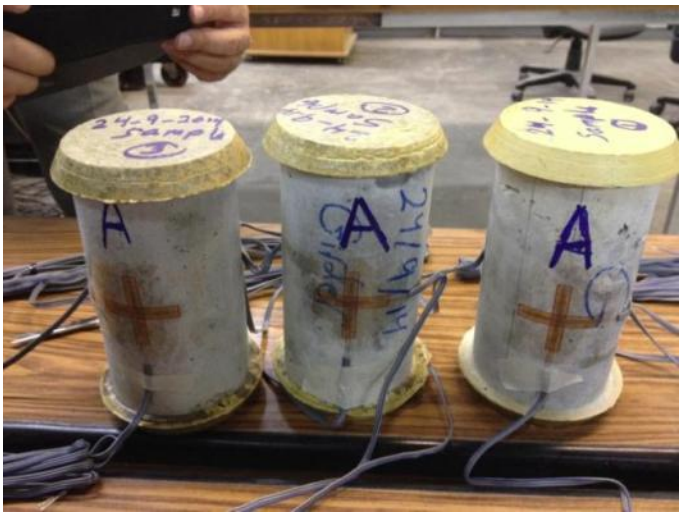

Figure 3: Prepared samples for compressive test

A screw type compressive machine with a speed rate of 0.2 mm/min was used. This speed rate is the idle rate according to the standard (ASTM-C39M 2003). Figure 4 shows specimen after failure. Failure types were cone and split, and shear fracture failure.

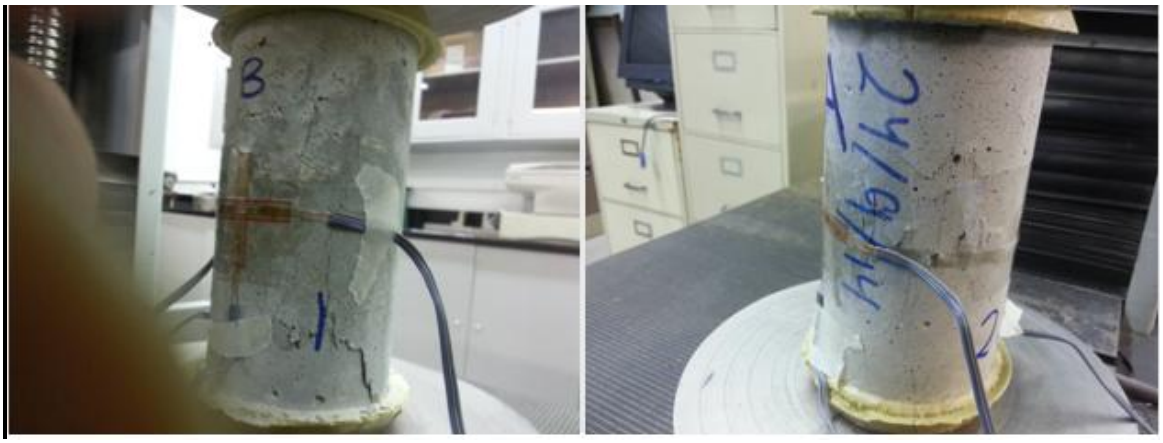

Figure 4: Fractured specimens compressive test

Deformations were recorded using strain gauges for the three specimens, Figure 5. The average concrete compressive strength was found to be 27.7 MPa, and the average Poisson's ratio 0.199. The modulus of elasticity was found to be 26216.22 MPa

according to (ASTM-C469 2002). The results of the three specimens are shown Table 2. Figure 6 show the Stress-Strain diagram of the three concrete specimens.

Table 2: Concrete compressive test results

Specimen #	Compressive Strength (MPa)	Poisson's Ratio
CSC-1	30.9	0.191
CSC-2	27.2	0.190
CSC-3	24.4	0.217
Average	27.7	0.199

Figure 5: Data logger for compressive test

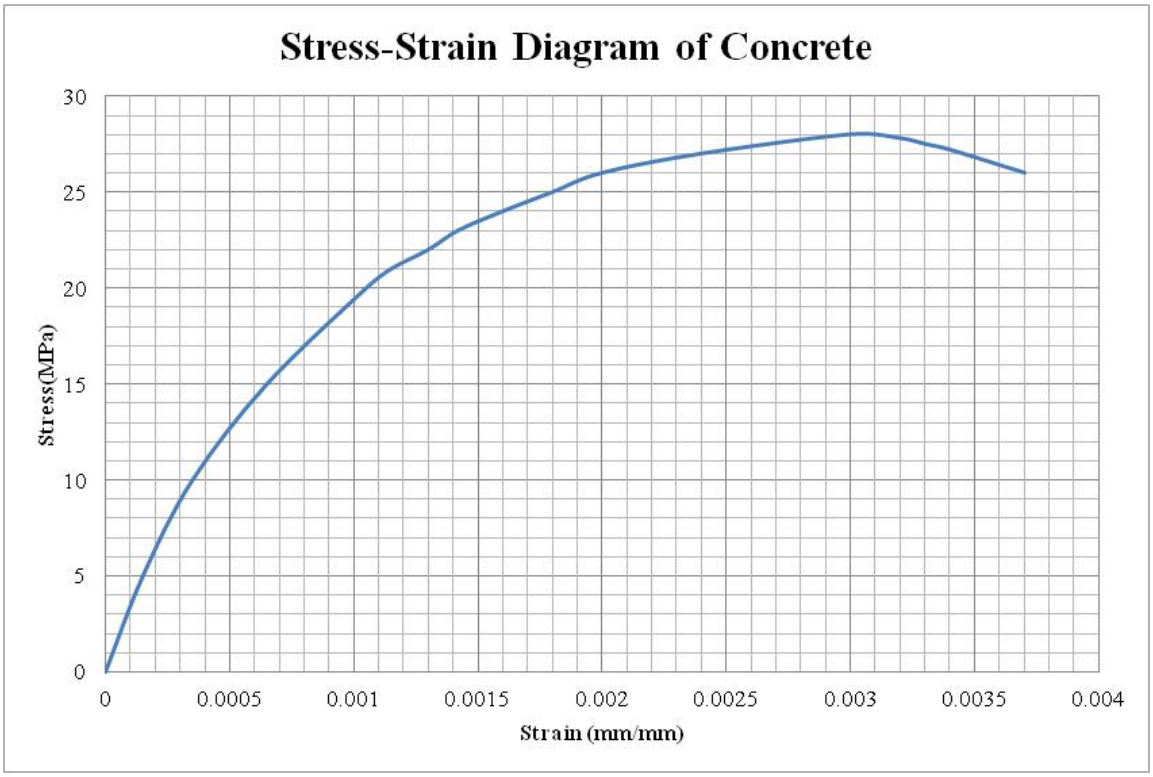

Figure 6: Stress-Strain diagram of concrete

3.2.1.2 Concrete Tensile Strength

The tensile strength was evaluated indirectly using split test (ASTM-C496M 2004). Three specimens were tested. Figure 7 shows the test and the positioning for one of the samples.

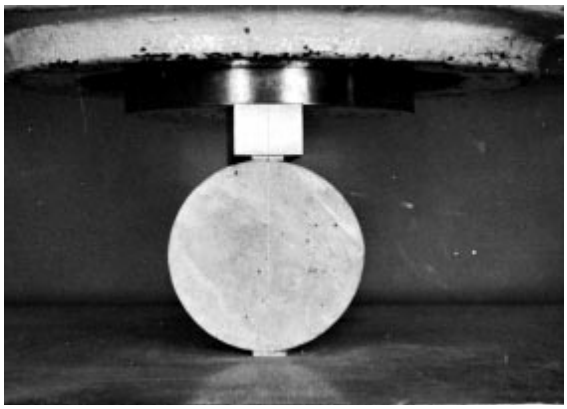

Figure 7: Testing machine for splitting tensile strength (ASTM-C496M 2004)

Table 3 contains the split test results for the three specimens. Concrete tensile strengths were calculated using the maximum load applied according to Equation 1 (ASTM-C496M 2004):

$$T = \frac{2\,P}{\pi\,l\,d} \qquad \text{Equation 1}$$

Where:

- T: is the split tensile strength (MPa)
- P: Maximum applied load (N)
- l: specimen length (mm)
- d: Specimen diameter (mm)

Table 3: Concrete split test results

Specimen #	Maximum load (KN)	Splitting tensile strength (MPa)
STC-1	50.7	2.78
STC-2	53.9	2.95
STC-2	56.7	3.10
Average	53.8	2.95

3.2.1.3 Concrete Flexural Strength

For concrete flexure strength three concrete prisms were tested under center point loading. The dimensions of each prism were 50x50x200 (mm). Figure 8 shows the prisms casting in the standard mold. Prisms were tested after 28 day of submerged curing.

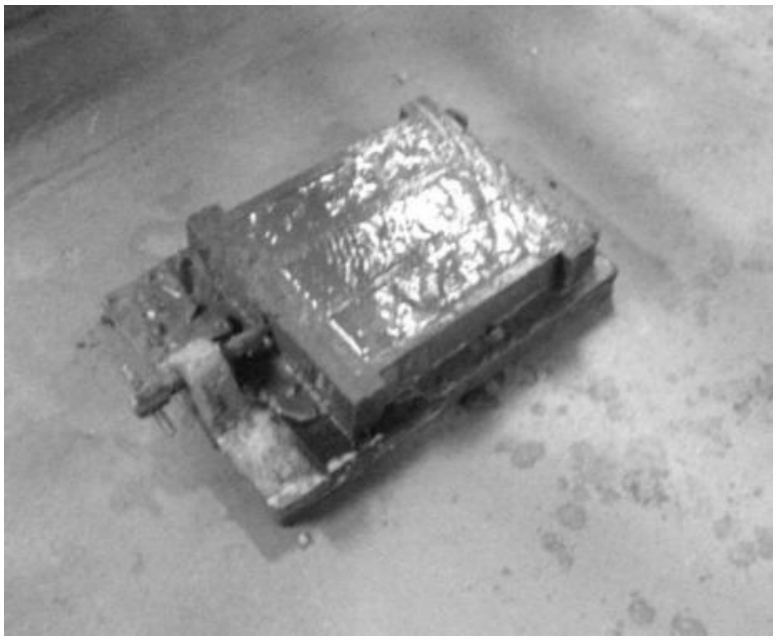

Figure 8: Casting of concrete prisms

Figure 9, a schematic diagram for the flexural testing. For the 50x50x200 mm prism, the span length was taken to be is 150 mm.

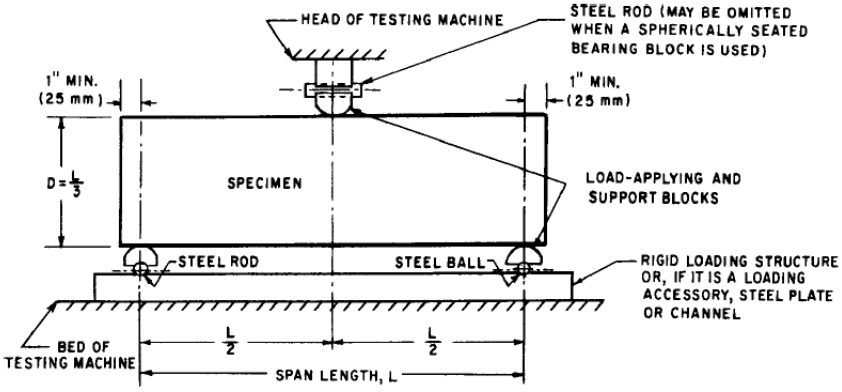

Figure 9: Diagrammatic view of the flexural test (ASTM-C293 2002)

Figure 10 shows the test for one specimen and the three prisms after the test.

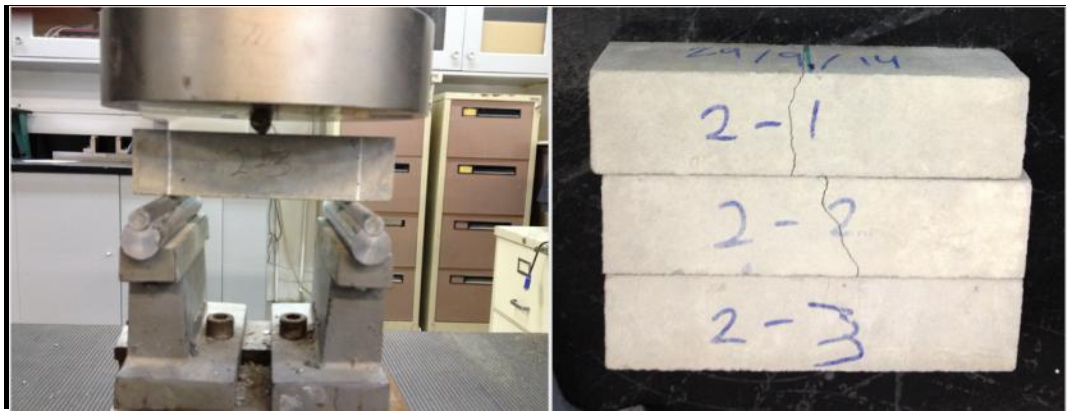

Figure 10: Concrete prisms testing

The modulus of rupture for the flexural test I calculated according to Equation 2:

$$F_R = \frac{3\,P\,L}{2\,b\,d^2} \qquad \text{Equation 2}$$

Where:

- F_R: is modulus of rapture (MPa),

- *P*: Maximum applied load (KN),
- *L*: Span length (mm),
- *b*: average width of prism (mm),
- *d*: average depth of prism (mm).

The results of the three specimens are in Table 4.

Table 4: Flexural test results

Specimen #	Maximum Load (KN)	Modulus of Rapture (MPa)
CFT-1	1.880	6.61
CFT-2	2.499	8.79
CFT-3	2.119	7.45
Average	2.166	7.61

The average results for concrete properties are summarized in Table 5.

Table 5: Summary of Material testing

Evaluated properties	Standard ASTM test	Strength (MPa)
Compressive strength	C39M	27.7
Tensile strength	C496M	2.95
Modulus of rupture	C293	7.61

3.2.2 STEEL REINFORCEMENT TENSILE STRENGTH TEST

Steel reinforcement was tested for its tensile strength. Grade 60 steel (420 MPa yield strength) 8 mm diameter steel bars were used for the girder top concrete slab. The tensile test was conducted according to (ASTM-E8M 2004). The three bars prepared for tensile test are shown in Figure 11.

Figure 11: Steel reinforcement bars for testing

Strain gauges were installed to evaluate the behavior of the bars. Figure 12 shows testing of sample 1 while reading the strains using the data logger.

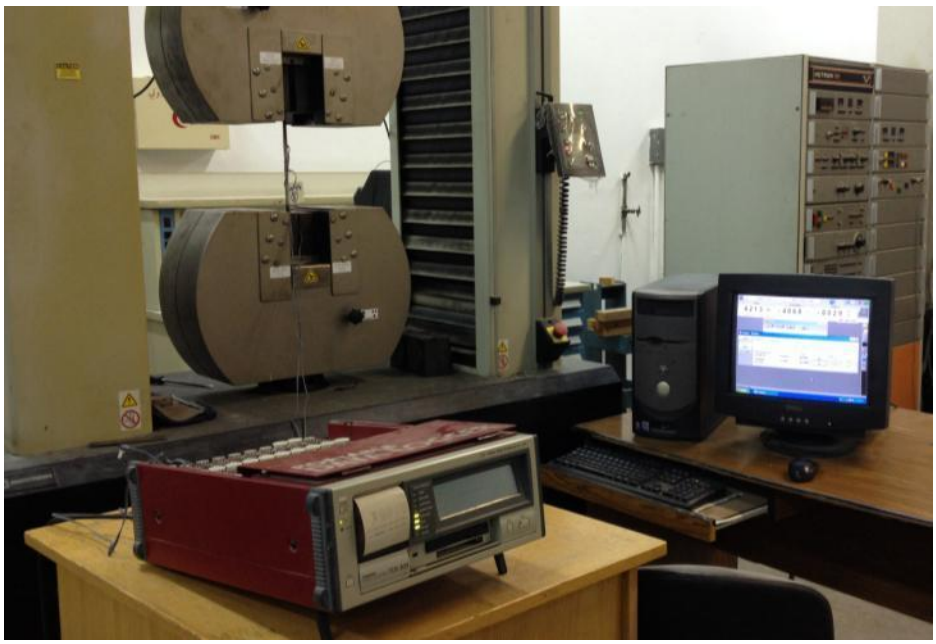

Figure 12: Testing of one of the bars

The stress versus strain diagram of the three samples is shown in Figure 13. The results of the tensile strength test for the steel bars are shown in Table 6.

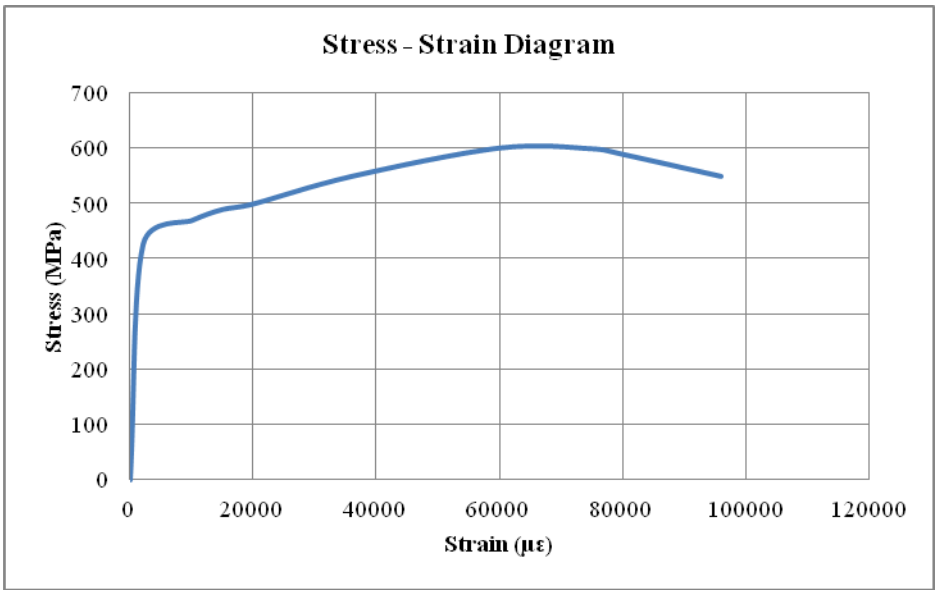

Figure 13: Stress-Strain diagram for steel reinforcement

Table 6: Steel reinforcement tensile test results

Specimen #	Yield Stress (MPa)	Ultimate Stress (MPa)
1	416.7	601
2	437	585
3	396	618
Average	416.57	601.33

3.2.3 STRUCTURAL STEEL TENSILE STRENGTH TEST

Three steel specimens were tested. Grade 36 steel (248 MPa yield strength) with a thickness of 8 mm was used to fabricate the steel girders. The tensile test was conducted according to ASTM-E8M. Figure 14 illustrate the dimensions for the steel plates to be tested, see Table 7 for abbreviations.

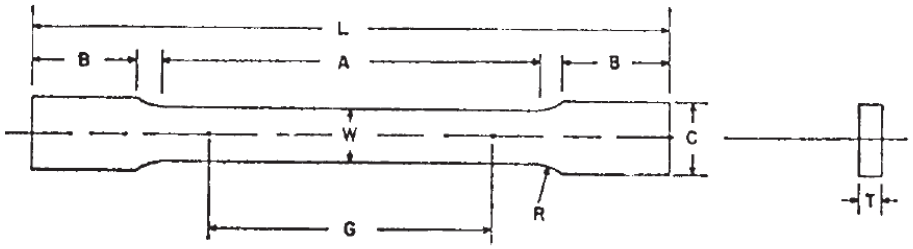

Figure 14: Standard test specimen dimensions (ASTM-E8M 2004)

Table 7: Dimensions for plate specimens

	Dimensions, mm
Nominal Width	Plate-Type 40 mm
G— Gage length	200.0 ± 0.2
W— Width	40.0 ± 2.0
T— Thickness	
R— Radius of fillet, min	25
L— Overall length,	450
A— Length of reduced section, min	225
B— Length of grip section,	75
C— Width of grip section, approximate	50

Strain gauges were installed to evaluate the plate's behavior. Figure 15 shows testing of sample 1 while reading the strains using the data logger. Figure 16 shows specimen 3 at failure. The results of the tensile tests are shown in Table 8. Figure 17 shows the average stress strain diagram for the steel plates.

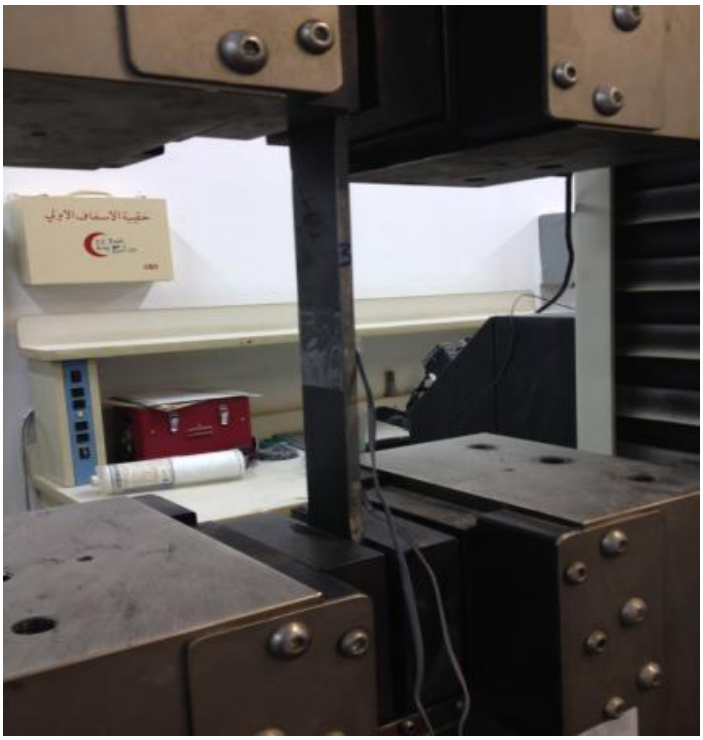

Figure 15: Tensile test of plate 1

Figure 16: Plate 1 after failure

Table 8: Results of steel plate tensile tests

Sample #	Yield Strength (MPa)	Ultimate Strength (MPa)
1	284.4	434
2	222.5	347.5
3	259	430
Average	255.3	403.8

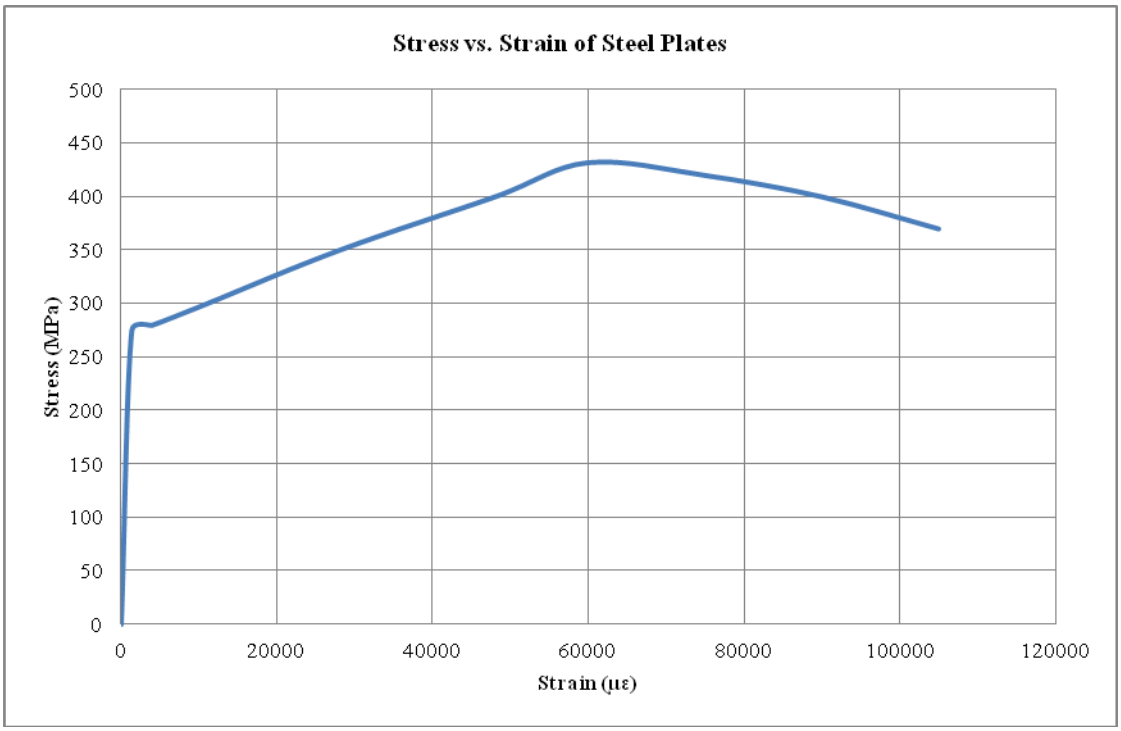

Figure 17: Stress strain diagram for the steel plates

3.2.4 CFRP PROPERTIES

Carbon Fiber Reinforced Polymers (CFRP) used in this project is Nitowrap FRC 230 from Fosroc Company. It is a unidirectional carbon fiber sheets used for strengthening load carrying capacity structures specifically to improve flexural and shear strength. Table 9 gives the physical properties of FRC 230 (FOSROC 2014).

Table 9: CFRP properties

Grade	FRC 230
Fiber Area Weight (g/m^2)	230
Design thickness (mm)	0.131
Tensile strength “design value” (MPa)	3480
Tensile E-modulus “design value” (MPa)	230500
Ultimate design strain (mm/mm)	0.015

Two types of adhesive were used in this project: Nitowrap Primer and Nitowrap Encapsulation Resin, Figure 18. Nitowrap Primer is used to penetrate the surface of the concrete, to improve the adhesive bond for the saturating resin or adhesive. Nitowrap Encapsulation Resin is used to impregnate the reinforcing fibers and to provide a shear load path to effectively transfer load between fibers. The saturating resin also serves as the adhesive between CFRP layers, providing a shear load path between the previously primed concrete substrate and the FRP systems. Both of the adhesives are two component epoxy and hardener. The ratio to be applied is 2:1 of epoxy to hardener. The physical properties of the adhesive material are given in Table 10. The weight per coverage area amount of the adhesives is given in Table 11

Table 10: Adhesive physical properties

Physical Property	Nitowrap Primer	Nitowrap Encapsulation Resin
Shear strength (MPa)	-	>30
Compressive strength (MPa)	-	>60
Flexural E-modulus (MPa)	-	>3500
Flexural strength (MPa)	-	>40
Adhesive strength (MPa)	>27.0	>2.0 (concrete failure)

Table 11:Weight of dhesive per area

Adhesive	Coverage
Nitowrap Primer	0.25 - 0.3 kg/m2
Nitowrap Encapsulation Resin	0.60 – 1.0 kg/m2

Figure 18: Adhesive used in the project

3.2.5 CFRP ADHESION STRENGTH TEST

The adhesive bond strength between concrete slab and CFRP sheets was evaluated using single shear test SST (Bilotta 2010) as shown in Figure 19. In the single shear test, CFRP sheet is adhered to a concrete prism. Then pulling load is applied to the CFRP sheet till the load reaches the debonding load as shown in Figure 20.

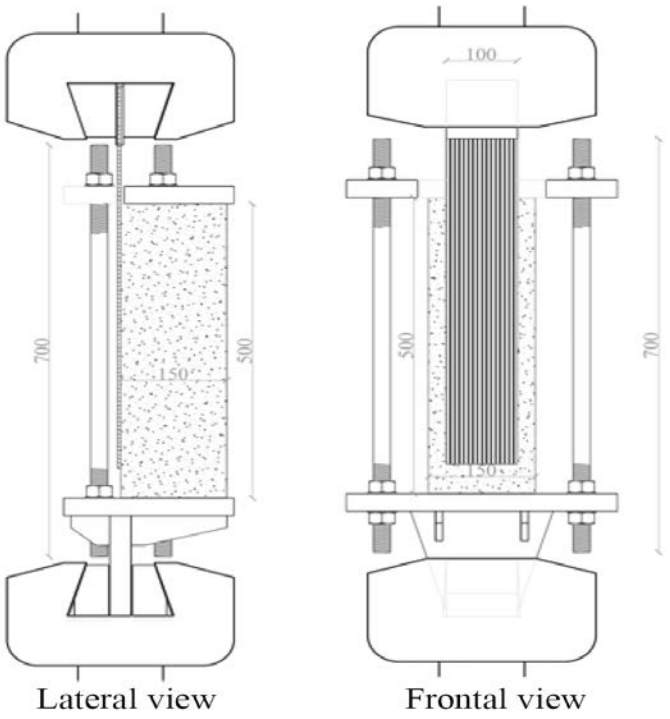

Figure 19: Single shear test schematic diagram (Bilotta 2010)

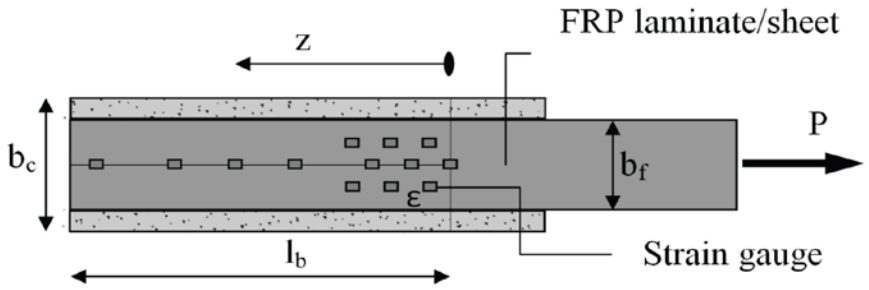

Figure 20: SST test direction of pulling load (Bilotta 2010)

Figure 21 shows the concrete prism dimensions, its width b_c = *150 mm*, height h_c = *200 mm* and length l_c = *500 mm*. the CFRP sheet has the following dimensions: the bond length l_b = *100 mm*, the un-bonded length of FRP L_{FREE} = *100 mm*, and width of FRP *bf* = *100 mm*.

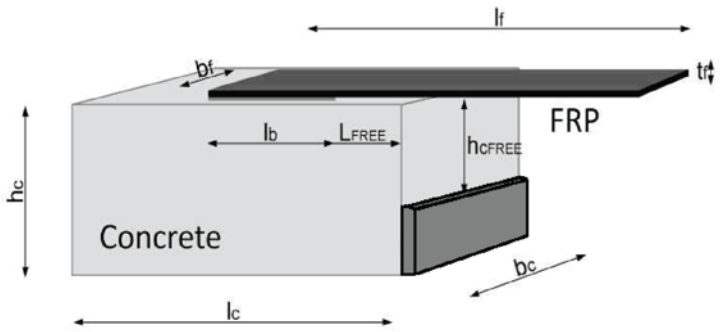

Figure 21: SST prism dimensions (Bilotta 2010)

Test was conducted on three samples. All samples were prepared according to the standard. CFRP sheets were adhered to the concrete prisms using the primer and let to be cured for 2 days. Figure 22 illustrates the specimen setup in the loading machine. Loading continued on the CFRP till it debonded from the concrete prism (concrete failure), see Figure 22. From the test the CFRP stress-slip is plotted, see Figure 23. It determines the behavior of the primer epoxy. The average adhesive strength of the primer was found to be 2.0 MPa with relative slip of 0.5 mm. these results satisfies with the manufacturer specifications of 2.0 MPa.

Figure 22: SST test

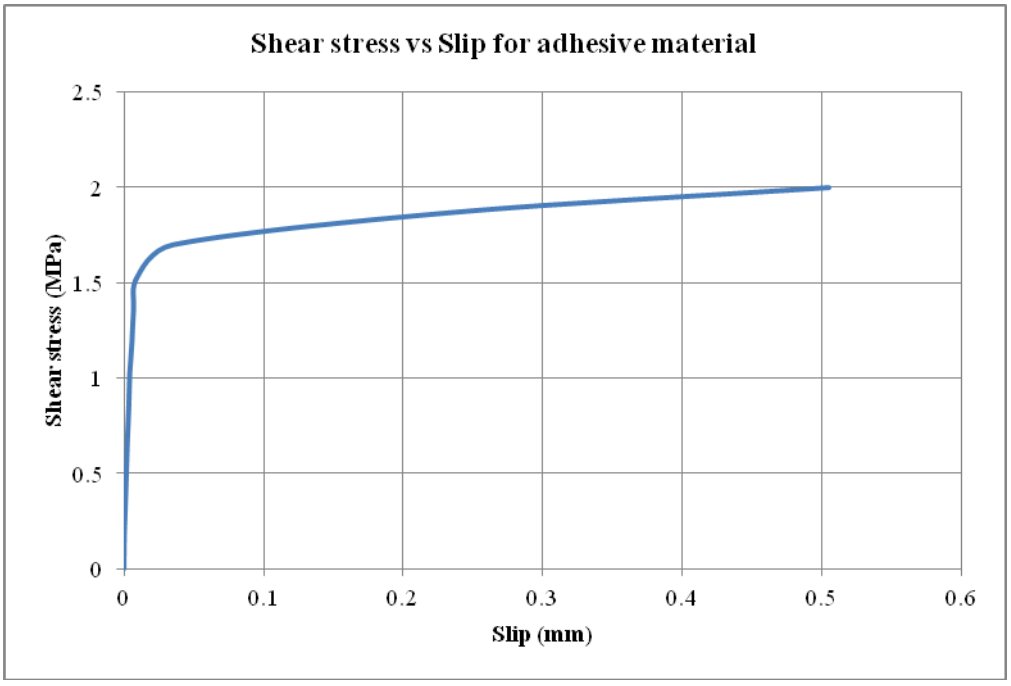

Figure 23: Shear stress vs. slip primer adhesive

3.2.6 PUSH-OUT TEST

Push out test was conducted to determine the capacity of steel studs. Maintaining the composite action between concrete slab and steel section depends in the behavior of steel studs. This test was conducted on three samples. It aimed to determine the capacity of each steel stud and its slip behavior. A schematic diagram of the sample is shown in Figure 24. The test was conducted in the heavy equipment and testing laboratory in KFUPM. Test set up is shown in Figure 25. The load is applied using a hydraulic jack and measured using a load cell. The slip between the concrete slab and steel section was measured using a LVDT.

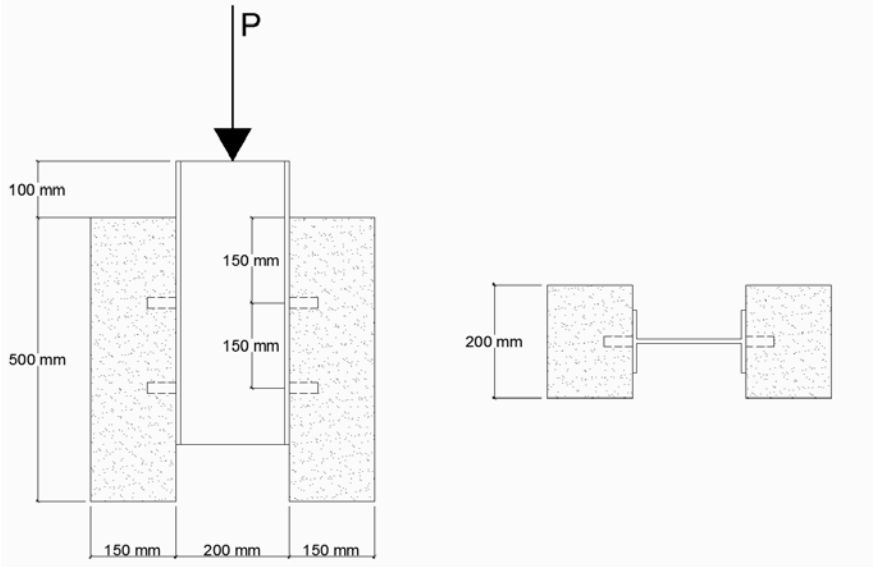

Figure 24: Push out test set up

Figure 25: Push out testing

The load versus slip behavior is plotted in Figure 27. The ultimate capacity of the each stud Q_u was found to be 71 KN per stud. The design capacity then shall be taken to be 90% of the ultimate (Johnson and Anderson 2004).

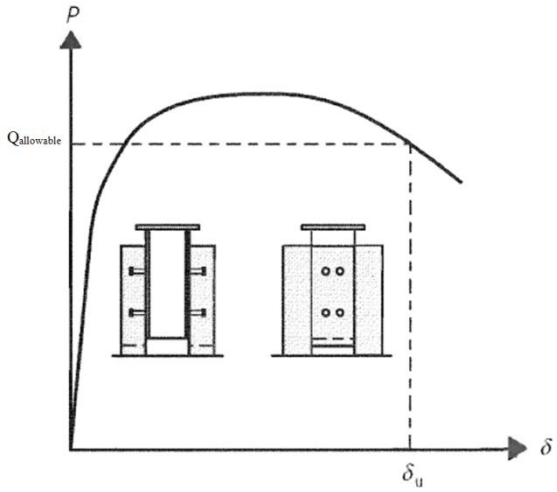

Figure 26: Determination of slip capacity (Johnson and Anderson 2004)

The value of $Q_{allowable}$ equals 64 KN. The ultimate slip is found by intersecting the Load $Q_{allowable}$ in the load vs. slip graph as shown in Figure 26 (Johnson and Anderson 2004). The ultimate slip was found to be 1.5 mm and thus the allowable slip is 90% of the ultimate slip. The allowable slip shall be taken to be 1.3 mm.

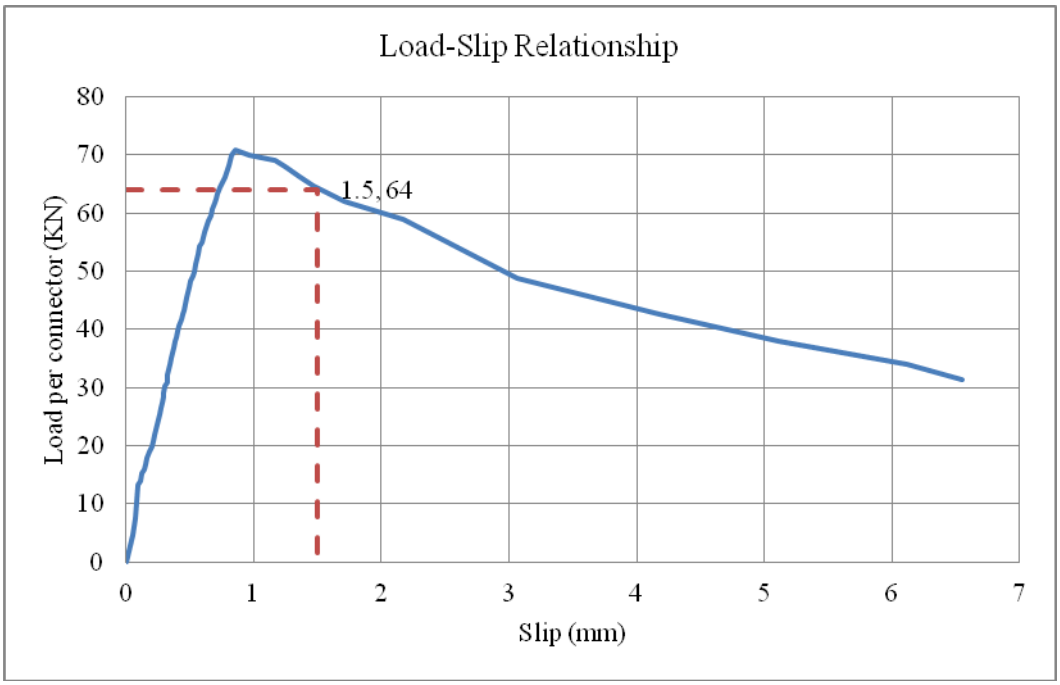

Figure 27: Push out test load vs. slip

3.3 COMPOSITE GIRDER TESTING

3.3.1 GENERAL

This section discusses the experimental program of testing the continuous composite girders. It covers the girder design, preparations for testing and finally the experimental testing variable. The experimental program was conducted in the Civil Engineering

Department Heavy Equipment and Testing Laboratories of King Fahd University of Petroleum and Minerals, see Figure 28.

Figure 28: Universal testing machine frame

3.3.2 CONTINUOUS COMPOSITE GIRDER DESIGN

Composite girder was designed based on the following criteria in order to satisfy the project objectives

1. Flexural failure is the required failure at ultimate load.
2. Shear failure prevented using proper thickness of web.
3. Plates local buckling prevented using proper length/thickness ratio.
4. Lateral torsional buckling prevented using proper cross section and lateral support over the interior support.

5. Shear connectors (studs) are designed to have full composite action between concrete slab and steel girder.
6. The expected ultimate capacity of the continuous composite beams with CFRP over the negative moment region should not exceed the ultimate capacity of Lab facilities (Loading cells, Loading Jack, Frame).

The detailed design procedure is shown in the Appendix. Figure 29 illustrates the final dimensions for the continuous composite girder to be prepared for testing.

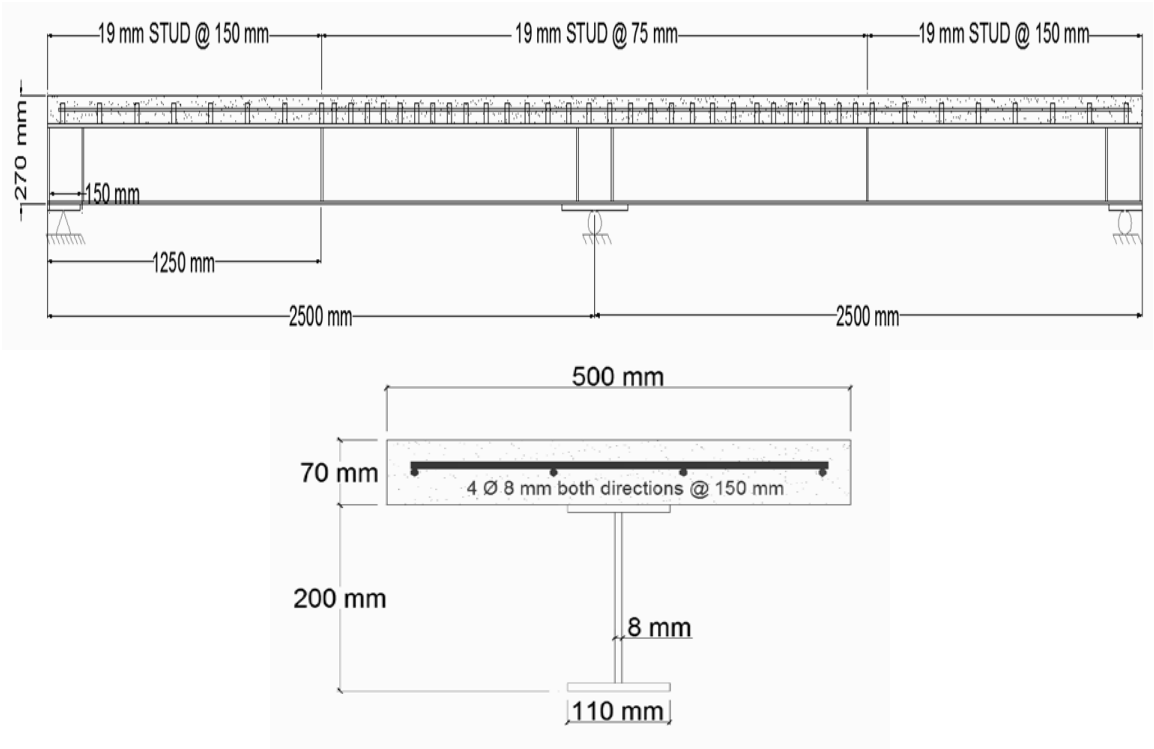

Figure 29: Girder drawing

3.3.3 SPECIMEN PREPARATION

Five continuous composite girders were tested in this project. The five girders were fabricated and cast at a local precast concrete factory (ABNIYAH) in the 2nd industrial

city of Dammam. Supervision was continuous during the girders preparation to insure the quality of the steel fabrication and concrete casting. Figure 30 shows the fabricated girders after preparations.

Figure 30: Fabricated steel girders

The factory was equipped with automated casting machines and vibrating tables which were used to cast the concrete slab. Seventy millimeters thick concrete slab was cast on top of the steel girder. Steel reinforcement in the concrete slab were placed according the design. Embedded strain gauges in the concrete slab were attached to the flange and steel reinforcement before concrete casting, Figure 31 (b). Steel surfaces were sand blasted to remove rust, and then cleaned with acetone to remove all oil residues, see Figure 31 (a).

Figure 31: (a) Steel surface preparation, (b) Strain gauges in steel surfaces

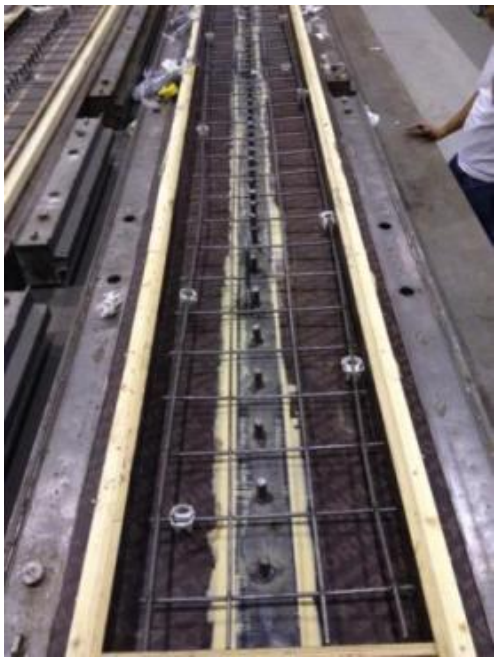

Figure 32: Steel reinforcement for the concrete slab

Concrete slab was cast in the forms and left for 24 hours before removing the forms. The automated pouring of concrete and final surface preparation of concrete slab is shown in Figures 33 and 34, respectively.

Figure 33: Automated concrete pouring

Figure 34: Concrete slab after pouring

Concrete slab surface preparation continued over night by the labors at the factory to provide smooth concrete surface. Curing was processed at controlled temperature and humidity for 28 days. Figure 35 shows the composite girder after demolding and curing. Composite girders were finally transported to KFUPM laboratory, see Figure 36.

Figure 35: Composite girders after demolding

Figure 36: Composite girder transportation

Before bonding CFRP sheets to the surface of concrete slab, concrete surface was prepared according to (ACI440.R-08). In this project CFRP strengthening is considered to be bond-critical application. According to 6.4.2 in (ACI440.R-08), bond critical application is when CFRP sheets are used for flexural or shear strengthening in beams, slabs, columns, and walls. For CFRP wrapping, concrete surfaces were grinded to have smooth surfaces and the edges were rounded to a radius of 15 mm to prevent stress concentrations in the CFRP.

For interior support zone, the bond between concrete and CFRP sheets should be adequate to achieve a full shear stress transfer. Diamond tip grinder was used to smooth the concrete surface, providing better adhesion surface. The weak surficial concrete layer was blasted by the grinder. Diamond tip grinder provided smooth surfaces with localized out of plane variation less than one millimeter.

3.3.4 INSTRUMENTATION

Strain gauges and LVDTs (Linear Variable Differential Transducers) were used to monitor the composite girder behavior.

Strain gauges were used to monitor material deformations in micro-strains (με). There are four different locations where strain gauges were attached. These locations are:

(1) At mid-span with 100 mm offset from the point load along the depth of the girder,

(2) At the interior support with an offset of 200 mm along the depth of the girder,

(3) Over the CFRP sheets at the negative moment zone along the girder's center line,

(4) Over the CFRP wrapping at positive moment region with an offset of 100 mm from the point load laterally.

Figure 37 illustrate the locations of the strain gauges in the girder. Two types of strain gauges were used in this project. For concrete and CFRP, thirty millimeters long electric resistance strain gauges were utilized to evaluate deformation in the members. For steel members (flanges, web and reinforcement), six millimeters long electric resistance strain gauges were used.

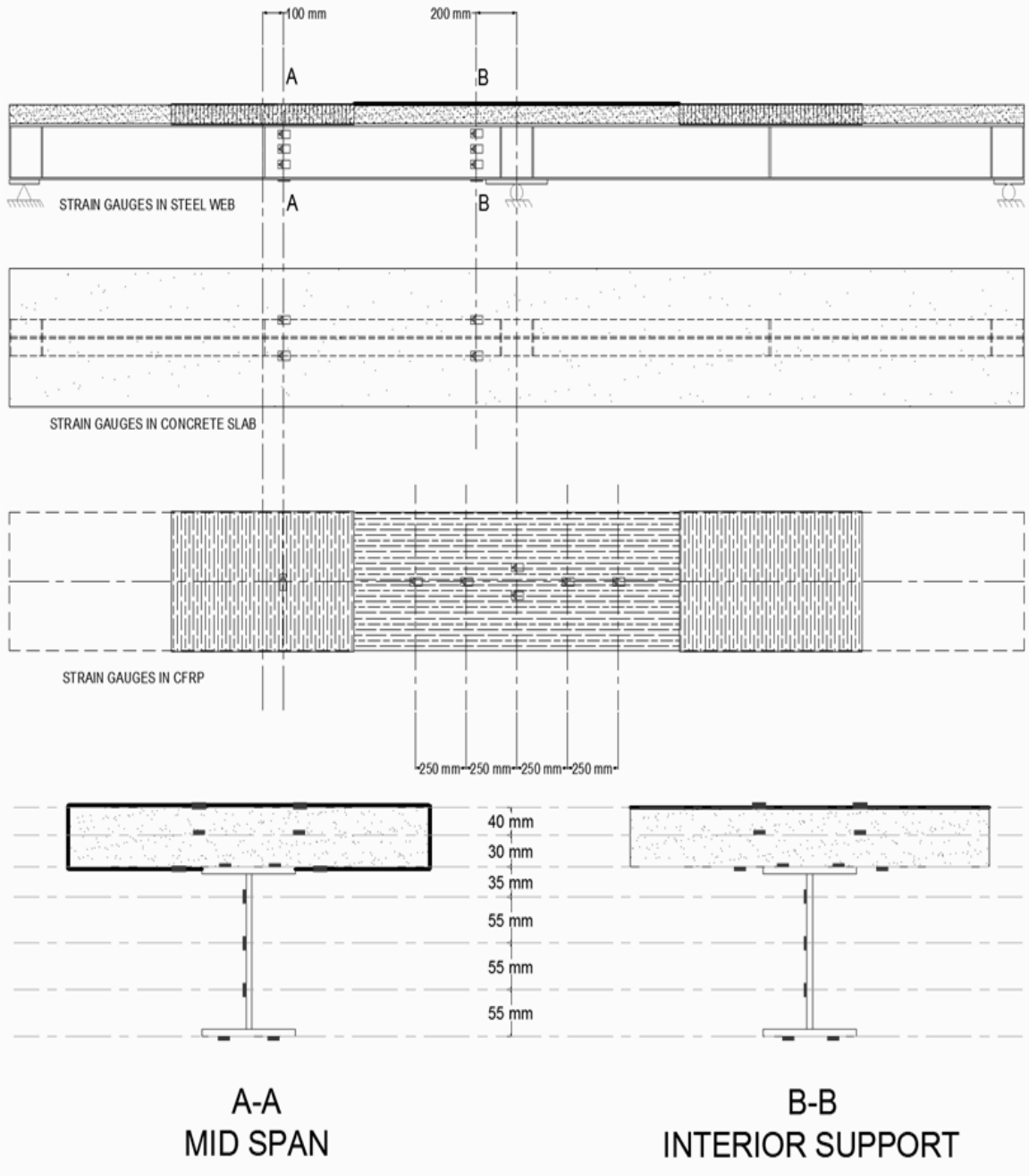

Figure 37: Locations of strain gauges

Deflections were measured at mid spans under the applied load. Two LVDTs were placed to measure vertical deflection at these locations. To measure the crack width, one LVDT was placed horizontally at the concrete top slab with a 50 mm offset from the girder's center. Slip between concrete slab and steel section was measured at three locations.

Three LVDTs were placed to measure the horizontal slip between the concrete and the steel girder at locations of maximum positive moment (under the applied load), maximum negative moment (at the internal support) and the point of moment inflection (zero moment). Figure 38 shows a schematic diagram for the locations of LVDTs.

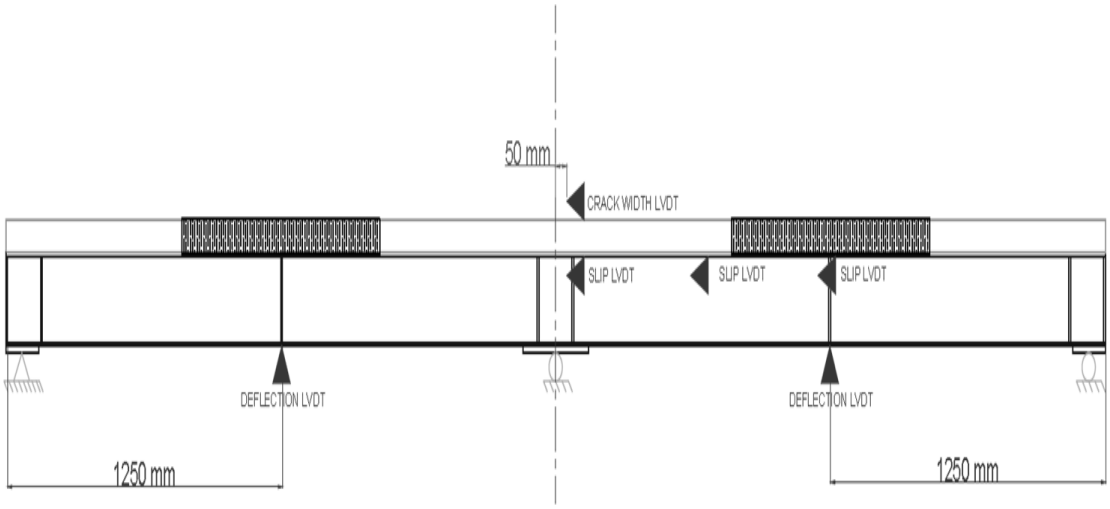

Figure 38: LVDTs locations

The heavy laboratory of the Civil Engineering department at KFUPM is equipped with a Universal Testing Frame, see Figure 28. It is also equipped with a 3000 KN hydraulic operated jack and a 2000 KN capacity load cell. To transfer the load from the jack to the continuous girder, a stiffened I beam was used. The chosen I-beam was HEB 450 which was available in the laboratory. It has a length of 3 meters and stiffeners were welded along the beam. Lateral supports were provided at the interior support to prevent lateral torsional buckling. The testing layout is shown in Figure 39, and Figure 40.

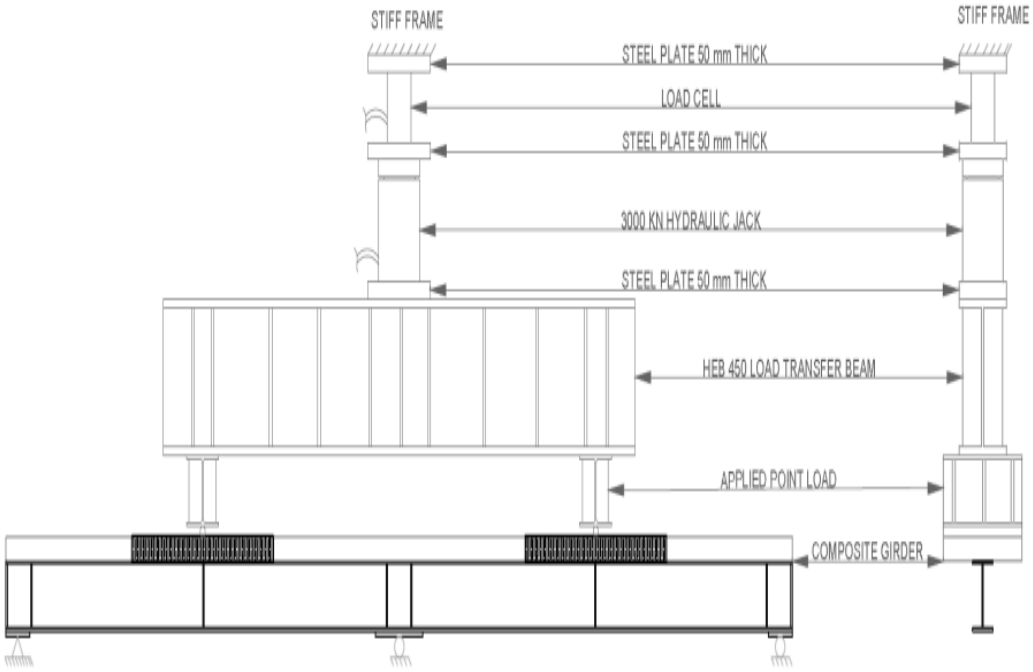

Figure 39: Schematic Testing Layout

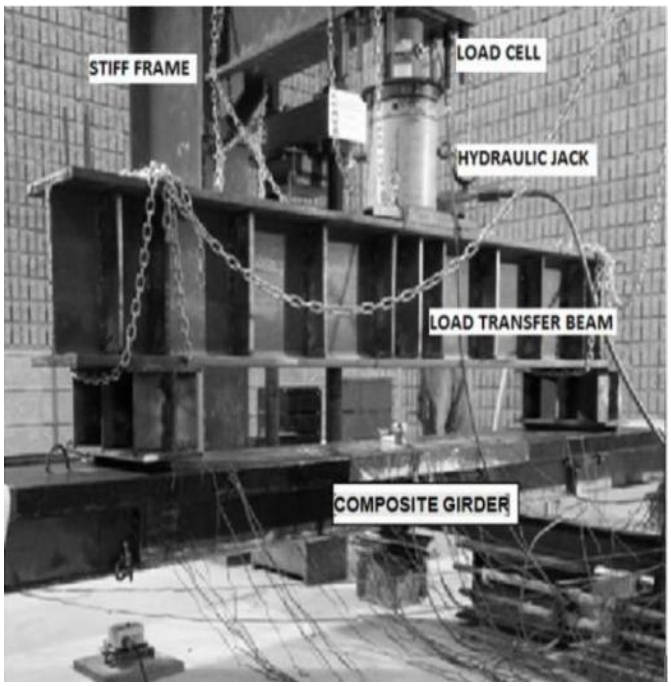

Figure 40: Testing Layout

3.3.5 GIRDERS TESTING

A total of 5 continuous composite girders were tested under 5 point loading. Different testing variables were applied to the continuous composite girders. The first continuous composite girder was tested without applying the CFRP in neither positive nor negative moment zones. It had a shear compression failure, see Figure 41. To prevent such failure mode, a layer of CFRP was wrapped around the concrete slab at the positive moment zone for the remaining 4 girders. To prevent such failure mode, a layer of CFRP was wrapped around the concrete slab at the positive moment zone for the remaining 4 girders, see Figure 42.

Figure 41: Shear compression failure

The four continuous composite girders were tested to achieve the objectives of this project. Reference girder (RFG) was tested without applying CFRP at the negative moment zone to determine the girder ultimate capacity. The other three girders (GR0.0,

GR0.4, and GR0.6) were tested after stressing them to a level of load equivalent to 0%, 40% and 60%, respectively, of the ultimate load obtained from RFG. Then CFRP will be applied at the negative moment zone.

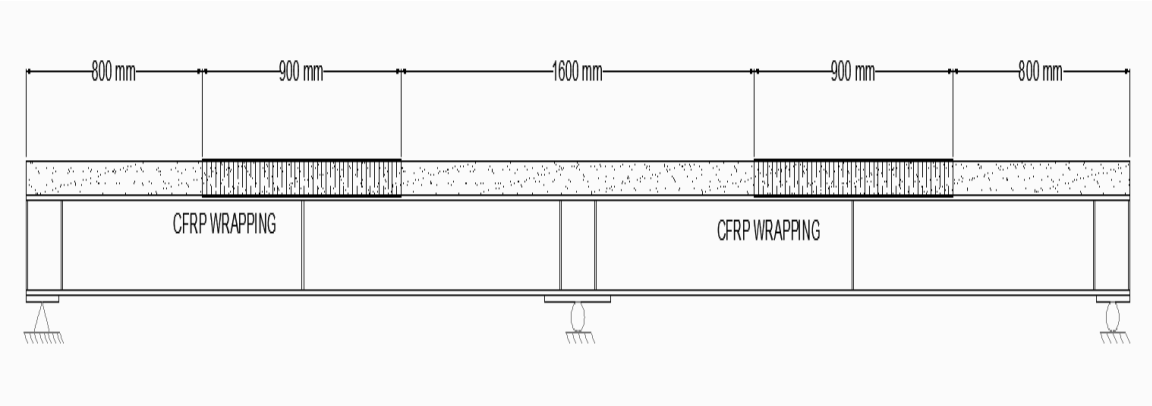

Figure 42: CFRP Wrapping locations

The specimen test matrix is shown in Table 12.

Table 12: Specimen variables

Sample #	Test Label	Specimen condition at negative moment zone	Distressing level
1	RFG	NO CFRP	0
2	GR0.0	With 2 layers of CFRP	0
3	GR0.4	With 2 layers of CFRP	40%
4	GR0.6	With 2 layers of CFRP	60%

CHAPTER 4

TEST RESULTS AND DISCUSSION

4.1 GENERAL

This chapter presents the results of the experimental program. The program objective is to evaluate the performance of CFRP sheets in restoring the stiffness and strength of distressed continuous composite girders. The experimental program variables were discussed in chapter 3.

Firstly, the characteristics of distressed girders are highlighted. Then the behavior of the strengthened girders was analyzed using the experimental results data. The data was recorded from the load cell, LVDTs and strain gauges through the data logger. The experimental results are discussed in the following manner:

1. Load-Deflection.
2. Strain distribution
3. Slip between concrete slab and steel section
4. CFRP sheet deformation.

4.2 DISTRESSED GIRDERS

Two girders (GR0.4 and GR0.6) were distressed by applying 40% (132 KN) and 60% (198.9 KN) of the ultimate load on each respectively. Then the load was gradually decreased to zero. The ultimate load was obtained from testing of girder RFG. The effects of distressing were observed in both girders. The girders had permanent deflection at mid span and lateral cracks in the concrete slab at the negative moment zone. All cracks were closed after the gradual unloading.

Distressing of girder GR0.4 caused plastic deformation at the mid span. The obtained residual strain at the bottom flange was 200 με (14% of yield strain). The concrete slab at the negative moment zone had the first crack at load of 70 KN. Also, mid span deflection after unloading was recorded to be 0.64 millimeters. Figure 43 shows the load deflection behavior of GR0.4 during the distressing stage.

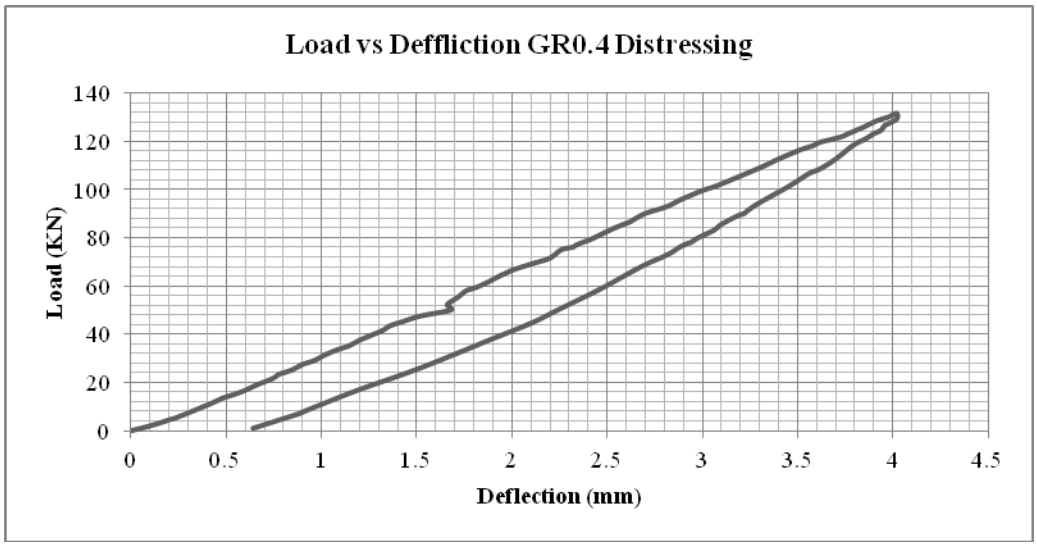

Figure 43: GR0.4 distressing behavior

For girder GR0.6, the observed plastic deformations were greater than GR0.4. The obtained residual strain at the bottom flange was 700 με (52% of yield strain). The first crack at the negative moment zone of the concrete slab appeared at load of 65 KN. Also, mid span deflection after unloading was recorded to be 1.82 millimeters. Figure 44 shows the behavior of girder GR0.6 during the distressing stage.

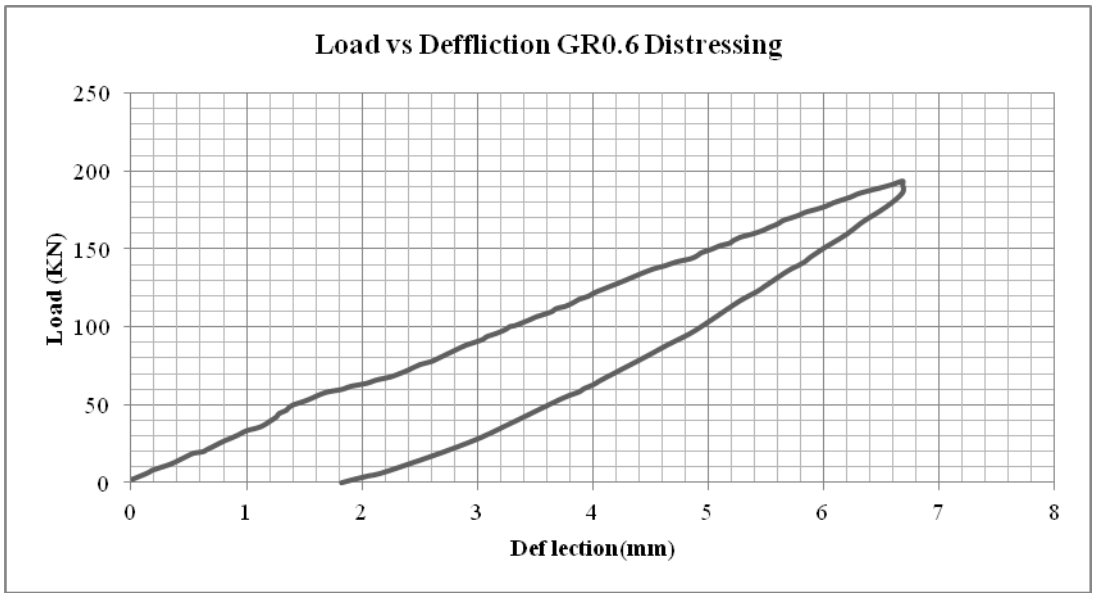

Figure 44: Girder GR0.6 distressing behavior

In the analysis, the residual strain and deflection values were included after repairing with CFRP sheets. CFRP performance evaluation on distressed continuous composite girders will be compared with the non-distressed girder GR0.0 and the reference girder RFG.

4.3 LOAD-DEFLECTION

This part discusses the load-deflection behavior of the girders at three main stages. The main stages of loading to be discussed are cracking stage, yielding stage and ultimate

stages. Cracking stage refers to the load causing concrete cracks at the negative moment zone. Yielding stage refers to the level of load at which steel yields. The ultimate stage refers to the load at failure. Figure 45 shows a schematic diagram for the locations of concrete cracks and bottom flange yielding. Figure 46 shows the load versus deflection for all girders. Table 13 summarizes the load deflection stages. It shows the corresponding load for each stage and its associated deflection at mid span.

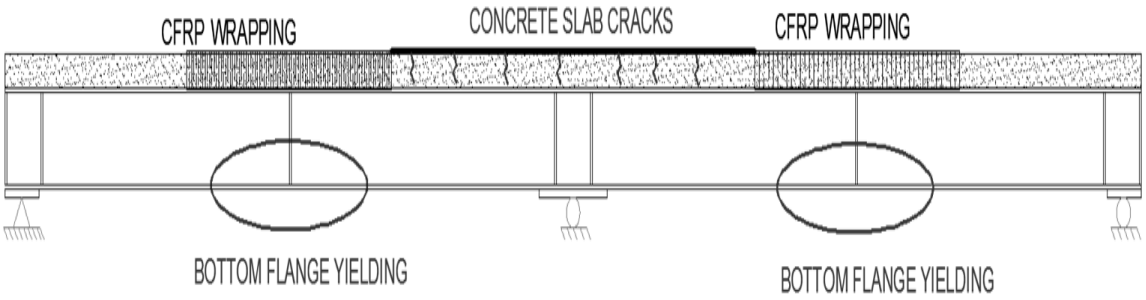

Figure 45: Schematic diagram for the location of concrete cracks and bottom flange yielding

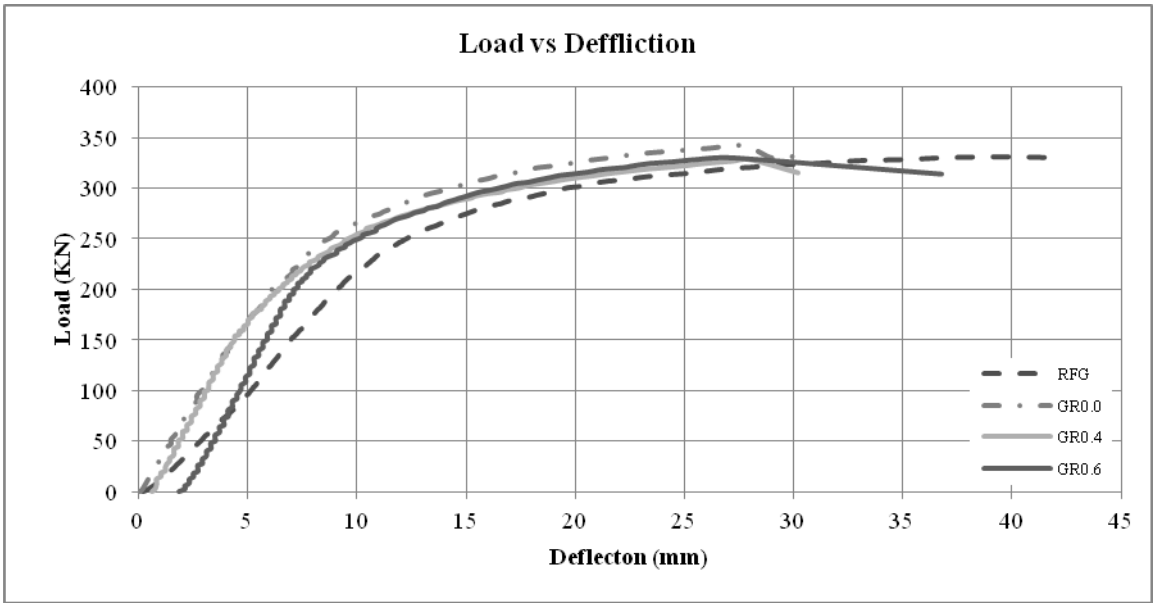

Figure 46: Load vs. deflection diagram

Table 13: Summary of load deflection stages

Stage	RFG	GR0.0	GR0.4	GR0.6
Cracking Load Pcr (KN)	75	150	55	40
Yield Load Py (KN)	152	171.5	166	154
Ultimate Load Pu (KN)	331.5	342	328.5	329.5
Deflection at crack Δcr (mm)	4.06	4.34	2.36	2.9
Deflection at yield Δy (mm)	7.02	5.039	5.14	5.8
Deflection at failure Δu (mm)	39.34	27.77	26.12	26.52

4.3.1 CONCRETE CRACKING STAGE

For girder RFG, the concrete slab at the negative moment zone had the first crack at a load of 75 KN. For the strengthened girders, the cracking load increased. For girder GR0.0, CFRP maintained the concrete slab un-cracked till 150 KN. The distressed girders (GR0.4 and GR0.6), concrete slab was previously cracked at the negative moment zone due to distressing. After retrofitting, CFRP maintained the uncracked concrete slab segments intact until the load reached 55 and 40 KN for girders GR0.4 and GR0.6, respectively. Subsequently, the existing cracks opened at the negative moment zone. The presence of these cracks delayed formation of new cracks for both girders.

At this stage, the girders deflection was recorded. For girder RFG, the mid span deflection was 4.06 mm. Girder RFG had less deflection at crack because the cracking load was less than the cracking load of the retrofitted girders. For the retrofitted girders, the deflections associated with concrete crack stage have slightly increased. Table 13 shows the associated deflections for the retrofitted girders.

4.3.2 YIELDING STAGE

Yielding of steel girder started at the bottom flange at mid span (Positive moment zone) for all girders, see Figure 45. The load at which the girders yielded was 152, 171.5, 166 and 154 KN for girders RFG, GR0.0, GR0.4 and GR0.6, respectively. At this stage of loading, the girders deflections were recorded. For girder RFG, the girder mid span deflection was 7.02 mm. For the retrofitted girders, the values of deflection at yielding stage were higher. Table 13 shows the associated deflections for the retrofitted girders at yielding stage.

The deflection at yield stage is important to determine the stiffness of the girder. From Figure 46, it is noticed that the deflection had a linear trend until yielding of bottom flange at mid span. The CFRP had a positive impact on deflection. The strengthened girders with CFRP had less deflection compared with the reference girder (RFG) at same load level as shown in Figure 46. This demonstrates the effect of carbon fibers in increasing the girder stiffness. For distressed girders, they deflected more at yield comparing to girder GR0.0.

4.3.3 FAILURE STAGE

Two failure modes developed in this study. The first was crushing of concrete at the positive moment zone. This mode of failure occurs when plastic hinges developed at mid span. The other failure mode was CFRP debonding at the interior support zone. This mode of failure was premature because the adhesive capacity was reached.

The post yielding load deflection behavior up to failure for all girders is shown in Figure 46. The load deflection behavior started to act in an inelastic plateau behavior after the yielding load until failure. There is an observed drop in the Load for the strengthened girders. The drop is caused by debonding of the CFRP. The ultimate loads were at 331.5, 342, 328.5 and 329.5 KN for girders RFG, GR0.0, GR0.4 and GR0.6, respectively. CFRP did not contribute in the ultimate strength as what expected due to debonding of the CFRP sheets. However other improvements were achieved; refer to section 4.3.4 page 62.

4.3.3.1 Girder RFG

The failure mode was crushing of concrete at the positive moment zone, see Figure 47. The collapse mechanism for girder RFG started by the formation of a plastic hinge at the interior support zone. When the interior support section became fully plastic, the girder acted as two simply supported beams. Plastic hinges occurred at the mid span at the failure of the girder by concrete crushing, Figure 48.

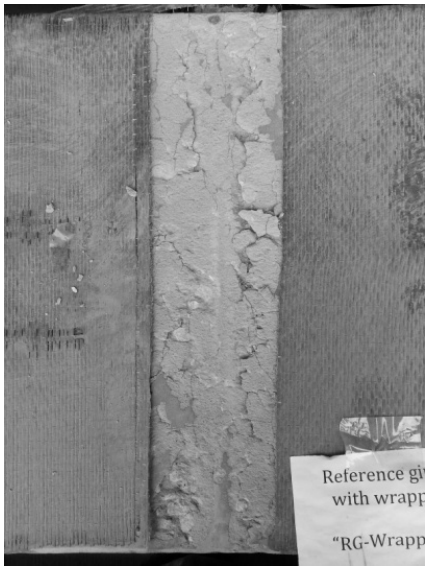

Figure 47: Crushing of Concrete of girder RFG

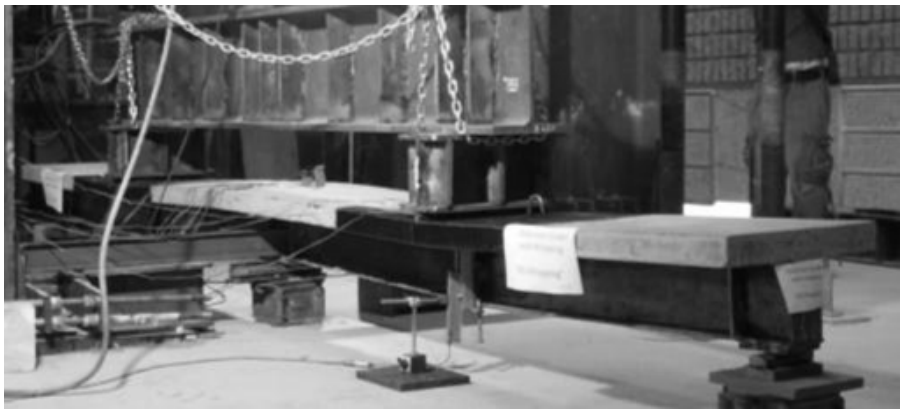

Figure 48: Girder RFG at failure

4.3.3.2 Girder GR0.0

The ultimate load reached was at 342.5 KN at each span. The failure mode was debonding of the CFRP sheet from its end toward the nearest crack in concrete slab. The CFRP debonding for girder GR0.0 specimen at failure are shown in Figure 49.

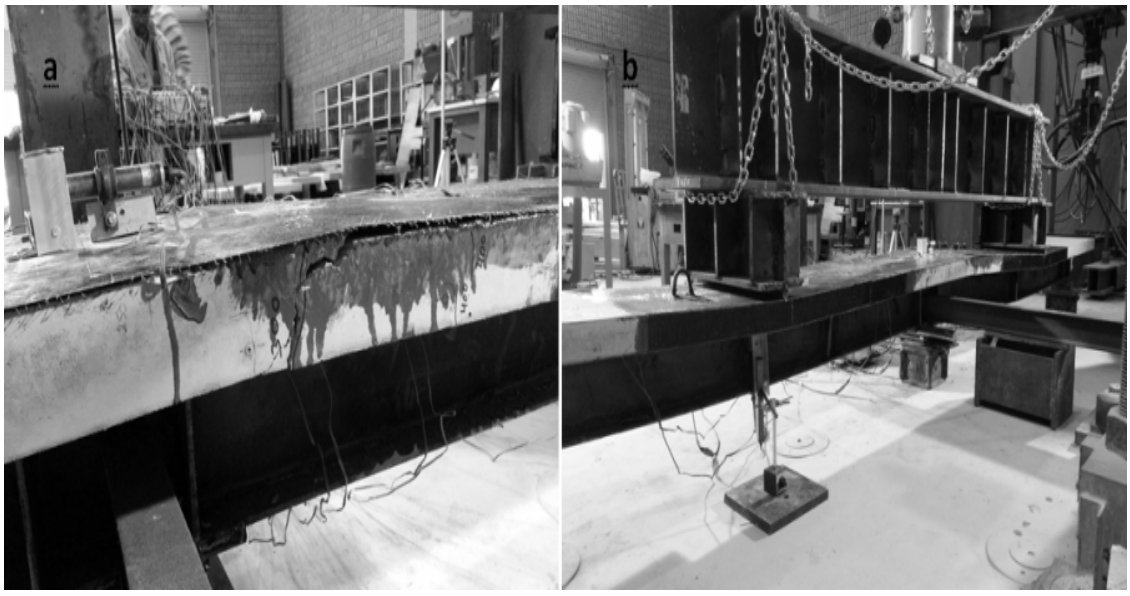

Figure 49: Girder GR0.0 CFRP debonding at failure

4.3.3.3 Girder GR0.4

The ultimate capacity of girder GR0.4 was 329 KN. The specimen failure mode was debonding of CFRP at the negative moment zone, Figure 50.

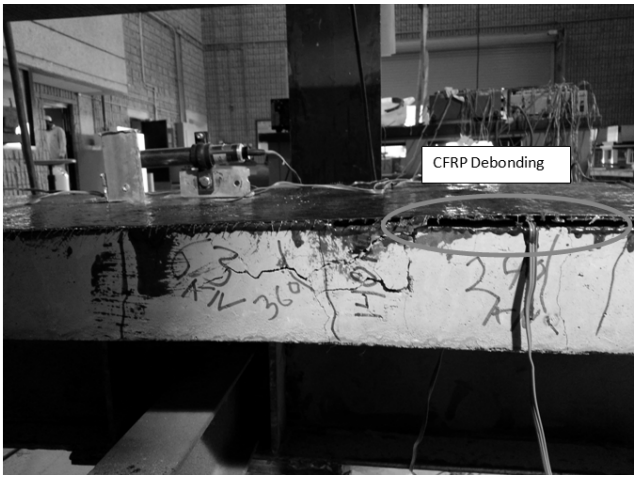

Figure 50: Girder GR0.4 CFRP debonding

4.3.3.4 Girder GR0.6

The ultimate capacity of girder GR0.6 was 330 KN. The specimen failure mode was debonding of CFRP at the negative moment zone, Figure 51.

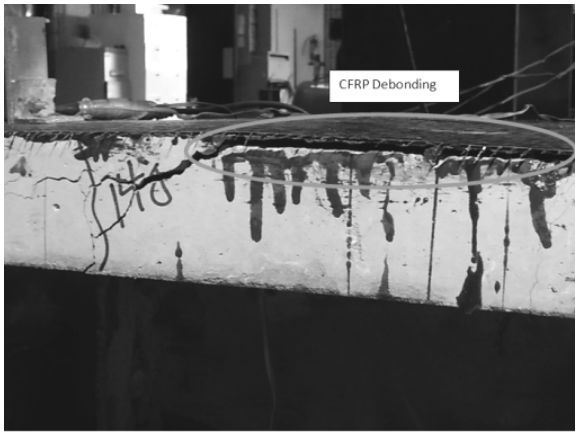

Figure 51: Girder GR0.6 CFRP debonding

4.3.3.5 Debonding Mechanism

For the strengthened girders with CFRP, flexural cracks caused large local strain concentration in CFRP sheets. The tensile stresses released by the cracked concrete are transferred to the CFRP sheet and steel reinforcements. High local interface stresses are provoked near the crack between the CFRP sheet and the concrete slab. As the loading increases, the interface stresses also increase between the CFRP sheet and the concrete near the crack. When these stresses reached the critical values, debonding started to propagate towards one of the CFRP sheet ends. For the distressed girders, presence of cracks led to CFRP debonding at a lower stage of loading compared to girder GR0.0.

From the single shear test SST in experimental program the adhesive bond strength was found to be 2.0 MPa. At the instance shear stresses in the adhesive reached this critical value, CFRP debonding failure occurred. Since the debonding occurred at one end of the CFRP sheet, shear stresses can be calculated to determine the debonding stress at that end. The distribution of these strains can be used to determine the interface shear stresses between the CFRP sheet adhesive and concrete (Rosenboom and Rizkalla 2008). Figure 52 shows the interface stress (τ_w) and the peeling stress (σ_c) between the CFRP sheet and concrete. The discussion in this project is limited to the interface stresses. It can be seen that the tensile stresses increase in the CFRP while approaching the center of the girder. Equation 3 evaluates the interface shear stress.

$$\tau_w(x) = \frac{d}{dx}\left[K_p \varepsilon_p(x)\right] \qquad \text{Equation 3}$$

Where:

- x is the distance along the girder in millimeters

- $\tau_w(x)$ the interface shear stress at a distance x along the girder
- K_p is the axial stiffness of the CFRP sheet
- $\varepsilon_p(x)$ CFRP strain distribution along the length of the CFRP sheet

Since the CFRP sheet configuration is constant along its length, then the axial stiffness K_p is constant.

$$K_p = t_{CFRP}\, E_{CFRP} \qquad \text{Equation 4}$$

Where: t_{CFRP} and E_{CFRP} are the thickness and modulus of elasticity of the fibers, respectively. The thickness was taken to be 0.5 millimeter including the thickness of epoxy. The modulus of elasticity for the CFRP is 230500 MPa.

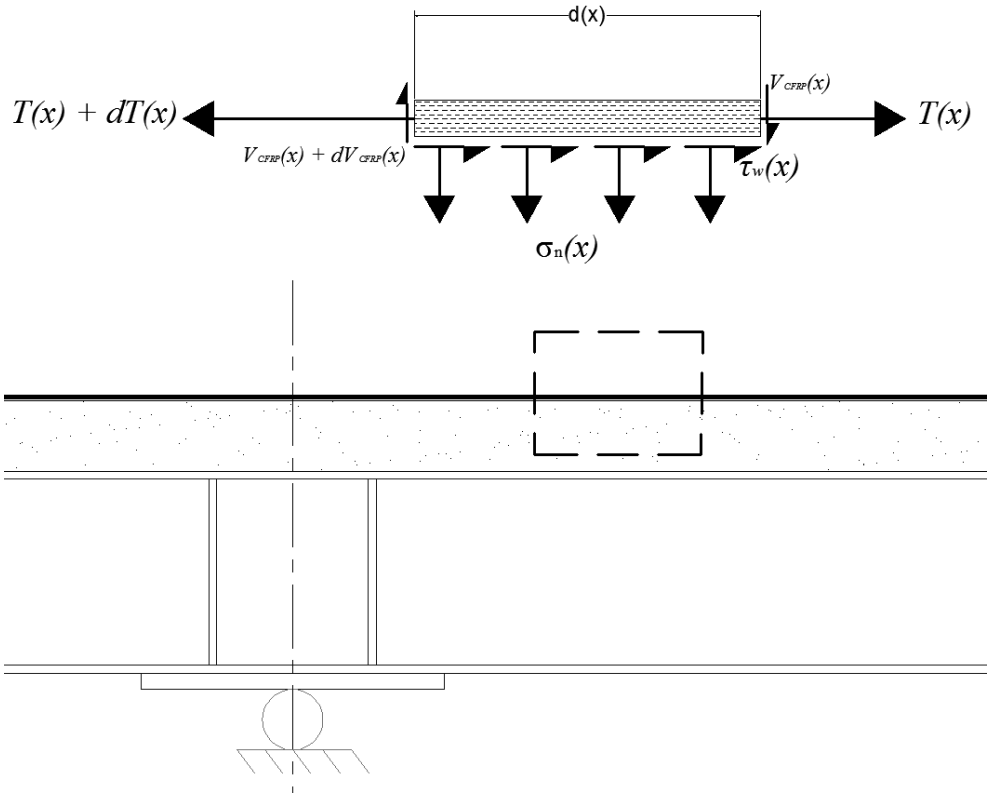

Figure 52: Interface shear stress $\tau_w(x)$

The strain distribution at debonding is shown in Figure 53. The behavior was fitted in a second degree polynomial to ease the differentiation as shown in Figure 53.

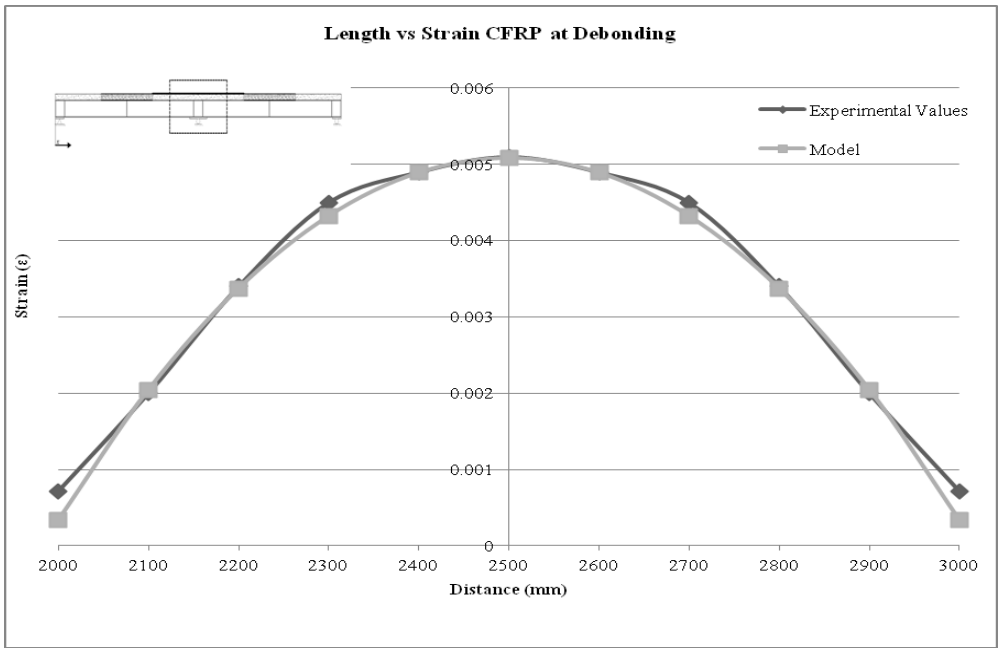

Figure 53: Strain disruption at debonding of CFRP

The strain along the length was fitted in the following equation:

$$\varepsilon_p(x) = -1.898 \times 10^{-8}\, x^2 + 9.49 \times 10^{-5}\, x - 0.114 \qquad \textbf{Equation 5}$$

Where: x is the distance in millimeters from the far end of the girder as shown in

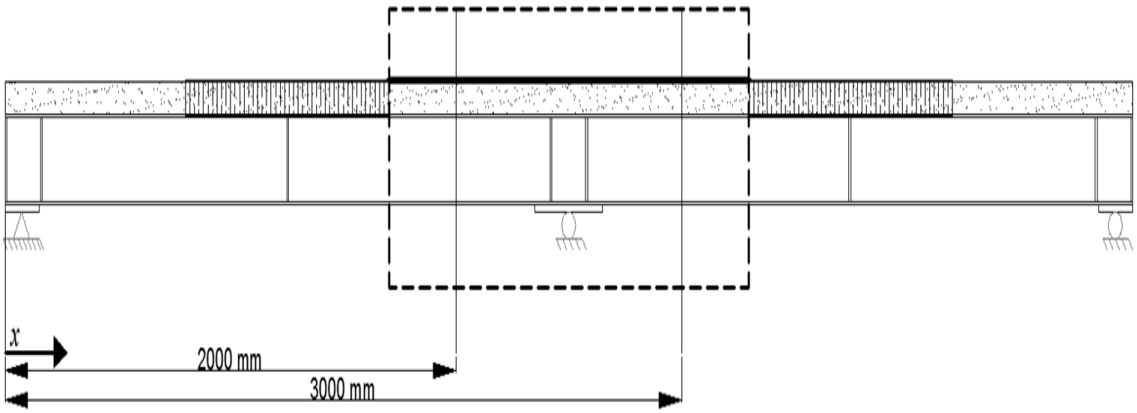

Figure 54: the location where the interface shear stresses equation is applicable

Thus by differentiation of Equation 5 and substitution of all values in Equation 3, the interface shear stresses at debonding are calculated by the following equation:

$$\tau_w(x) = -4.375 \times 10^{-3}\, x + \ 10.937 \qquad \textbf{Equation 6}$$

The shear stress in the CFRP at one end (at length of 2000 mm):

$$\tau_w(2000) = 2.18\, MPa > 2.0\, MPa$$

Thus debonding failure occurred in the girder. The interface shear stresses between the CFRP sheet adhesive and concrete is plotted along the CFRP sheet length in Figure 55. The curve shows that the stress takes a linear trend from zero at the maximum moment location to the critical shear stress value at the end of the CFRP sheet.

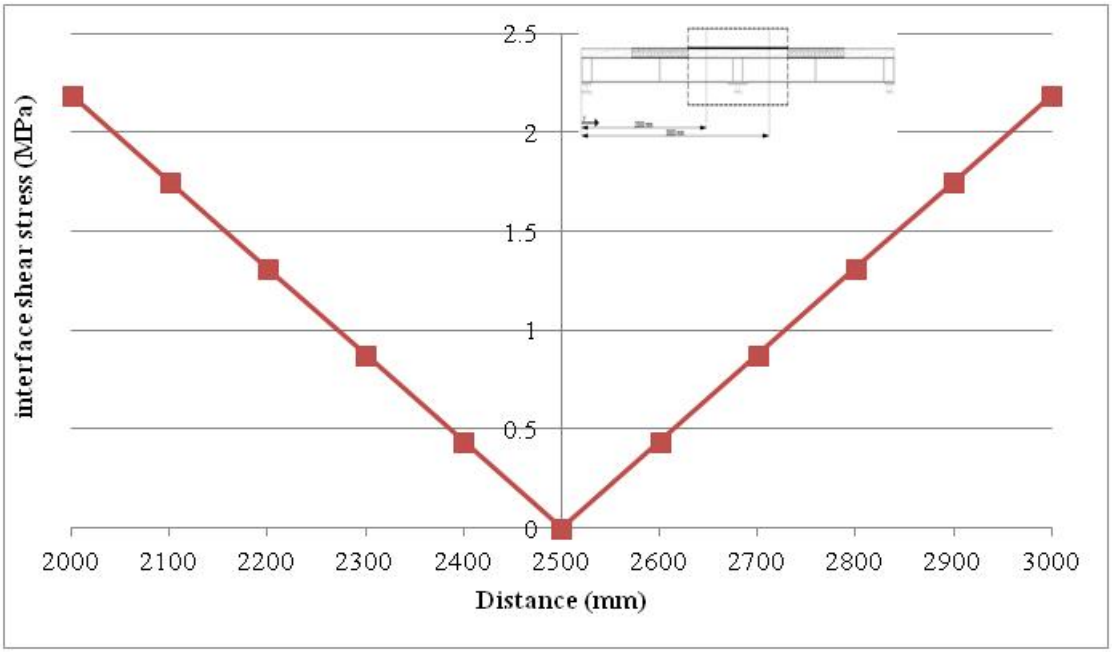

Figure 55: Interface shear stresses

4.3.3.6 Deformed Shapes

Figure 56 shows the continuous composite girders deformed shapes at yield stage and at failure stage. The effect of CFRP in reducing the deflection of the girders can be seen. The profiles reflect the difference in deflection between girder RFG and girders strengthened with CFRP.

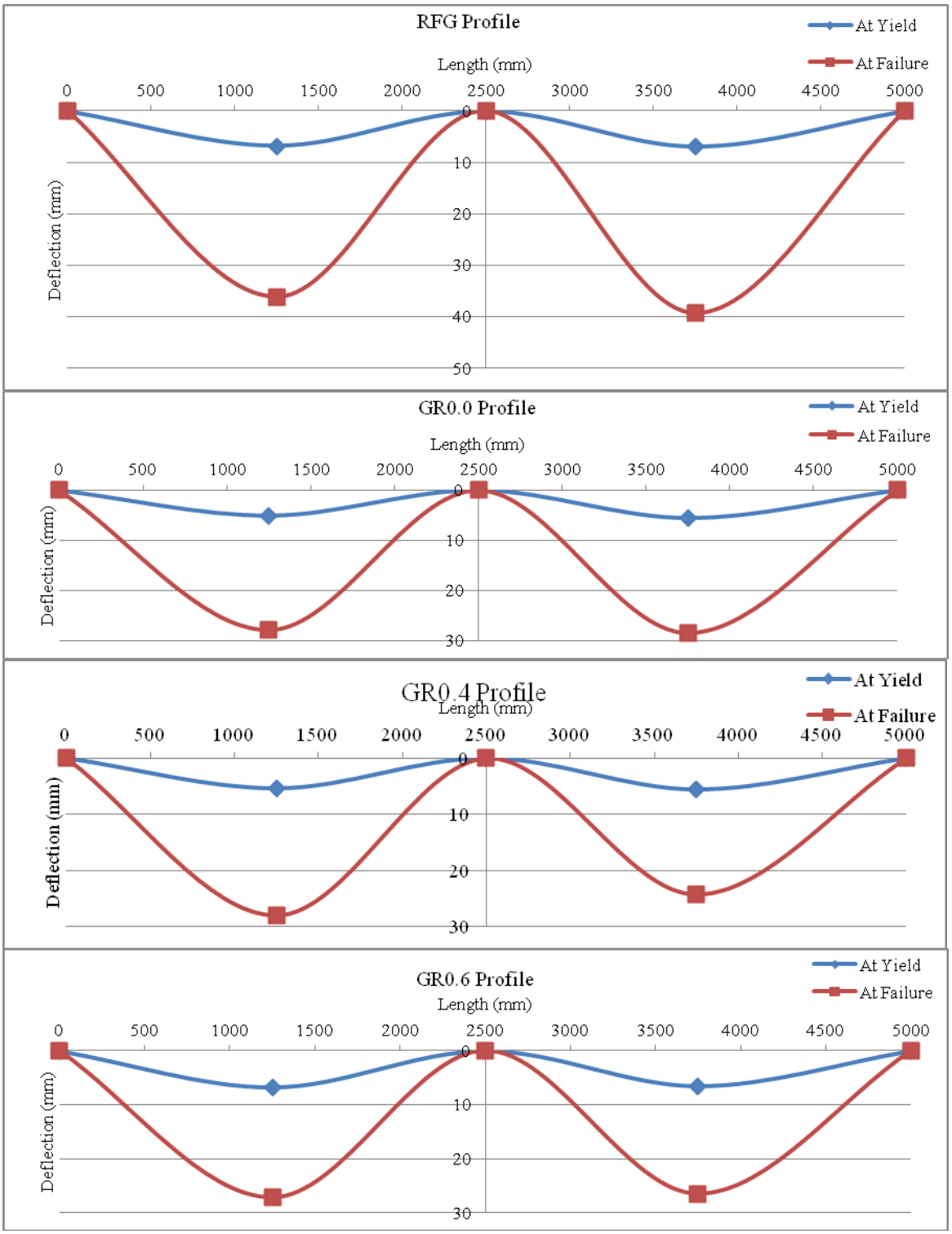

Figure 56: Girder deformed shapes

4.3.4 EFFECTIVENESS OF CFRP STRENGTHENING SYSTEM

This part discusses the effectiveness of CFRP materials as strengthening scheme for the distressed continuous composite girders. Table 14 shows a summary of the improvements on the behavior.

Table 14: Results of CFRP on loading stages

Beam	P_{cr}/P_y	$P_y/P_{y(RFG)}$	K	$K/K_{(RFG)}$	$\Delta_y/\Delta_{y(RFG)}$	Δ_u/Δ_y
	Ratio	% gain	KN/mm	% gain	% less	Ratio
RFG	0.59	0.00	21.65	0.00	0.00	5.60
GR0.0	0.87	12.83	34.03	57.19	28.22	5.51
GR0.4	0.33	9.21	32.30	49.16	26.78	5.08
GR0.6	0.26	1.32	26.55	22.63	17.38	4.57

4.3.4.1 CFRP Ability to Restore the Service Capacity

It's noted that CFRP have increased the yielding load of girder GR0.0 by 12.83%. For the distressed girders, the CFRP have restored and increased the yield load of girder GR0.4 and girder GR0.6 by 9.2% and 1.32%, respectively. For girder GR0.6, although the yielding of bottom flange due to distressing, CFRP have restored the service capacity of the girder to its original state. This increase in yielding load satisfies the proposed design guidelines for strengthening steel bridges with FRP materials.

4.3.4.2 CFRP Improvements on Crack Load Behavior

For the retrofitted girders, CFRP has increased the cracking load to level close to yielding load. Table 14 shows the improvements on the girders' strengths achieved by CFRP. The cracking load increased by 66.67% for girder GR0.0. For the deteriorated girders GR0.4

and GR0.6, cracks existed in the concrete slab due to distressing. However, the epoxy primer with the CFRP sheets maintained the cracks closed until a level of load equals 33% and 26% of the yielding load. The positive impact of this action is for durability concerns.

4.3.4.3 CFRP Effect on Deflection at Yield

The improvement on the service deflection at yield achieved by the CFRP was noticed during the experiment, see Table 14. CFRP has reduced the deflection at yielding by up to 28% for strengthened girders compared to girder RFG ($\Delta_y/\Delta_{y\ (RFG)}$). The distressed girders had less improvement than girder GR0.0 because the distressing stage caused plastic deformations in the girders causing permanent deflection at mid span.

4.3.4.4 CFRP Improvements on Stiffness

One of the important aspects for CFRP strengthening is the increase in stiffness, see Table 14. The stiffness (K) is found from the slope of the linear part (before yielding) in the load-deflection curve. The retrofitted girders showed improvements in the stiffness due do utilizing CFRP. The stiffness has increased by 57.19%, 49.16% and 22.63% for girders GR0.0, GR0.4 and GR0.6, respectively. For the distressed girders, the ratio is less because the yielding occurred at a lower load. Furthermore, crack propagation in the concrete slab at the negative moment zone for the distressed girders has not affected the stiffness due to utilizing CFRP. CFRP aided in increasing the stiffness of the distressed girders.

4.3.4.5 CFRP Effect on Ductility

Displacement ductility (Δ_u/Δ_y) characterizes the deformation capacity of members (structures) after yielding, or their ability to dissipate energy. It is the ratio of the midspan deflection at the ultimate load to the mid span deflection at yield. The retrofitted girders did not reach their full capacity due to premature CFRP debonding. As a result, the actual ultimate deflection was not determined. However, the Δ_u/Δ_y ratio shows that CFRP affected the girders by reducing their ductile behavior. For the distressed girders, they showed less ductile behavior compared to the non-distressed girder GR0.0.

4.4 STRAIN DISTRIBUTION

To show the strain distribution of the girders, data was acquired from strain gauges along the depth of the girder. The considered stages of loading are: yielding of bottom flange and at load equals 300 KN. The variation is shown along the depth at mid span (positive moment zone) and at interior support (negative moment zone). Figure 57 shows the girder RFG curvature at stage of yielding and at load equal to 300 KN. For the strengthened girders, the strain variations are shown in Figures 58, 59, and 60 for girders GR0.0, GR0.4 and GR0.6, respectively.

At yielding stage of the girder, linear strain variation is noticed. Later, the strains along the section depths varied between the concrete slab and the steel section. This variation was due to slip between concrete slab and steel girder. Slip was measured using LVDTs between the concrete slab and steel section. The strain distribution can also give an indication of the slip between these layers.

At the negative moment zone, cracking of concrete slab in reference girder RFG led to losing of the strain gauges at the concrete slab as shown in Figure 57. For the reference girder, the composite action at the negative moment zone was between the steel section and steel reinforcement. For the strengthened girder the composite action at the negative moment zone was between steel section, steel reinforcement and CFRP sheet. The CFRP has increased the stiffness of the section. That aided in reducing the rotational capacity of the plastic hinge at the negative moment zone.

It also can be visualized from the strain distribution curves the CFRP effect on the depth of natural axis in the negative moment zone. For girders RFG the natural axis was at a distance of 105 mm from the bottom flange. While for the strengthened girder the natural axis depth increased to around 130 mm from the bottom flange. This represents an increase in the natural axis depth by 24%.

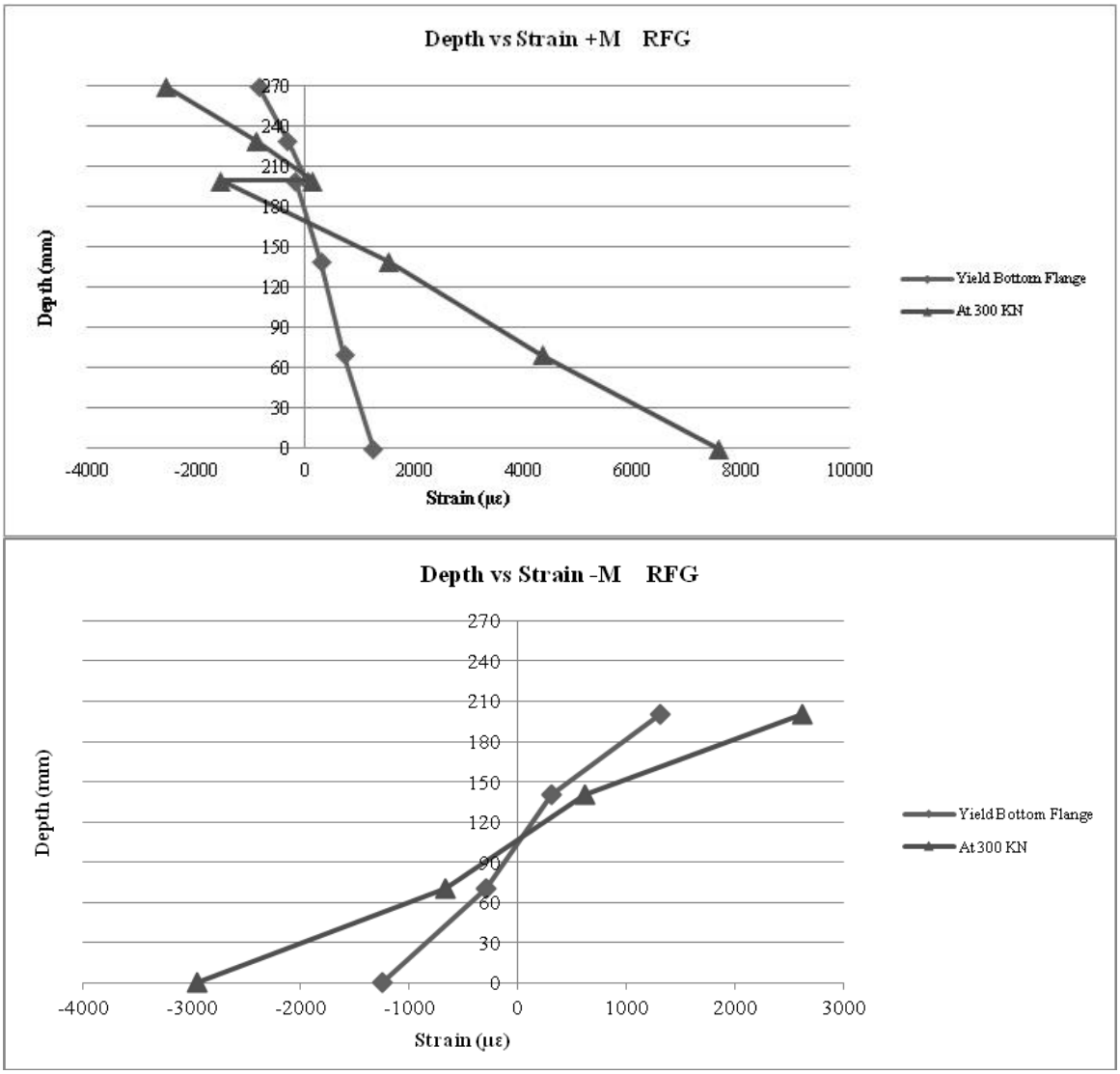

Figure 57: Girder RFG strain distribution

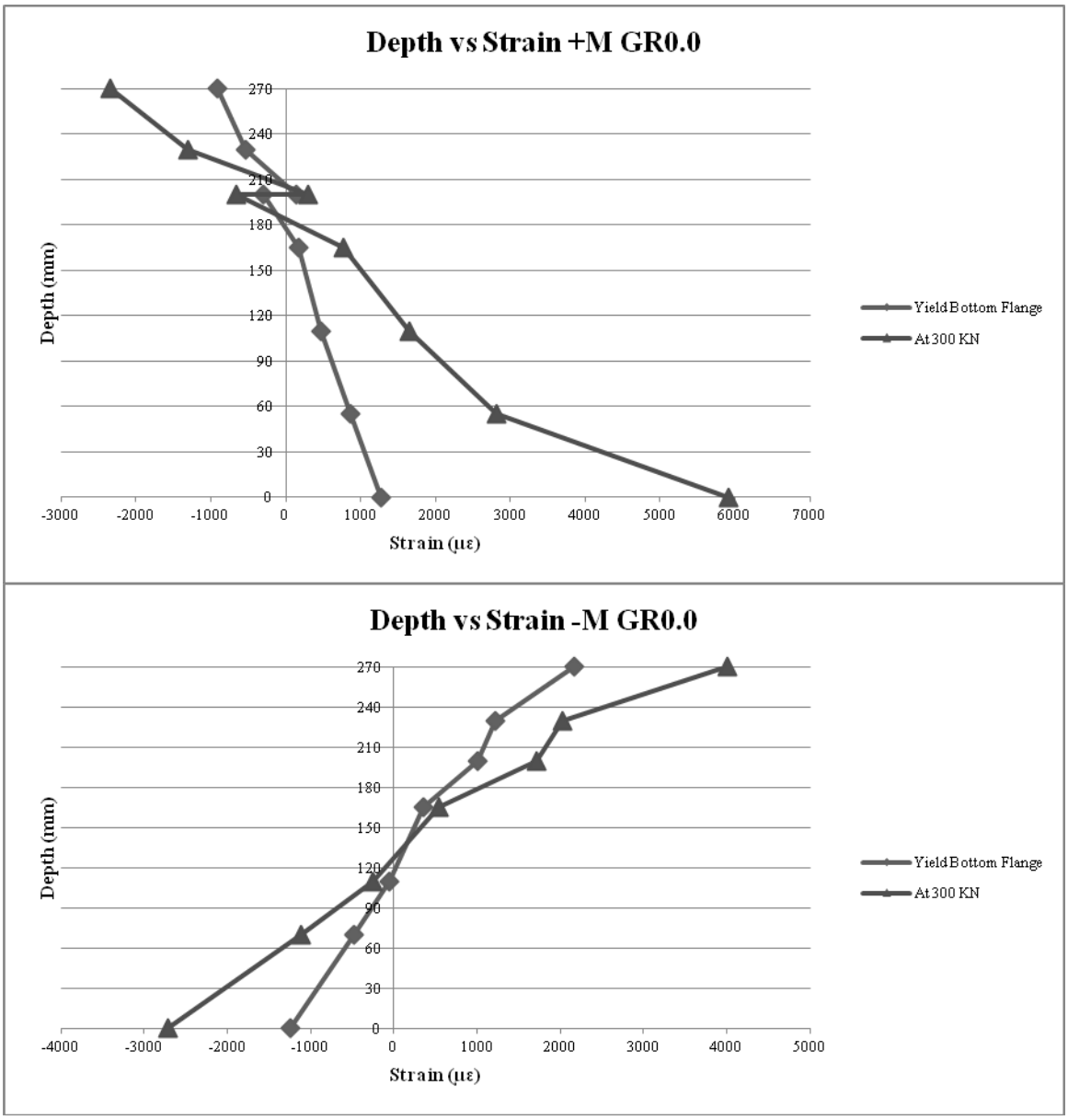

Figure 58: Girder GR0.0 strain distribution

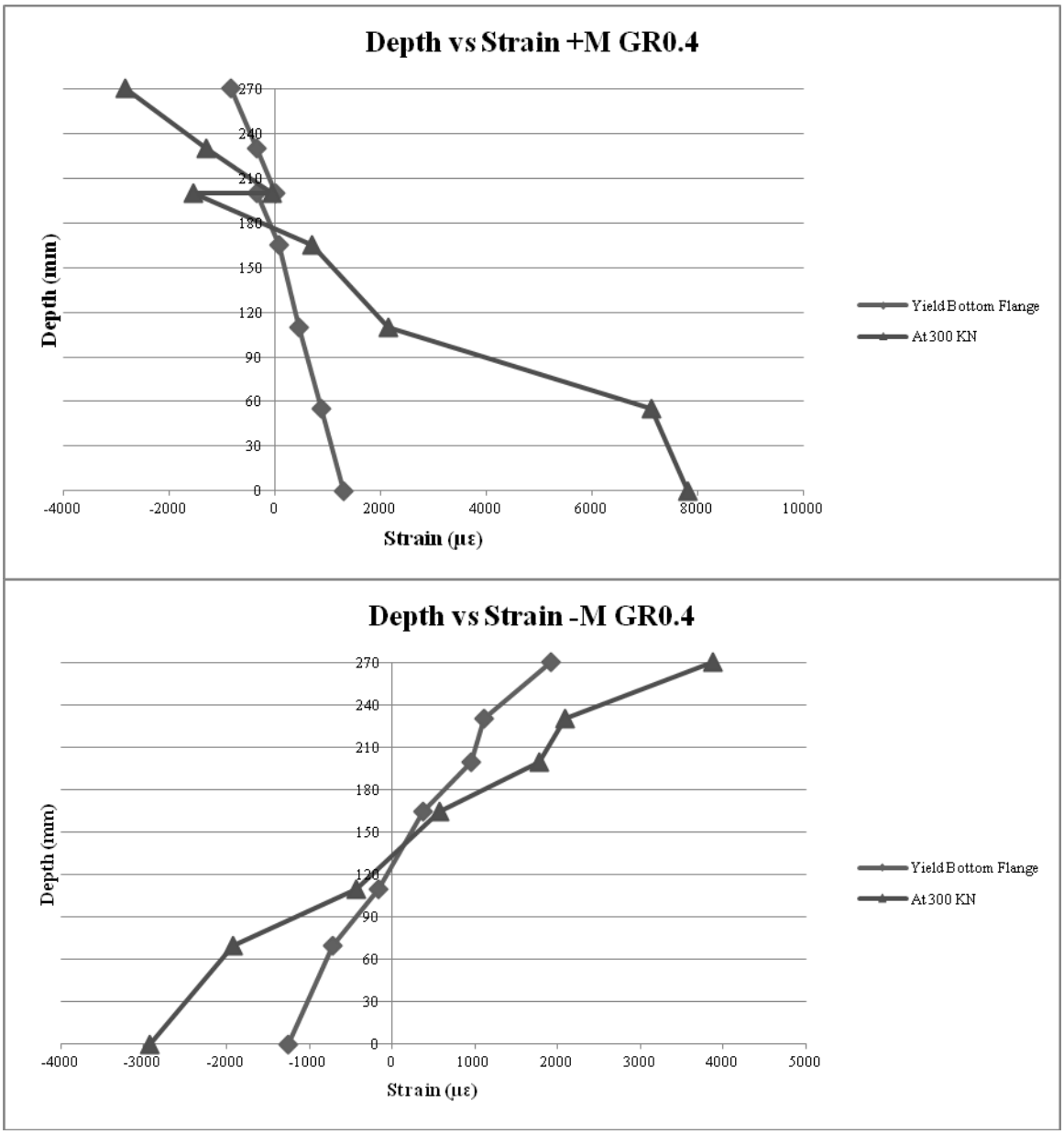

Figure 59: Girder GR0.4 strain distribution

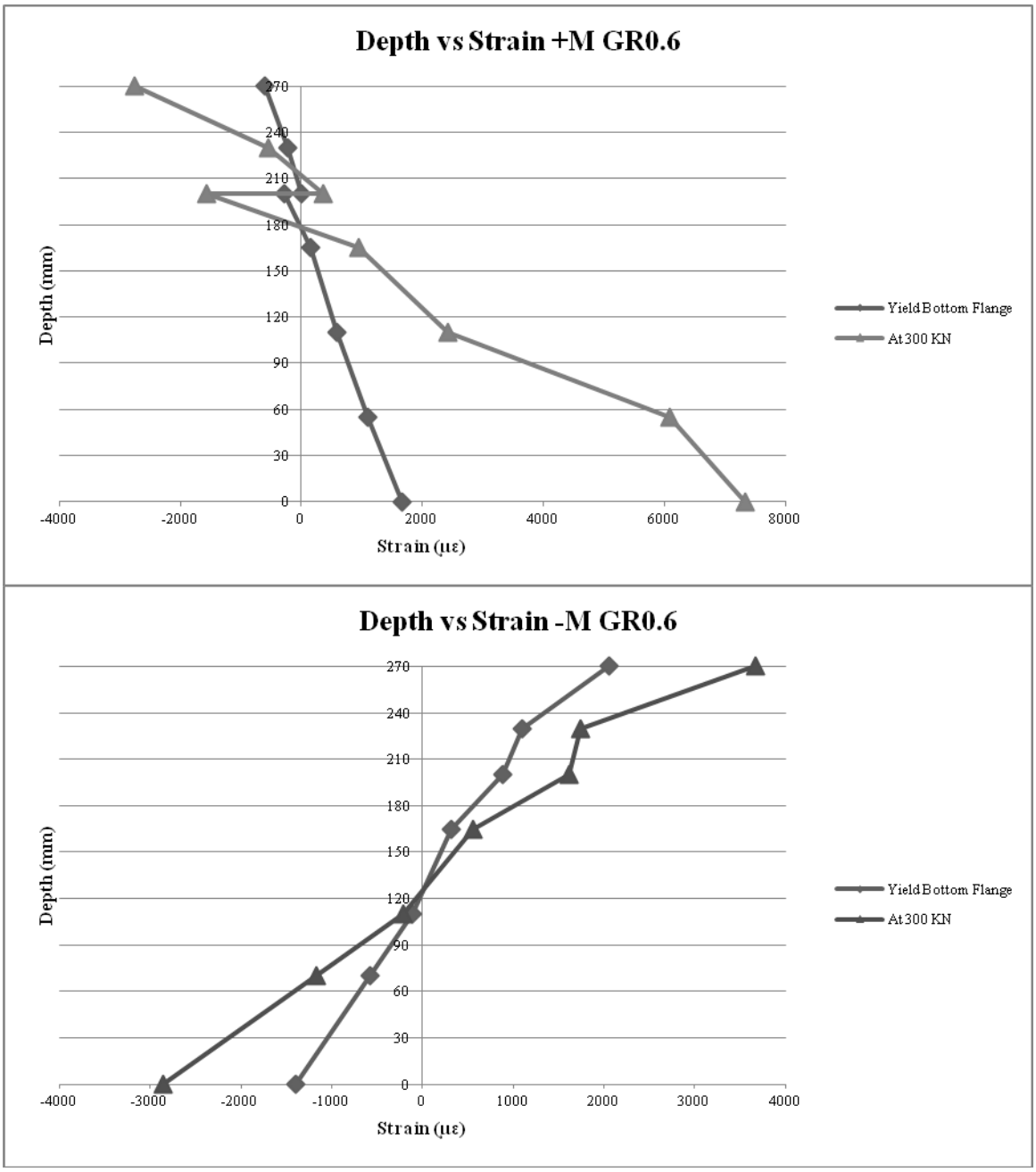

Figure 60: Girder GR0.6 strain distribution

4.5 SLIP BETWEEN CONCRETE SLAB AND STEEL SECTION

Slip was monitored to analyze the stud behavior. Steel studs were utilized to maintain the composite action between the concrete slab and steel section. That is achieved by transferring the shear stresses between the steel section and concrete slab. Figure 61 and Figure 62 show the load versus slip for strengthened girders at mid span and internal support, respectively. Slip was recorded at the mid span and internal support between the concrete slab and steel section using the LVDTs. Slip between the concrete slab and steel section follows a linear trend till yielding of bottom flange. Then the slip behaves in plateau behavior till failure. The distressed girders had initial slip between concrete slab and steel section. These initial values where within the limit specified by the push out test, refer to section 3.2.6.

At the positive moment zone (mid span), girder RFG exceeded the ultimate slip capacity found from the push out test (<1.3 mm). On the other hand, the slip at failure reached by the strengthened girders was within the limit (<1.3 mm), although the deboning failure. CFRP has maintained the full composite action between the steel section and concrete. At the negative moment zone (internal support), distressed girders exhibited more slip comparing to girder GR0.0.

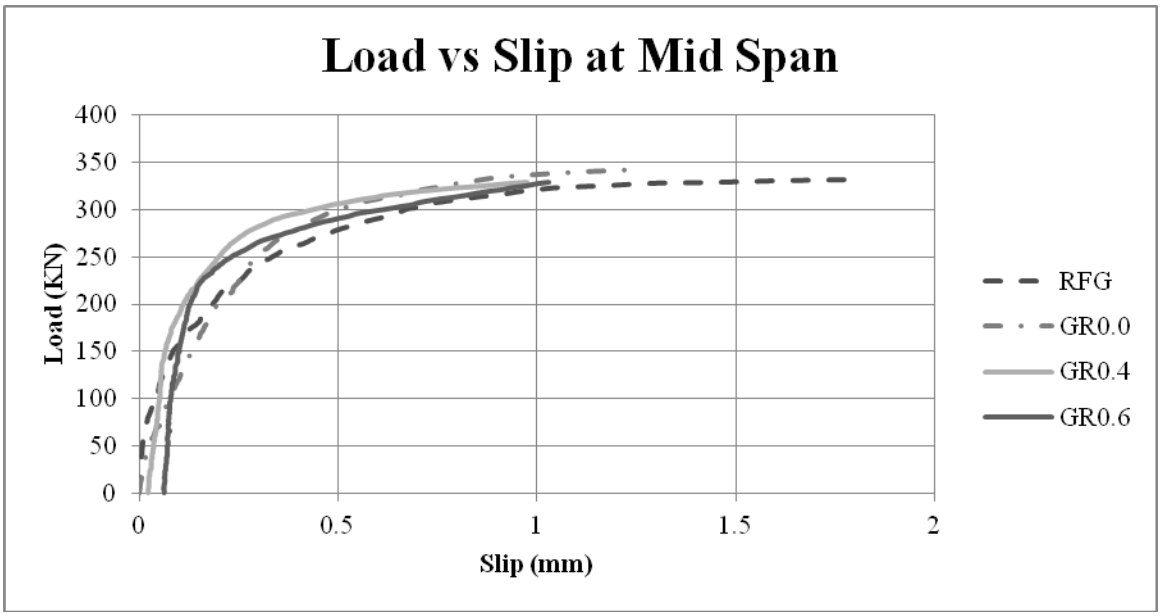

Figure 61: Load vs. Slip curve at mid span

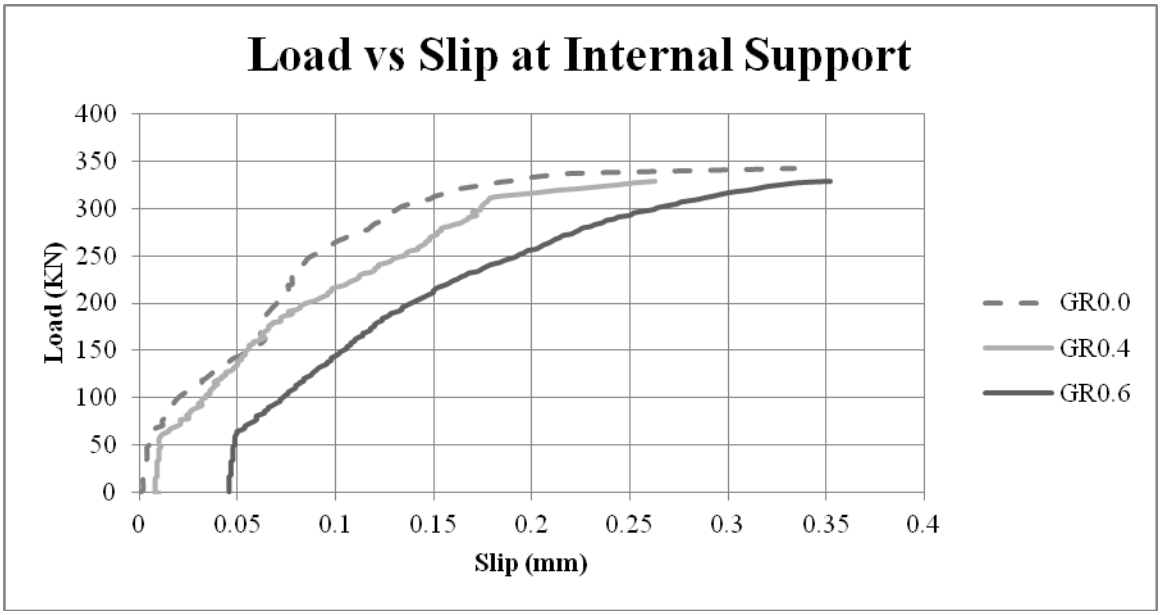

Figure 62: Load vs. Slip curve at internal support

Furthermore, from the figures, the slip at the mid span had greater values than at the interior support at the same load level. One of the reasons for such behavior is the number of shear studs. At the negative moment zone the number of shear studs was

double the number at the positive moment zone. That provided better interface between concrete slab and steel section. Also, the transferred shear stresses at mid span are much greater than at internal support. Figure 63 shows the schematic diagram of stresses to be transferred though the shear studs. The compression stresses from concrete slab is more than the tensile stresses from CFRP and steel reinforcement at internal support.

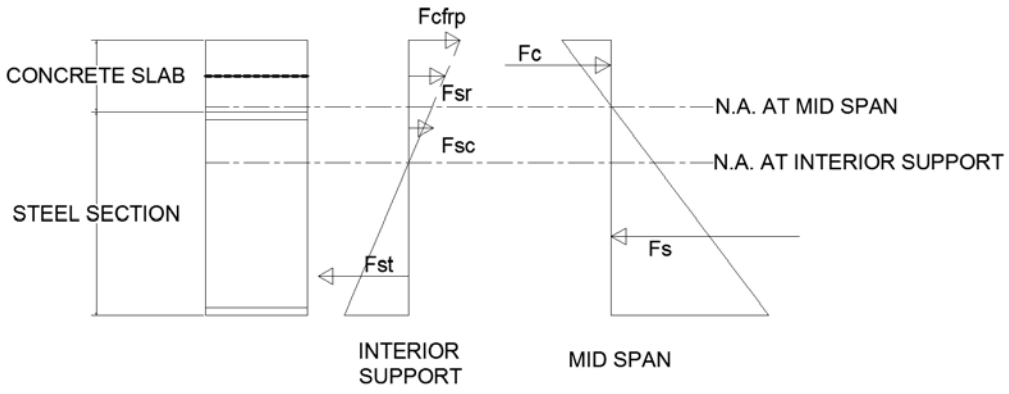

Figure 63: Schematic diagram of the section stresses

4.6 CFRP SHEET DEFORMATIONS

Strain gauges were installed at the CFRP sheet to monitor its deformations. CFRP is known of having a linear stress-strain behavior. Figure 64 shows the applied load versus strain in CFRP. CFRP sheets for girder GR0.0 behaved linearly while increasing the applied load till the section started to yield at 219 KN. For the distressed girders GR0.4 and GR0.6, the CFRP behaved in a linear behavior prior to yielding of the section. However, the stress in the CFRP sheet in the distressed girders was higher compared to the stress in girder GR0.0. Presence of cracks in the distressed slab caused development of stresses in CFRP sheets. That caused more straining in the CFRP sheets compared to

girder GR0.0, see Figure 65. After steel section yielded at the interior support zone, the CFRP sheets tended to have similar plateau behavior.

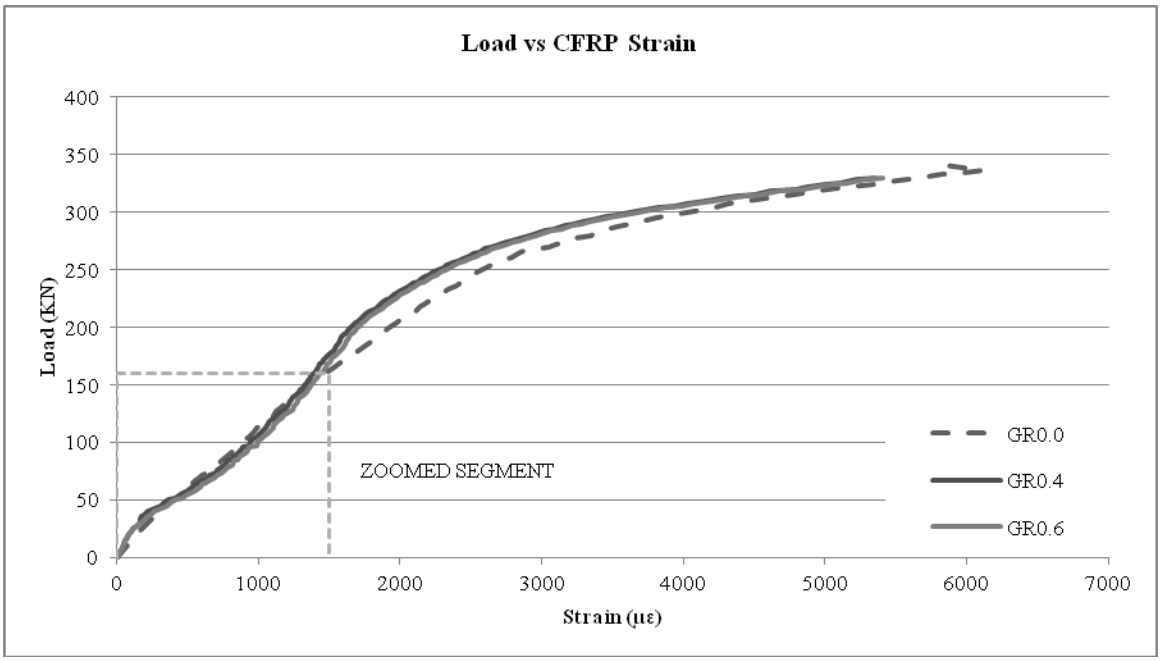

Figure 64: Load vs. Strain CFRP at interior support

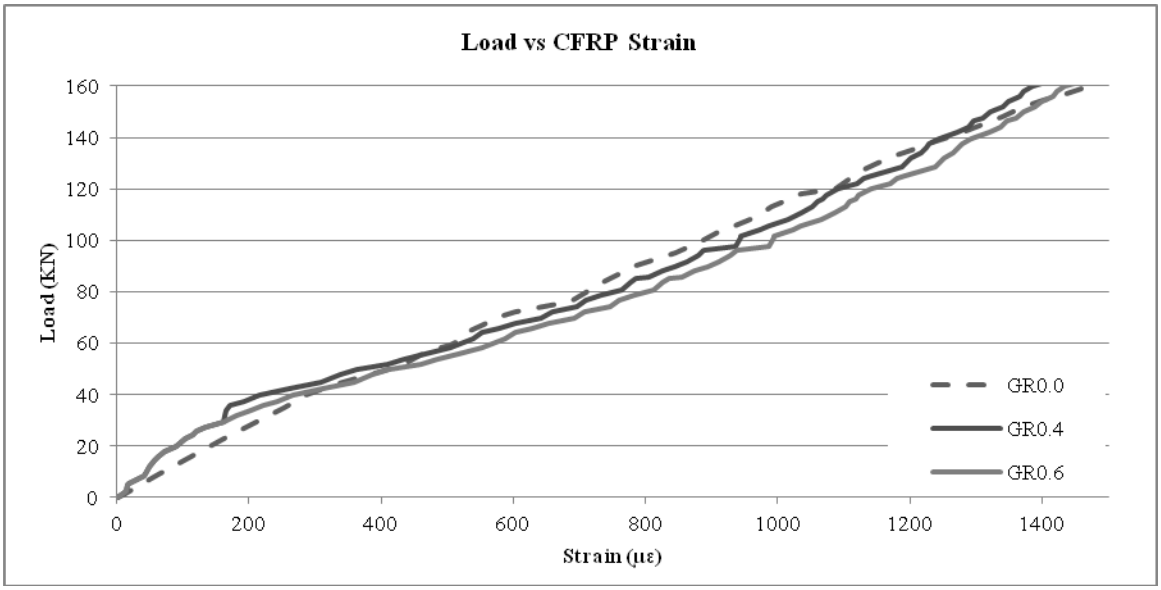

Figure 65: Load vs. Strain CFRP at interior support "load up to 160 KN"

Figures 66 and 67 present CFRP strain measurements along its length for girders GR0.0, GR0.4 and GR0.6. Strain measurements are taken at 300 KN close to ultimate load and at 100 KN close to yield load. It noticed the CFRP used for retrofitting distressed girders was strained more before yielding of the section. At later stages of loading after yielding, CFRP sheets behaved the same for all girders.

It should be highlighted that the girders have failed by debonding without utilizing full tensile strength of CFRP. In the experiment, CFRP reached up to 40% of its ultimate strain for girder GR0.0, and 35% for distressed girders GR0.4 and GR0.6. These strains were at the instant of CFRP debonding.

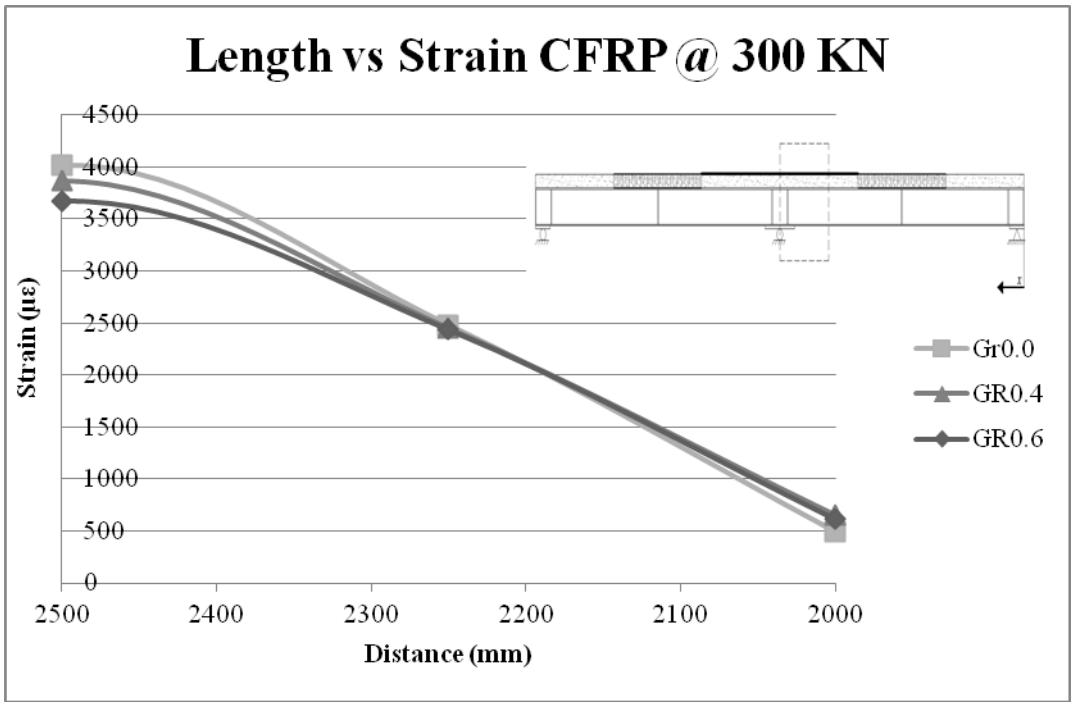

Figure 66: Length vs. Strain CFRP @ 300 KN

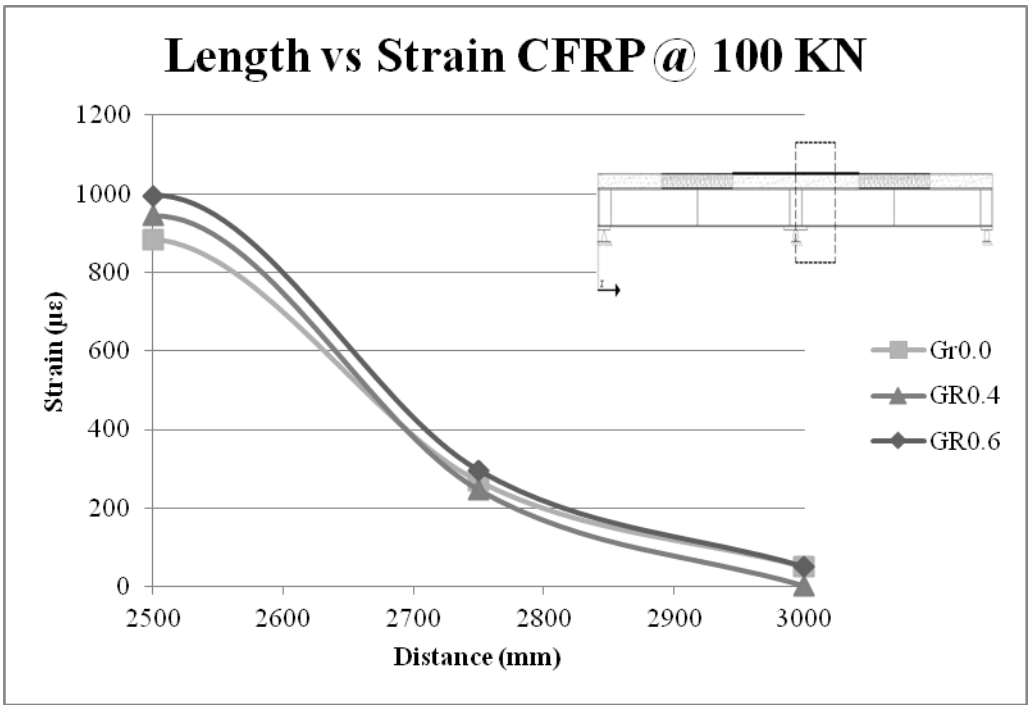

Figure 67: Length vs. Strain CFRP @ 100 KN

4.7 SUMMARY OF RESULTS

This section summarizes the experimental testing results. Table 15 contains the summary of testing results for the girders. It contains the yielding and ultimate load with the associated deflection and failure mode. The table also includes the CFRP strain at yield and at ultimate load.

Table 15: Summary of test results

Beam	Crack load	At Yield			At Ultimate			Failure mode
		Load	deflection	CFRP Strain	Load	deflection	CFRP Strain	
	KN	KN	mm	με	KN	mm	με	
RFG	75	152	7.02	N/A	331.5	39.34	N/A	Concrete Crushing
GR0.0	150	171.5	5.039	1607	342	27.77	6112	CFRP Debonding
GR0.4	55	166	5.14	1434	328.5	26.12	5356	CFRP Debonding
GR0.6	40	154	5.8	1416	329.5	26.52	5400	CFRP Debonding

Table 16 presents a summary of the gain in strength and stiffness due to utilizing CFRP. The flexural stiffness is computed as the slope of the load deflection graph along the linear elastic part. The results showed that utilizing CFRP at the negative moment zone has improved the stiffness by 57.19%, 49.16% and 22.63% for girders GR0.0, GR0.4 and GR0.6, respectively. For the ultimate strength, there was no noticeable strength gain. That is due to failure by CFRP debonding. On the other hand, the yield capacity has increased by 12.83%, 9.21% and 1.32% for girders GR0.0, GR0.4 and GR0.6, respectively. This gain satisfies what with the proposed design guidelines for strengthening steel bridges with FRP materials. This is mainly essential from the design point of view as it can noticeably increase the service load margins.

Table 16: Summary of the comparison results

Beam	Pu/Py	Δu/Δy	Py/Py(RFG)	K=Py/Δy	K/K (RFG)	Pu/Pu(RFG)	Δy/Δy(RFG)	Δu/Δu(RFG)
			%	KN/mm	%	%	%	%
RFG	2.18	5.60	0.00	21.65	0.00	0.00	0.00	0.00
GR0.0	1.99	5.51	12.83	34.03	57.19	3.17	28.22	29.41
GR0.4	1.98	5.08	9.21	32.30	49.16	-0.90	26.78	33.60
GR0.6	2.14	4.57	1.32	26.55	22.63	-0.60	17.38	32.59

CHAPTER 5

ANALYTICAL ANALYSIS

5.1 GENERAL

This chapter presents the analytical analysis to predict the flexural strength and the behavior of distressed continuous composite girders strengthened with CFRP sheets. The results of the analysis will be verified using the experimental results. It is noted that this chapter discussion is limited to the flexural analysis of girders using bonded CFRP sheets at the top of concrete slab at the negative moment zone. Plastic analysis was used to determine the ultimate capacity of distressed continuous composite girders. Finally, a proposed method for retrofitting distressed continuous girders at the negative moment zone is presented. This method can be used by designers for strengthening deteriorated steel concrete composite girders.

5.2 INTRODUCTION TO PLASTIC ANALYSIS

Plastic analysis is considered to determine the ultimate load capacity of the whole structure. In the plastic analysis, the section capacity is found from the post yield strength of the steel. Using this method of analysis, economical sections are designed from weight point of view. That is because the required sections by this method are smaller comparing

to elastic design. Plastic analysis is mainly used to analyze and design statically indeterminate structures. By using this method the chosen section should achieve its plastic moment capacity. Then it undergoes a significant rotation maintaining its plastic moment. In the plastic analysis, the collapse mechanism occurs when all possible plastic hinges are formed. In this study the plastic analysis is conducted using the virtual work method. The plastic moment capacity is calculated using strain compatibility approach.

5.2.1 ASSUMPTIONS

Assumption regarding the materials and the geometry of the structure are considered to achieve the full plastic capacity of the section. These assumptions are undertaken to simplify the analytical approach and develop the ultimate capacity of the girders.

5.2.1.1 Geometrical Assumptions

1. Width to thickness ratio of steel elements is controlled to prevent local buckling (compact sections).
2. Lateral torsional buckling is prevented by providing adequate lateral bracing.
3. Concentrated forces problems are prevented by using proper stiffeners and bearing plates.
4. Sections remain plane after deformation.

5.2.1.2 Material Assumptions

1. The tensile strength of concrete slab is neglected ($\sigma_{ct}=0$).

2. The compressive capacity of concrete is given as 0.85f'c. Concrete stress strain behavior is assumed to follow a second degree parabola that fits the compressive behavior of concrete test.
3. Steel is considered as an elastic-perfectly plastic material.
4. CFRP have linear stress strain behavior.
5. Steel members behave in compressive as in tension and yield at F_y.
6. Full composite behavior between steel section and concrete slab, and between concrete slab and CFRP sheet (zero slip between the materials)

5.2.2 PLASTIC ANALYSIS FUNDAMENTAL CONDITIONS

1. Mechanism condition: The ultimate load is attained when all possible plastic hinges are formed. The number of plastic hinges developed should be just sufficient to form a mechanism.
2. Equilibrium condition : $\sum F_x = 0, \sum F_y = 0, \sum M_{xy} = 0$
3. Plastic moment condition: bending moment at any location should not be more than the full plastic moment of the section.

5.2.3 VIRTUAL WORK METHOD

This method is also named the energy method. The required plastic load of a structure is found using the principle of virtual work. It is assumed that the structure remains rigid between supports and plastic hinges. The plastic deformations at failure load are considered larger than elastic deformations. All plastic rotations take place at the plastic

hinges. The entire energy is absorbed by the plastic hinge rotation while the rest of the beam will remain undeformed.

5.2.4 STRAIN COMPATIBILITY APPROACH

This approach allows using reasonable strain stress constitutive models for steel and concrete. In order to calculate the moment capacity of the section, the strain at the top fiber is assumed. This project considered three cases:

Case 1. At the positive moment zone: the compressive strain in at the top concrete fiber is assumed.

Case 2. At the negative moment zone without CFRP: the tensile strain in steel reinforcement is assumed.

Case 3. At the negative moment zone with CFRP: the tensile strain in CFRP is assumed.

The cross section of the composite girder is divided into horizontal layers as shown in Figure 68. It is noted that steel reinforcement in compression is ignored. After establishing these layers and assuming the top fiber strain, then the strain at each layer can be determined using similarity of triangles as shown in Equation 7.

$$\varepsilon_i = \left(\frac{d_i}{c} - 1\right) \times \varepsilon_{top} \qquad \text{Equation 7}$$

Where:

- ε_i is the strain in the element
- d_i the distance from the element to the fiber with assumed strain
- ε_{top} the assumed strain

- *c* the depth of the natural axis from top of concrete

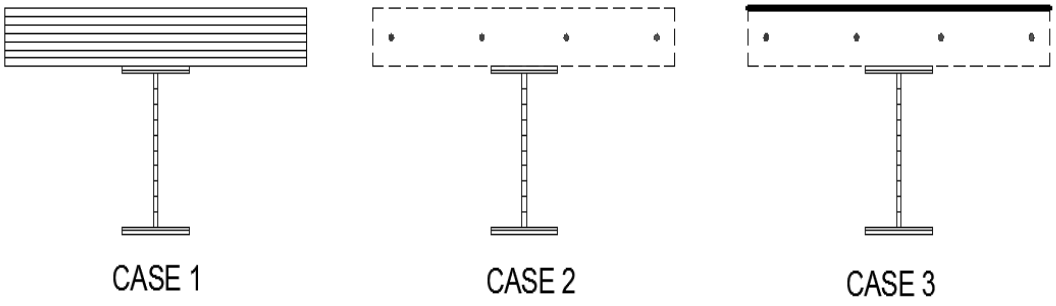

Figure 68: Cross sections of the composite girder

The stress integration and the internal forces of the cross section are determined using the following summation:

$$\Sigma F = \Sigma_{concrete}(\sigma_{ci}A_{ci}) + \Sigma_{Steel\ Reinforcement}(\sigma_{SR}A_{SR}) + \Sigma_{CFRP}(\sigma_{CFRP}A_{CFRP}) + \Sigma_{Steel}(\sigma_S A_S) \quad \textbf{Equation 8}$$

Where:

- σ_{ci}, σ_{SR}, σ_{CFRP} and σ_S are the stresses of concrete, steel reinforcement, CFRP and structural steel elements, respectively. These stresses are determined using Equations 10 to 12.
- A_{ci}, A_{SR}, A_{CFRP} and A_S are the cross section areas of concrete, steel reinforcement, CFRP and structural steel elements, respectively.

An iterative approach is conducted to determine the depth of the natural axis (*c*) until force equilibrium is satisfied (thus $\Sigma F=0$). The moment capacity is then determined for

the cross section by summation of the bending moments of the element forces about the top fiber as shown in Equation 9.

$$M = \Sigma_{concrete}(\sigma_{ci}A_{ci}d_i) + \Sigma_{Steel\ Reinforcement}(\sigma_{SR}A_{SR}d_i) + \Sigma_{CFRP}(\sigma_{CFRP}A_{CFRP}d_i) + \Sigma_{Steel}(\sigma_S A_S d_i) \quad \text{Equation 9}$$

The obtained moment capacity of the section will be used in the plastic analysis to determine the ultimate load.

5.3 MATERIAL CONSTITUTIVE MODELS

5.3.1 CONCRETE

Concrete is assumed to follow a second degree polynomial. Equation 10 defines the stress in the concrete element as a function of strain at that element. This model was obtained by fitting the stress strain curve of the concrete compressive test from the experimental part as shown in Figure 69.

$$\sigma_c = -372313.84 * \varepsilon_c^2 + 19818.24 * \varepsilon_c + 2.25 \quad \text{Equation 10}$$

Where:

- σ_c is the compressive stress in concrete
- ε_c is the compressive strain in concrete

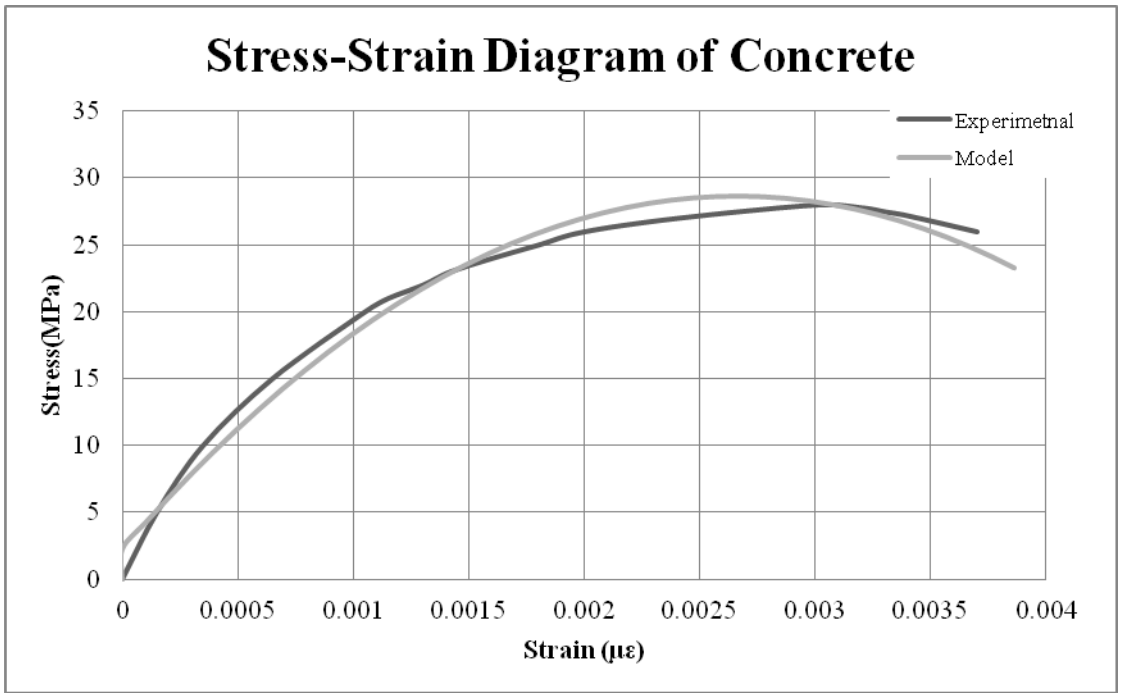

Figure 69: Stress-Strain diagram of concrete model

5.3.2 STEEL ELEMENTS

Steel is assumed to follow elastic-perfect plastic behavior in the analytical analysis. Equation 11 defines the stress in the steel element as a function of strain at that element.

$$\sigma_S = \begin{cases} E_S \varepsilon_S & \text{if } \varepsilon_S \leq \varepsilon_Y \\ F_Y & \text{if } \varepsilon_S > \varepsilon_Y \end{cases} \qquad \text{Equation 11}$$

Where:

- σ_S is the stress in the steel
- ε_S is the strain in the steel element
- E_S equals 205 GPa
- F_Y equals 430 MPa for steel reinforcement and 275 MPa for structural steel
- ε_Y is yield strain for steel:

- for steel reinforcement it equals 0.0021 mm/mm
- for structural steel it equals 0.00135 mm/mm

5.3.3 CFRP MATERIAL

CFRP follows linear elastic behavior. Equation 12 defines the stress in the CFRP sheet as a function of its strain.

$$\sigma_{CFRP} = E_{CFRP} \times \varepsilon_{CFRP}$$ Equation 12

Where:

- σ_{CFRP} is the stress in the CFRP
- E_{CFRP} equals 230.5 GPa
- ε_{CFRP} is the strain in CFRP

5.4 CALCULATION OF MOMENT CAPACITY

To determine the moment capacity of the composite girder section the strain compatibility approach is used. Three cases are considered in the analysis as shown in section 5.2.4 in page 82. The assumed strain in the top fiber is taken from the experimental results at failure of each girder. For case 1 at the positive moment zone, the assumed top strain at the top fiber is the crushing strain of concrete 0.0035 mm/mm for all girders. For case 2 at the negative moment zone, from girder RFG, the strain in the steel reinforcement at failure was .01 mm/mm. this value of strain will be considered for case 2. For case 3, since three girders are retrofitted, each girder will be analyzed for the maximum strain found in the CFRP. For girder GR0.0 the maximum strain reached 40%

of the CFRP ultimate strain. For the distressed girders GR0.4 and GR0.6, the maximum strain reached by CFRP sheet was 36% of the CFRP ultimate strain. Table 17 shows the strains at the top fiber element for each girder.

Table 17: Top fiber strain for each case

Case	Applicable For girder	Top fiber element	Assumed Strain at top fiber (με)
1	All girders	Concrete	3500
2	RFG	Steel Reinforcement	10000
3	GR0.0	CFRP	6100
	GR0.4	CFRP	5400
	GR0.6	CFRP	5400

5.4.1 CASE 1 AT THE POSITIVE MOMENT ZONE

The plastic moment capacity is determined at the positive moment zone by assuming a strain of 0.0035 mm/mm in the top concrete element as shown in Figure 70. Then the natural axis depth (c) is iterated till Equation 9 is satisfied.

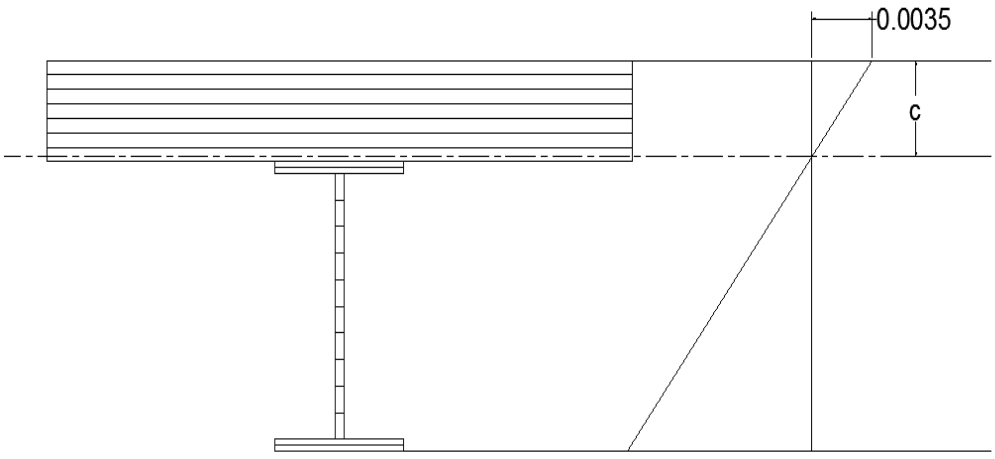

Figure 70: Strain distribution at positive moment section

From the analysis the value of c was found to be 67.6 mm from the top of concrete. The obtained moment capacity was 114.2 KN.m at mid span. The location of the natural axis was within the concrete slab. The internal forces and strain distribution along the depth of the section are plotted in Figure 71. It is visible that the section became fully plastic the instant of concrete crushing.

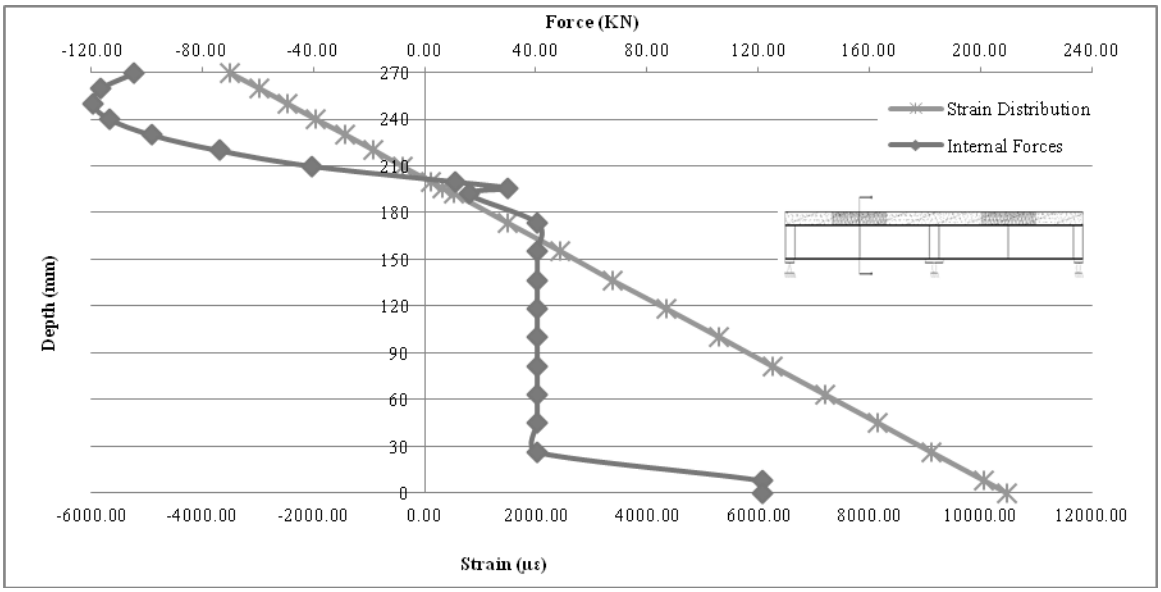

Figure 71: Section strain distribution and internal forces at positive moment zone

5.4.2 CASE 2 AT THE NEGATIVE MOMENT ZONE WITHOUT CFRP

The plastic moment capacity is determined at the negative moment zone by assuming a strain of 0.01 mm/mm in the steel reinforcement as shown in Figure 72. Then the natural axis depth (c) is iterated till Equation 9 is satisfied.

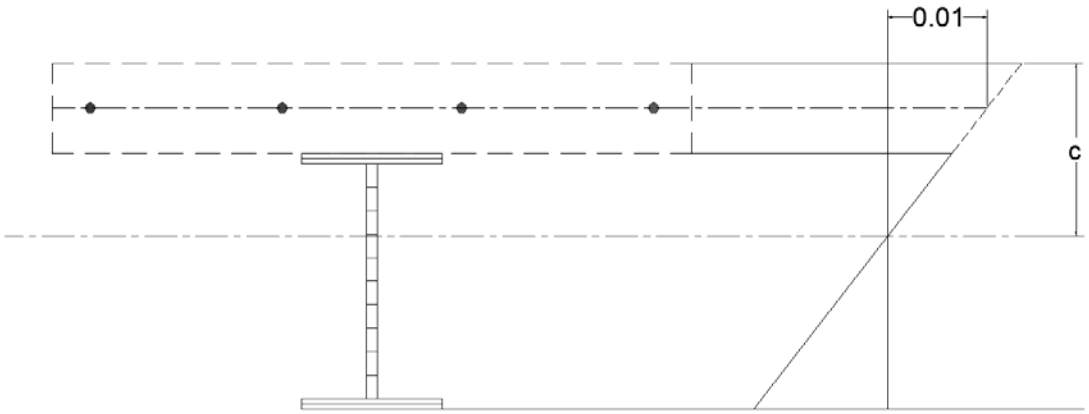

Figure 72: Strain distribution at negative moment section whithout CFRP

From the analysis the value of c was found to be 150.8 mm from the top of concrete. The obtained moment capacity was 76.3 KN.m at the interior support zone. The location of the natural axis was within the web of the steel section. The internal forces and strain distribution along the depth of the section are plotted in Figure 73. It is visible that the section became fully plastic.

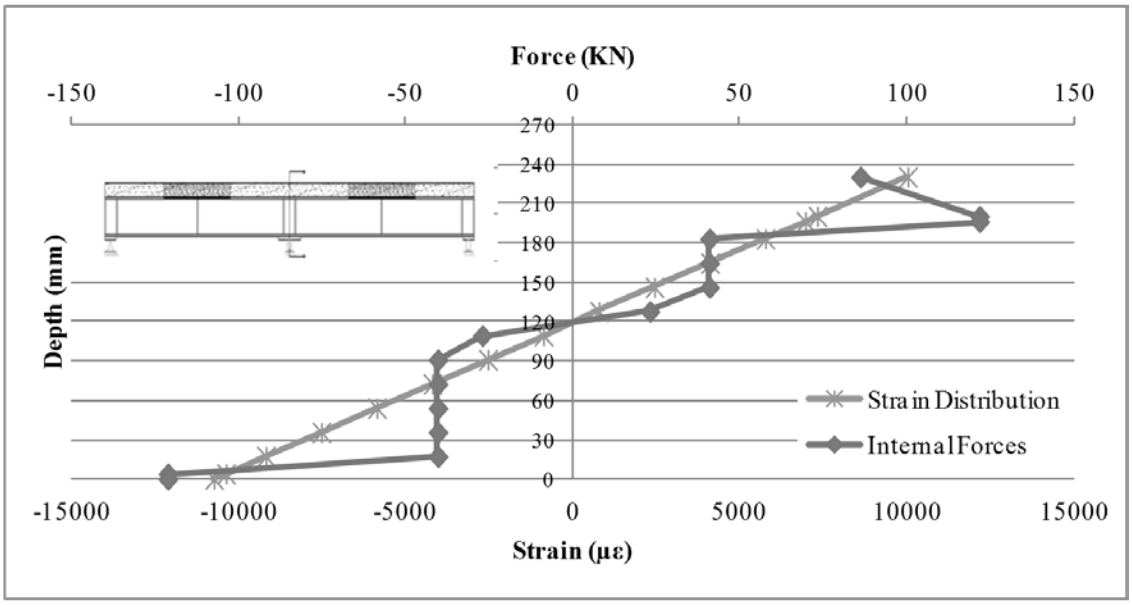

Figure 73: Section strain distribution and internal forces at negative moment zone without CFRP

5.4.3 CASE 3 AT THE NEGATIVE MOMENT ZONE WITH CFRP

The plastic moment capacity is determined at the negative moment zone by assuming the strain in the CFRP for the non distressed girder GR0.0 as shown in Figure 74. For the distressed girders GR0.4 and GR0.6, the assumed strain is shown in Figure 75. Then the natural axis depth (c) is iterated till Equation 9 is satisfied.

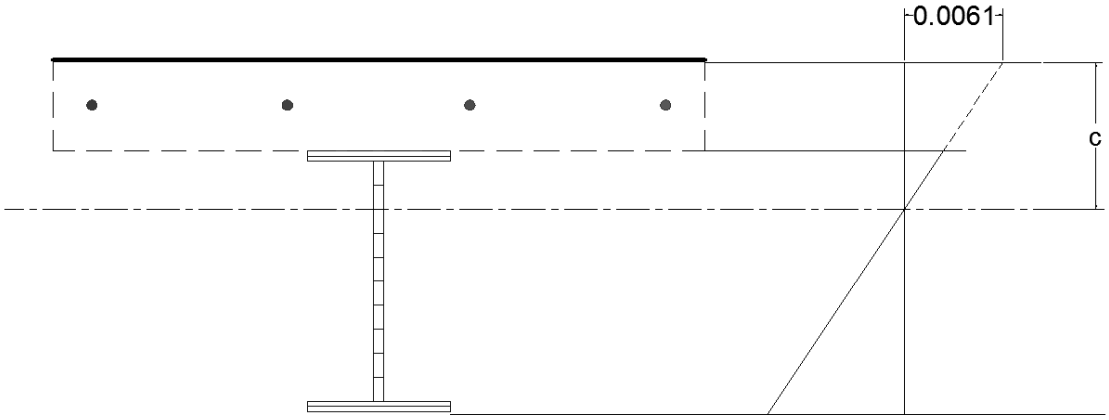

Figure 74: Strain distribution at negative moment section with CFRP for GR0.0

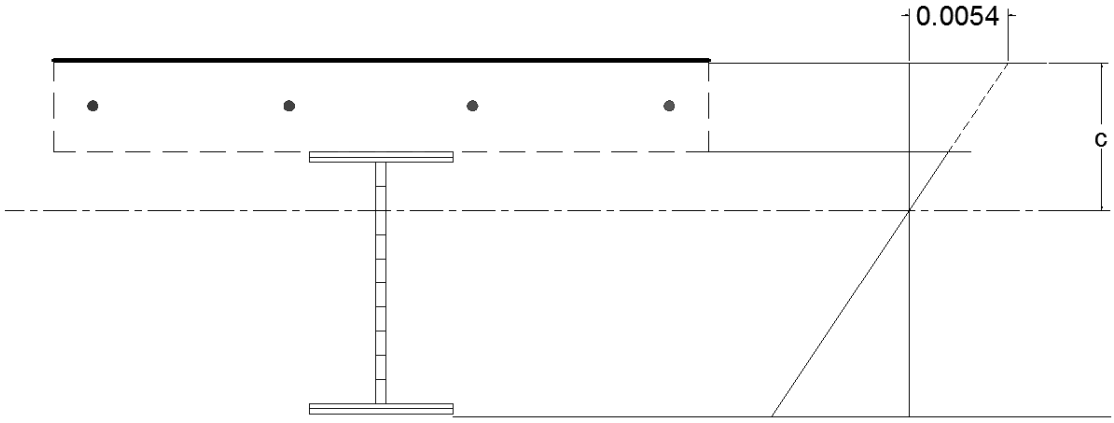

Figure 75: Strain distribution at negative moment section with CFRP for the distressed girders

From the analysis the value of c was found to be 108.4 mm from the top of concrete for girder GR0.0. For the distressed girders the depth was found to be 113.9 mm. The obtained moment capacity was 99.5 KN.m at the interior support zone for girder GR0.0. For the distressed girders the moment capacity was 97.1 KN.m at the interior support zone. The location of the natural axis was within the web of the steel section. The internal forces and strain distribution along the depth of the section are plotted in Figure 76. It is visible that the sections for both cases became fully plastic.

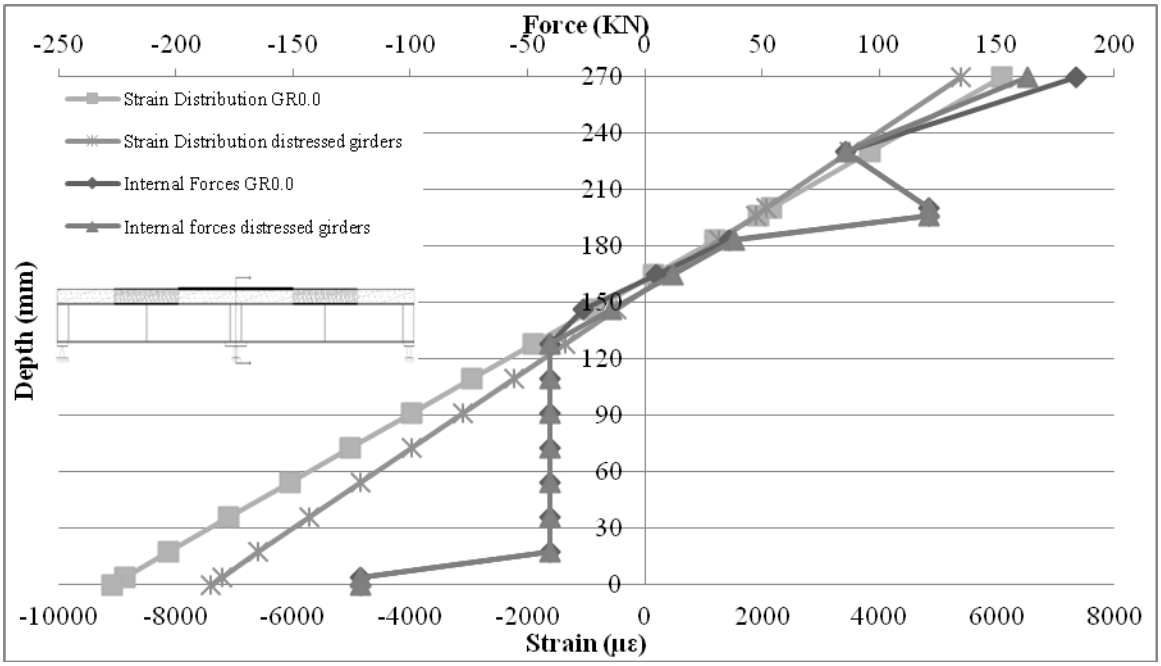

Figure 76: Section strain distribution and internal forces at negative moment zone with CFRP

5.5 PLASTIC ANALYSIS

Assuming that capacity of section at mid span is α Mp (Mp is the plastic moment) and at the interior support is Mp as shown in Figure 77. Then the ultimate load at plastic moment can be calculated as follows:

$$\Delta W = \Delta E \quad \text{Equation 13}$$

$$P \times \frac{L}{2} \times \theta = \alpha Mp(2\theta) + Mp(\theta) \quad \text{Equation 14}$$

$$P = \frac{2(2\alpha + 1)}{L} \times M_p \quad \text{Equation 15}$$

Where:

$$\alpha = \frac{M_{+zone}}{M_{-zone}} \quad \text{Equation 16}$$

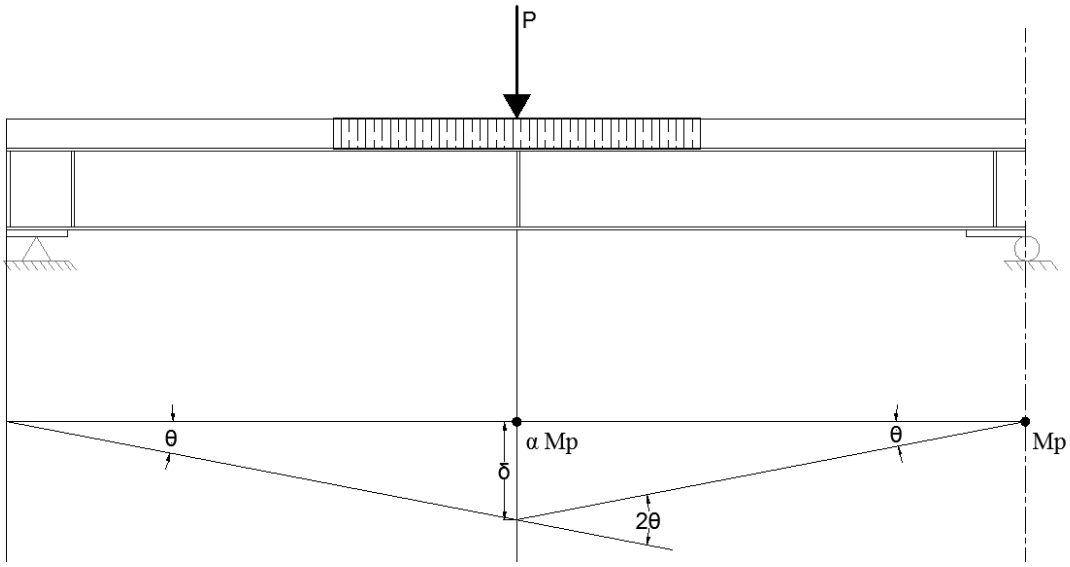

Figure 77: Plastic moment diagram

Equation 15 is used to determine the ultimate load for each girder.

Table 18: Plastic ultimate loads of the girders

Girder	Mp (KN.m)	α Mp (KN.m)	α	P_{UP} (KN)	% increase	P_{UT} (KN)	P_{UP} / P_{UT} (%)
RFG	76.3	114.2	1.50	243.76	0	331.5	74
GR0.0	99.5	114.2	1.15	262.32	8	342	77
GR0.4	97.1	114.2	1.18	260.4	7	328.5	79
GR0.6	97.1	114.2	1.18	260.4	7	329.5	79

Where: P_{UP} is analytical plastic ultimate load and P_{UT} is experimental testing ultimate load

The results of the analytical analysis gave conservative values of ultimate load comparing to the experimental testing. In the experimental testing, steel strain hardening, caused increase in strength leading to a higher ultimate load. The analytical study, steel elements were assumed to have elastic-perfect plastic behavior.

5.6 SIMPLIFIED DESIGN METHODOLOGY

The aim of this methodology is to provide engineers with a simple approach to strengthen distressed composite girders utilizing CFRP. This proposed method provides conservative limits for the deteriorated continuous composite girders.

From the experimental results, CFRP sheets utilized 35% of their ultimate capacity to strengthen distressed continuous composite girders. This limit will be used as the ultimate strength for CFRP sheets in order to design for strengthening distressed continuous composite girders. This limit will be used to avoid CFRP sheet debonding failure. This simplified methodology gives the appropriate thickness of the CFRP to be installed in the concrete slab at the negative moment zone.

Note that this methodology is applicable for distressed composite girder where distressing didn’t cause plastic deformations in the steel members upon unloading. It is noted that this method illustrate the flexural design of girders using bonded CFRP sheets at the top of concrete slab at the negative moment zone.

After satisfying the previous conditions, the following steps shall be taken to design for strengthening continuous composite girders with CFRP at the negative moment zone:

1. Evaluate the capacity of the existing distressed continuous composite girder. Plastic analysis can be used to determine the ultimate load capacity of the girder. The

plastic moment analysis of the girder is shown in Figure 77. The capacity of mid span and interior support zones shall be determined using plastic stress distribution or strain compatibility approach as described in section 5.2.4. An iterative approach is conducted to determine the depth of the natural axis (*c*) until force equilibrium is satisfied (thus $\Sigma F=0$). As follows:

$$\Sigma F = 0.85\, f_c' a\, b + F_{YSR}\, A_{SR} + F_{YS}\, A_S \qquad \text{Equation 17}$$

$$\alpha\, M_p = M_{+\text{zone}} = 0.85\, f'_c\, a\, b\, d_c + F_{YS}\, A_S\, d_S \qquad \text{Equation 18}$$

$$M_p = M_{-\text{zone}} = F_{YSR}\, A_{SR}\, d_{SR} + F_{YS}\, A_S\, d_S \qquad \text{Equation 19}$$

$$P_{UE} \times \frac{L}{2} \times \theta = \alpha Mp(2\theta) + Mp(\theta) \qquad \text{Equation 20}$$

$$P_{UE} = \frac{2(2\alpha + 1)}{L} \times M_p \qquad \text{Equation 21}$$

Where:

$$\alpha = \frac{M_{+zone}}{M_{-zone}} \qquad \text{Equation 22}$$

- d_i the distance from the centroid of the element to the natural axis *c*
- *b* the width of concrete slab
- P_{UE} is the existing ultimate load
- $A_{SR,}$ *and* A_S are the cross section areas of concrete, steel reinforcement, CFRP and structural steel elements, respectively.

2. The increase in strength capacity of the girder (*h* %) is determined based on the new loading requirements. Determine the ultimate load (P_{UR}) of the continuous girder as follow:

$$P_{UR} = P_{UE} \times (1 + h\%) \qquad \text{Equation 23}$$

Where: P_{UR} and P_{UE} are the ultimate load after repair and existing ultimate load, respectively.

3. CFRP increases the negative moment capacity and thus changes the value of α. The new value of α' can be determined. Then the required moment capacity at the negative moment zone ($M'_{-zone} = M_p$) can be calculated as follow:

$$\alpha' = \frac{2\ M_{+zone}}{P_{UR}\ l - 4\ M_{+zone}} \quad \text{Equation 24}$$

$$M'_{-zone} = \frac{M_{+zone}}{\alpha'} \quad \text{Equation 25}$$

4. The required cross section area of CFRP can be found by utilizing 35% of the CFRP strength. This value is based on the experimental and analytical results.

$$A_{CFRP} = \frac{M'_{-\text{zone}} - F_{YSR}\ A_{SR}\ d_{SR} - F_{YS}\ A_S\ d_S}{0.35\ \sigma_{uCFRP}\ \ d_{CFRP}} \quad \text{Equation 26}$$

$$\Sigma F = F_{YSR}\ A_{SR} + F_{YS}\ A_S\ + 0.35\ \sigma_{uCFRP}\ A_{CFRP} \quad \text{Equation 27}$$

This is an iterative method were the natural axis depth is assumed (c). Then the required area of CFRP is calculated using Equation 26. Finally, the equilibrium of internal forces is checked.

5. The width of the CFRP sheet is chosen based on the available products in the market. Regarding the width, it shall not be taken more than the concrete slab effective width. The thickness is then determined. The sheet length shall be the length of the negative moment zone plus the cutoff length of the sheet from both sides.

6. Surface preparation prior adhesion of the sheets shall satisfy with ACI 546R (ACI-546R 2004).

5.6.1 SOLVED EXAMPLE USING THE SIMPLIFIED DESIGN METHOD

In this example, a two span composite bridge is to be retrofitted using CFRP. The elevation and cross section are shown in Figures 78 and 79, respectively. The material properties and shown in Table 19. The girder shall retrofitted and to increase its capacity by 6% to meet the new loading requirements. The design will determine the required thickness of CFRP sheets to achieve the new requirement. The available CFRP products are shown in Table 20.

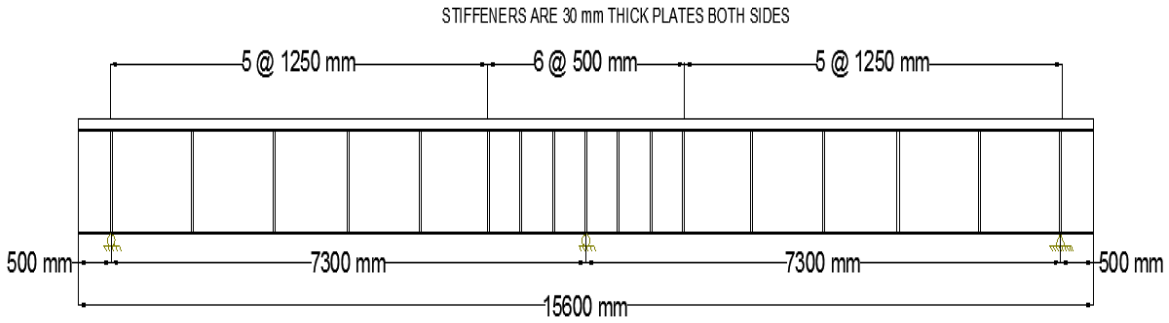

Figure 78: Elevation of the girder

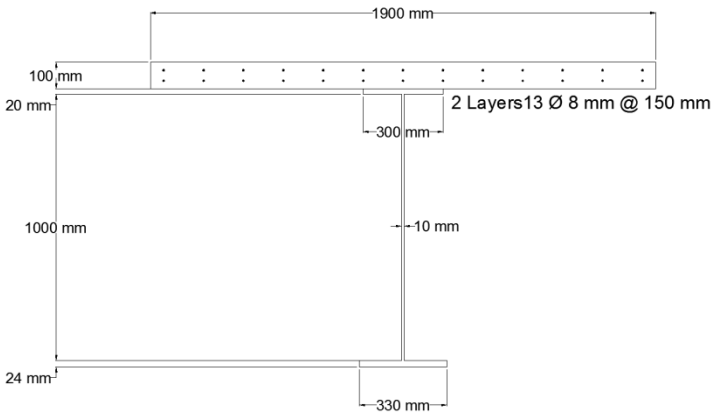

Figure 79: Cross section of the girder

Table 19: Material properties

Material	Property	
Concrete	f'c (MPa)	40
	ε_{uc} (mm/mm)	0.0035
Structural Steel	F_{ys} (MPa)	248
	E_s (GPa)	205
Steel Reinforcement	F_{ysr} (MPa)	420
	E_s (GPa)	205
CFRP	f_{uCFRP} (MPa)	3460
	E_{CFRP} (GPa)	230.5
	ε_{uCFRP} (mm/mm)	0.015

Table 20: Available CFRP products

Grade	FRC 200	FRC 230	FRC 300	FRC 530
Fiber Area Weight (g/m^2)	200	230	300	530
Design thickness (mm)	0.111	0.131	0.167	0.293

the design steps are illustrated in Table 21.

Table 21: Example solution steps

Step	Comment	Procedure
1	Check section is compact	$\frac{b_f}{t_f} = \frac{150}{24} = 6.25 < 0.38\sqrt{\frac{205000}{248}} = 10.92\ OK\ \frac{b_w}{t_w} = \frac{1000}{10}$ $= 100 < 3.76\sqrt{\frac{205000}{248}} = 108.1\ OK$
	Find M_{+zone}	$M_{+zone} = 0.85\ f'_c\ a\ b\ d_c + F_{YS}\ A_S\ d_S = 3977.2\ KN.m$
	Find M_{-zone}	$M_{-zone} = F_{YSR}\ A_{SR}\ d_{SR} + F_{YS}\ A_S\ d_S = 2969.8\ KN.m$

	Find α	$\alpha = \frac{M_{+zone}}{M_{-zone}} = \frac{3977.2}{2969.8} = 1.34$
	Find P_{UE}	$P_{UE} = \frac{2(2\alpha + 1)}{7.3} \times M_p = \frac{2(2 \times 1.34 + 1)}{7.3} \times 2969.8 = 2993\ KN$
2	Find P_{UR}	$P_{UR} = 2993 \times (1 + 6\%) = 3172.6\ KN$
3	Find α’	$\alpha' = \frac{2 \times 3977.2}{3172.6 \times 7.3\ - 4 \times 3977.2} = 1.09$
	Find M'_{-zone}	$M'_{-zone} = \frac{3977.2}{1.09} = 3615.6\ KN.m$
4	Trail 1 Assume c=300mm	$A_{CFRP} = \frac{3615.6 - 610.3 - 1418.02}{0.35 \times 3460 \times 1144} = 1145.7\ mm^2$
		$\Sigma F = 558 + 1386.5 - 1981.67 = -37.17\ KN\ \neq 0$
	By iteration the depth of the natural axis c was found to be 332.9 mm	
	c=332.9 mm	$A_{CFRP} = \frac{3615.6 - 610.34 - 1526.06}{0.35 \times 3460 \times 1144} = 1067.7\ mm^2$
		$\Sigma F = 558 + 1286.6 - 1844.54 = 0.06\ KN\ \approx 0$
5	Find thickness of CFRP t_{CFRP}	$t_{CFRP} = \frac{1067.7}{1900} = 0.562\ mm$
	Based on the available products, 2 layers of FRC 530 will be used. total thickness of the CFRP sheets equals t_{CFRP}=2 x 0.293 =0.586 mm → A_{CFRP} = 1113.4 mm^2	
Check		
	Find M_{+zone}	$M_{+zone} = 0.85\ f'_c\ a\ b\ d_c + F_{YS}\ A_S\ d_S = 3977.2\ KN.m$
	Find M_{-zone}	$M_{-zone} = F_{YSR}\ A_{SR}\ d_{SR} + F_{YS}\ A_S\ d_S + 0.35\ \sigma_{uCFRP}\ A_{CFRP} = 3628.8\ KN.m$

	Find α	$\alpha = \frac{M_{+zone}}{M_{-zone}} = \frac{3977.2}{3628.8} = 1.1$
	Find P_{UR}	$P_{UR} = \frac{2(2\alpha + 1)}{7.3} \times M_p = \frac{2(2 \times 1.1 + 1)}{7.3} \times 3628.8 = 3173.5\ KN$
		$\frac{P_{UR}}{P_{UE}} = \frac{3173.5}{2992.95} = 1.0603 \rightarrow 6.03\%\ increase\ OK$
6	Surface preparation prior adhesion of the sheets shall satisfy with ACI 546R	

The length of the sheet shall be along the negative moment zone plus the cutoff distance. To determine the cutoff points for the two layers:

- development length is found using Equation 28

$$l_{dCFRP} = \sqrt{\frac{t_{CFRP} E_{CFRP}}{\sqrt{f_c'}}} = \sqrt{\frac{0.586 \times 230500}{\sqrt{40}}} = 146\ mm \qquad \text{Equation 28}$$

Where: l_{dCFRP} is the development length of the CFRP

l_{dCFRP} shall taken to be 150 mm

- Since two layers are applied, the first layer shall extend by 150 mm than second layer.

The length of the negative moment zone is 3600 mm. From the previous points, the length of the first layer shall be 4200 mm and the length of the second layer shall be 3900 mm. Figure 80 shows a shcematic diagram of the retroffited girder.

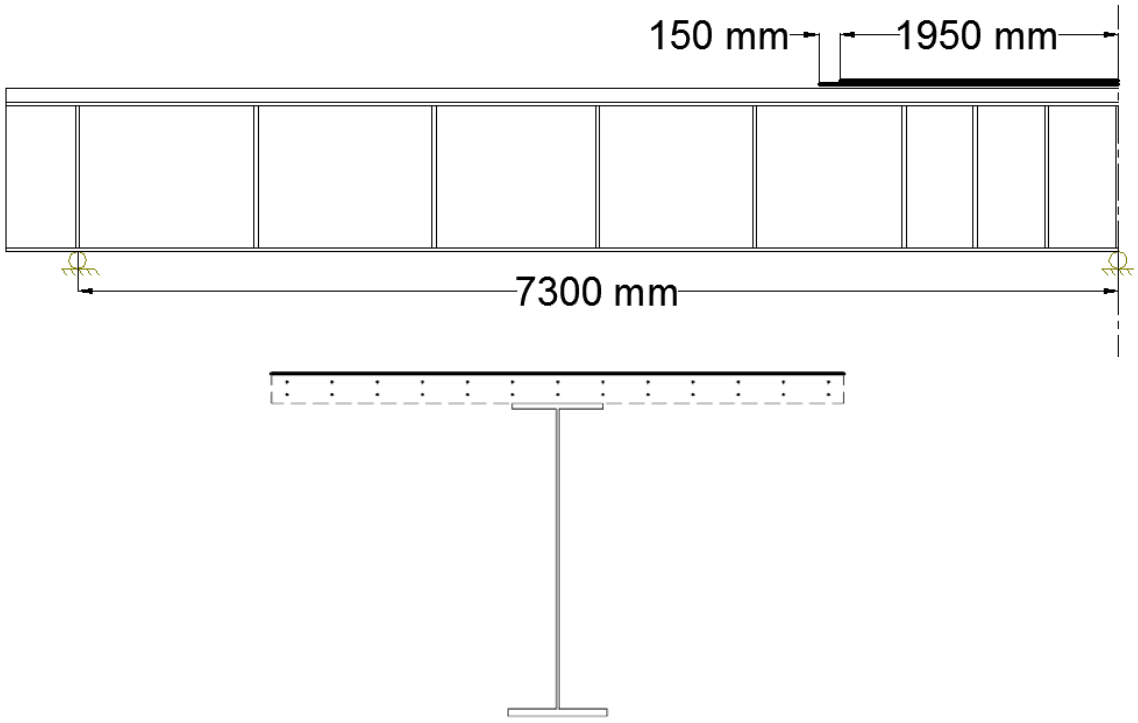

Figure 80: Elevation and cross section at interior support zone of the retrofitted girder

CHAPTER 6

CONCLUSIONS AND FUTURE WORK

6.1 CONCLUSIONS

- Composite girders are commonly used for long span structures such as in bridges. It is highly efficient structure due to utilizing the properties of the materials. Concrete is used for it high compressive strength and stiffness. Structural steel is utilized because of high tensile strength.
- In continuous composite girders, concrete will be under tensile stresses in the negative moment zone. This reduces the efficiency of the structure and causes cracks in the concrete slab. Steel reinforcement and steel section act compositely at the negative moment zone.
- Deterioration of the girders can affect its behavior and reduce it capacity. New rehabilitation techniques are required for restoring and increasing the stuffiness of continuous composite girders.
- The aim of this project was to evaluate distressed composite girder strengthened with CFRP sheet at the negative moment zone. Experimental and analytical approaches were used to achieve the objectives of this project.
- For experimental results, four girders were tested to determine the ability of CFRP to restore the capacity of the distressed girders. Two out of the four girders

were distressed to 40% and 60% of the ultimate load. CFRP showed improvements in the behavior of the continuous composite girders. Increase of both strength and stiffness were achieved. The yield capacity of the distressed girders increased up to 9%. Whereas stiffness have increased up to 50% compared to non-strengthened girder.

- Two failure modes developed in the study. The first was crushing of concrete at the positive moment zone. The other was CFRP debonding at the negative moment zone. The deboning occurred because the interface stress between the CFRP sheet and the concrete reached the critical stress value.
- The analytical approach was based on the plastic analysis – virtual work method. Strain compatibility approach was used to determine the section capacity. At the positive moment section capacity was determined by choosing the crushing strain of concrete at the top fiber. For the negative moment capacity to the top fiber strain was based on the experimental findings. CFRP sheet utilized 35% of its ultimate capacity. This limit was chosen to avoid CFRP debonding.
- Simplified design approach was presented for retrofitting of continuous composite girders at the negative moment zone. The approach was based on the experimental and analytical results. This design approach aimed to give a conservative load capacity for the distressed composite girders.
- A solved example for retrofitting two span continuous composite girder with CFRP was given to illustrate of the simplified design method.

6.2 FUTURE WORK

The following suggestions are proposed for future work as an extension of this study:

1. Study of cyclic behavior of distressed continuous composite girders after retrofitting with CFRP.
2. Finite element modeling of distressed continuous composite girders retrofitted with CFRP at the negative moment zone.
3. To study the behavior of the girder with prestressing the CFRP plates in the negative moment zone.

APPENDIX

CONTINUOUS COMPOSITE GIRDER DESIGN

From chapter 3, composite girder was designed based on the following criteria in order to satisfy the project objectives

7. Flexural failure is the required failure at ultimate load.
8. Shear failure prevented using proper thickness of web.
9. Plates local buckling prevented using proper length/thickness ratio.
10. Lateral torsional buckling prevented using proper cross section and lateral support over the interior support.
11. The expected ultimate capacity of the continuous composite beams with CFRP over the negative moment region should not exceed the ultimate capacity of Lab facilities (Loading cells, Loading Jack, Frame).

Composite girder was designed using concrete with a compressive strength of 28MPa, and yield strength of steel section is F_{ys}=248MPa (Gr. 36), whereas the yield strength of steel reinforcement is F_{ySR}=420MPa.

The composite girder geometry was controlled by the laboratory frame dimensions. Composite beams designed as two spans of 2500 millimeters, such that full length is 5000 millimeters, and a full depth of 270 millimeters, see Figure 81.

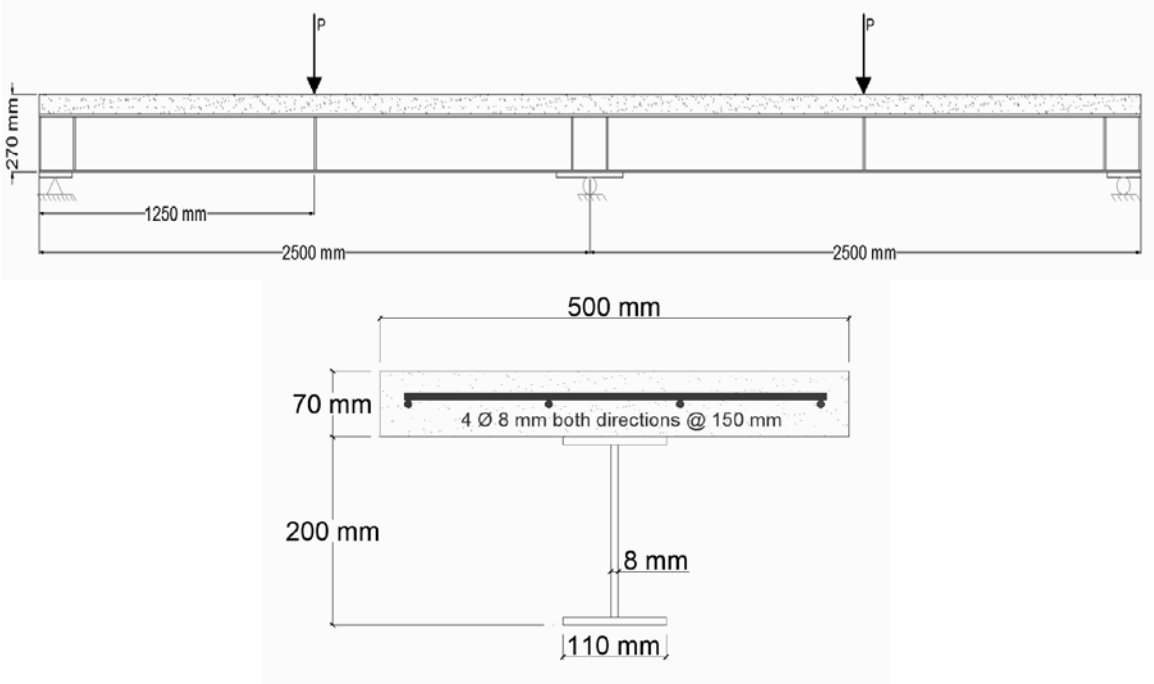

Figure 81: Composite girder geometry

Based on the design criteria which mentioned above, the composite steel concrete designed as follow:

Area of steel reinforcement ($A_{S.R}$) =201mm^2

F_{ysr}=420MPa

Area of steel section (A_s) =3232mm^2

F_{ys}=248MPa

Capacity of section at +v moment (M_{+v})

Assume that the neutral axis (N.A) in the concrete slab, Figure 82 , then the depth of compression block (a) calculated as:

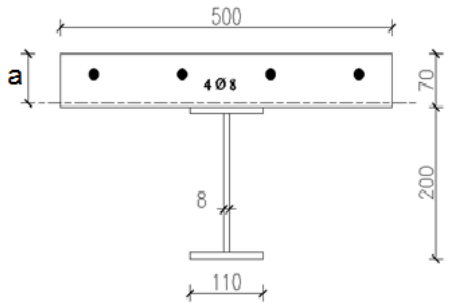

Figure 82: location of N.A. at positive moment section (mm)

$$0.85\, f'c * b * a + A_{SR} * F_{ysr} = A_S * F_{ys}$$

$$0.85\, f'c * 500\, a + 201 * 420 = 3232 * 248a = 60.3\, mm$$

$$M_{+v} = 0.85\ f'c \times b \times (0.5 \times a) + A_{SR} \times F_{ySR} \times d_{SR} + A_S \times F_{yS} \times d_S$$

$$M_{+v} = 0.85\ f'c \times 500 \times (0.5 \times 60.3) + 201 \times 420 \times (60.3 - 20) + 3232 \times 248$$

$$\times 105.7 M_{+v} = 92\ KN.m$$

Capacity of section at -v moment ($M\text{-}_v$)

In the negative moment section, concrete slab is neglected. Only steel reinforcement and steel section are considered in the calculations, Figure 83.

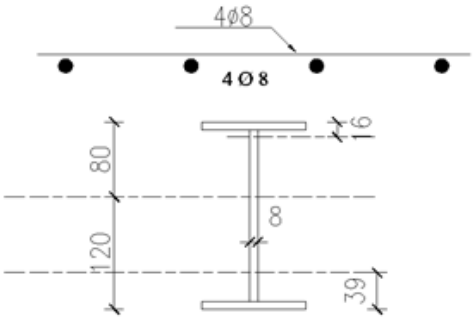

Figure 83: location of N.A. at negative moment section (mm)

$$M_{-v} = A_{SR} \times F_{ySR} \times d'_{SR} + A_{ST} \times F_{ySR} \times d'_{ST} + A_{SC} \times F_{ySR} \times d'_{SC}$$

$$M_{-v} = 201 \times 420 \times 130 + \left(110x8.0 + (72 \times 8.0)\right)64 \times 248$$

$$+ \left(110 \times 8.0 + (112 \times 8.0)\right)81 \times 248 M_{-v} = 70 \text{ KN. m}$$

Assuming that capacity of section at mid span is α Mp (Mp is the plastic moment) and over the interior support is Mp, then the ultimate load at plastic moment could be calculated as follows:

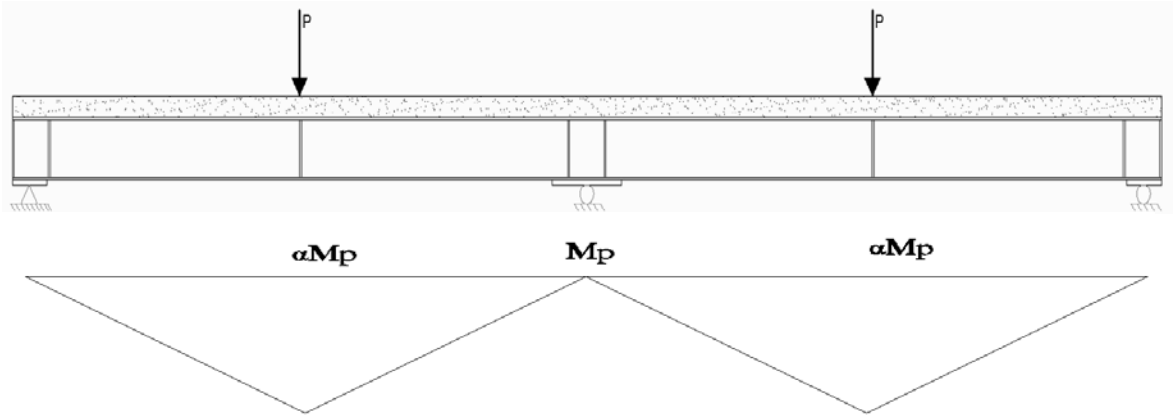

Figure 84: Plastic moment diagram

$$\alpha = \frac{M_{+v}}{M_{-v}} = 1.31$$

$$P = \frac{2(2\alpha+1)}{L} \times M_p = 205 \; KN \text{ (Expected ultimate load without CFRP)}$$

Shear studs design

The concrete slab designed to be fully composite with the steel section, so proper number of steel connectors (headed studs) was provided to ensure the composite action. Number of headed studs calculated as follows:

The N.A in the concrete slab, then

The compression strength of concrete slab (Cc) is

Cc =0.85x28x500x60.3/1000 =720KN

The compression strength of steel reinforcement (C_{SR}) is

C_{SR}=201x420/1000 = 85 KN

Total compression is C = Cc+ C_{SR} = 805 KN

Tension strength of steel section (T_s) is

T_s= 3232x248/1000 =805 KN

Shear stud should resist this load (805 KN)

For f'$_c$ =28 MPa, using of 50 mm long of 19.05 mm diameter headed studs

$$Q_n = 0.5xA_{stud}x\sqrt{f'_cE_c} = 0.5 * 283.4x\sqrt{28x25000} = 118.6\ KN$$

$$NO.of\ studs = \frac{805}{118} = 6.8\ stud\ \ ==>\ use\ 8\ studs$$

This means that 8 headed studs are needed between max moment points and zero moment based on the moment diagram. Figure 85 show headed studs in the girder.

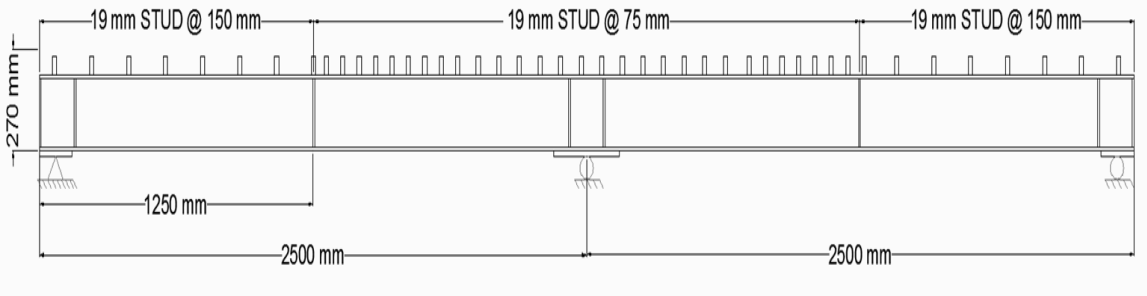

Figure 85: Steel studs

Check local buckling

$$\frac{110/2}{8} = 6.88\ \ < 0.38\sqrt{\frac{E}{Fy}} \qquad \text{OK}$$

$$\frac{184}{8} = 23\ \ < 2.5\sqrt{\frac{E}{Fy}} \qquad \text{OK}$$

Check Lateral Torsional Buckling

The first plastic hinge is going to be formed over the interior support which means that section should have enough rotational capacity. The maximum length for this beam to ensure the plastic moment with enough rotational capacity (Lpd) is

$Lpd = \left(0.12 + 0.076\frac{M1}{M2}\right)\frac{E}{Fy}\, ry$ = 2270 mm

M_{+v} is protected by slab

Only lateral support need at interior support

Welding of shear connectors

Shear connectors will be welded for the full capacity (12mm fillet weld E70)

Design of plates for concentrated force

Steel plates needed over supports and under the point load to prevent web local buckling and web crippling.

Web local buckling

$Rn = (5k + N)f_{rw}t_w$

$(5x0.3346 + N)36x\ 0.3346 = \frac{500}{4.45(1.5)}$ Assume P_{ult} = 450 KN

Use plates of N=150 mm and 20 mm thickness

Check Shear design

Shear diagram at ultimate plastic load is shown in Figure 86. The shear is assumed to be resisted by the web of the girder. The capacity of web to resist shear force (V_{steel}) calculated as follows

V_{steel}= 0.6x248x (8.0x200) = 238 KN > $V_{Ult.}$

$V_{Ult.\ (plastic)}$ = 250 KN

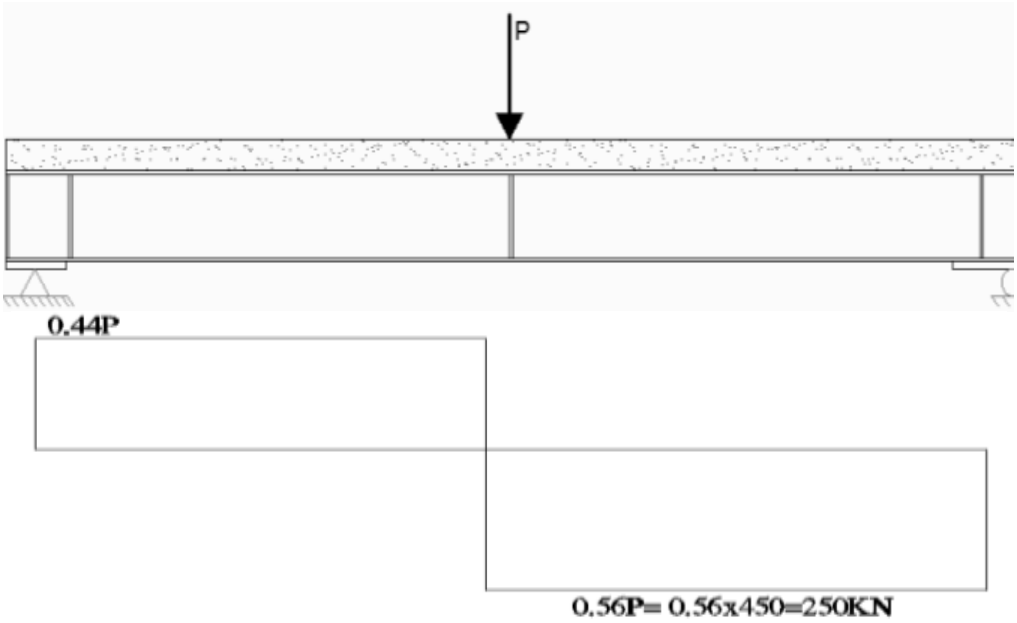

Figure 86: Shear diagram

Welding design for the fabricated girder

Since the steel beams designed as built up section, proper welding should be provided to prevent plate connection failure.

Plate thickness = 8 mm

AISC16.1.96: the maximum size of fillet weld edge of material > 6mm

Use 6mm fillet weld E70

$$\emptyset R_{nw} = 0.75\left(0.707\left(\frac{6}{2.54}\right)\right)0.6x70 = 5.26\frac{k}{in} = 922\ N/mm$$

Max capacity = 922x2x570/1000 =1345 KN

2 = sides of welding

570 mm= max length between zero and max moment

Max shear = 0.85x25x500x90 + 110x8.0x248 =976 KN OK

Note: Slab compression and stud tension whereas considered in same direction

Use 6mm E70 for full length

Design of stiffeners

Provide stiffeners of 8mm thickness under the point loads and over the interior supports as will show in the final drawings.

Check deflection for steel beam

$$\Delta = \frac{Pl^3}{48EI}$$

Max deflection assuming load of 1400 KN doesn't exceed three millimeters.

Flexural capacity = 1650 KN.m

Shear capacity = 1200 >800 KN OK

Continuous composite girder drawing

Figure 87 illustrates the final dimensions for the continuous composite girder to be prepared for testing.

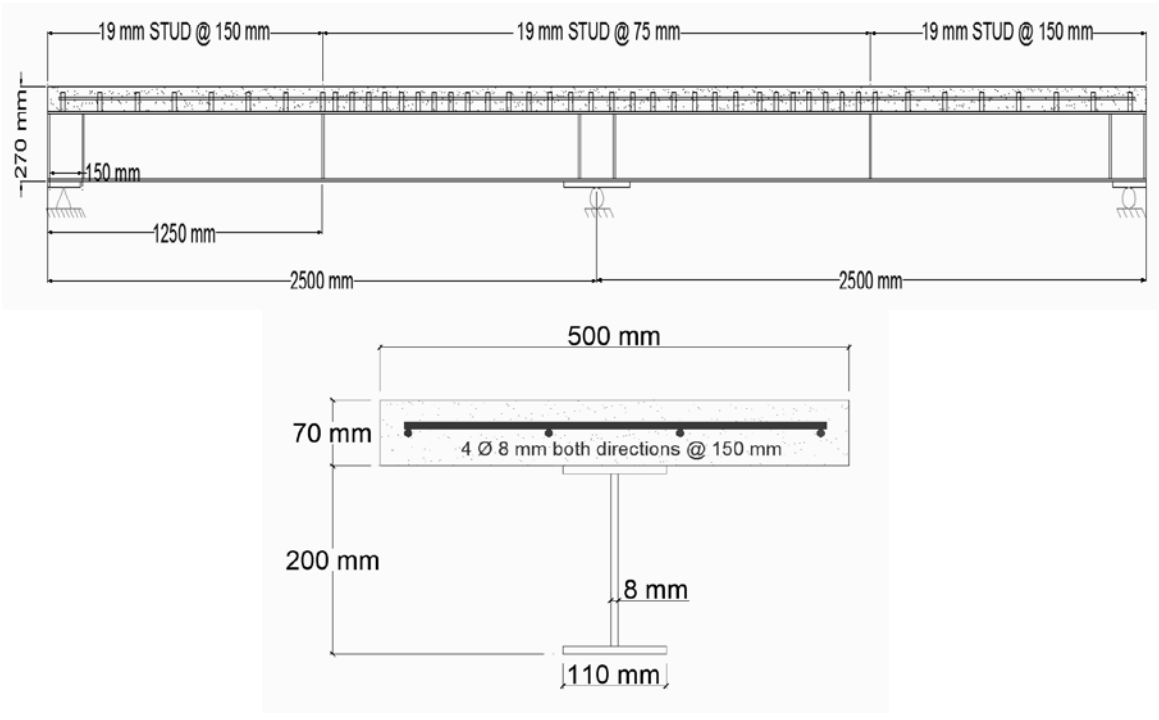

Figure 87: Girder drawing

REFERENCES

ACI440.R-08 ACI 440.R-08. Guide for the design and construction of externally bonded FRP systems for strengthening concrete structures, American Concrete Institute.

ACI-546R (2004). ACI 546. Concrete repair guide.

Aidoo, J., K. A. Harries and M. F. Petrou (2006). "Full-scale experimental investigation of repair of reinforced concrete interstate bridge using CFRP materials." *Journal of Bridge Engineering* **11**(3): 350-358.

AISC (2010). Steel Construction Manual 13th, American Institute of Steel Construction.

Al-Saidy, A., F. Klaiber and T. Wipf (2007). "Strengthening of steel–concrete composite girders using carbon fiber reinforced polymer plates." *Construction and Building Materials* **21**(2): 295-302.

ASTM-C39M (2003). Compressive Strength of Cylindrical Concrete Specimens, ASTM.

ASTM-C293 (2002). Flexural Strength of Concrete (Using Simple Beam With Center-Point Loading), ASTM.

ASTM-C469 (2002). Static Modulus of Elasticity and Poisson's Ratio of Concrete in Compression. West Conshohocken, PA, ASTM.

ASTM-C496M (2004). Splitting Tensile Strength of Cylindrical Concrete Specimens, ASTM.

ASTM-E8M (2004). Tension Testing of Metallic Materials, ASTM.

Basu, P. K., A. M. Sharif and N. U. Ahmed (1987). "Partially prestressed composite beams. II." *Journal of Structural Engineering* **113**(9): 1926-1938.

Bilotta, A. (2010). *Behavior of FRP-to-concrete interface: theoretical models and experimental results* Dissertation, Università degli Studi di Napoli Federico II.

Dong, Y., M. Zhao and F. Ansari (2002). "Failure characteristics of reinforced concrete beams repaired with CFRP composites." *strain* **304**(25.4): 12.17.

El-Hacha, R. and N. Ragab (2006). Flexural strengthening of composite steel-concrete girders using advanced composite materials. Third international conference on FRP composites in civil engineering.

FOSROC (2014). Nitowrap FRC.

Higgins, C., G. Williams and L. Elkins (2006). Capabilities of diagonally-cracked girders repaired with CFRP.

Johnson, R. P. and D. Anderson (2004). *Designers' Guide to EN 1994-1-1: Eurocode 4: Design of Composite Steel and Concrete Structures. General Rules and Rules for Buildings*, Thomas Telford.

Miller, T. C., M. J. Chajes, D. R. Mertz and J. N. Hastings (2001). "Strengthening of a steel bridge girder using CFRP plates." *Journal of Bridge Engineering* **6**(6): 514-522.

Namboorimadathil, S. M., J. G. Tumialan and A. Nanni (2002). "BEHAVIOR OF RC TBeams STRENGTHENED IN THE NEGATIVE MOMENT REGION WITH CFRP LAMINATES." *ICCI 2002*.

Nguyen, D. M., T. K. Chan and H. K. Cheong (2001). "Brittle failure and bond development length of CFRP-concrete beams." *Journal of Composites for Construction* **5**(1): 12-17.

Prodyot, K. B., M. Alfarabi and U. Nesar (1987). "Partially prestressed continuous composite beams." *Journal of Structural Engineering* **113**(9): 1909-1925.

Rosenboom, O. and S. Rizkalla (2008). "Modeling of IC debonding of FRP-strengthened concrete flexural members." *Journal of Composites for Construction* **12**(2): 168-179.

Salomon, C. G., J. E. Johnson and F. A. Malhas (2009). *Steel Structures: Design and Behavior*, Pearson Prentice Hall.

Samaaneh, M. A. R. (2012). *Modeling of continuous composite partially reinforced girders with CFRP*. MSc, King Fahd University of Petroleum and Minerals (Saudi Arabia).

Schnerch, D., M. Dawood and S. Rizkalla (2005). Strengthening steel-concrete composite bridges with high modulus carbon fiber reinforced polymer (CFRP) laminates. Proceedings of the Third International Conference on Composites in Construction (CCC 2005).

Schnerch, D., M. Dawood, S. Rizkalla and E. Sumner (2007). "Proposed design guidelines for strengthening of steel bridges with FRP materials." *Construction and Building Materials* **21**(5): 1001-1010.

Sen, R., L. Liby and G. Mullins (2001). "Strengthening steel bridge sections using CFRP laminates." *Composites Part B: Engineering* **32**(4): 309-322.

Sharif, A. and M. Samaaneh (2014). "Modeling of continuous composite girders partially reinforced with CFRP." *Concrete Solutions 2014*: 361.

Spadea, G., R. Swamy and F. Bencardino (2001). "Strength and ductility of RC beams repaired with bonded CFRP laminates." *Journal of Bridge Engineering* **6**(5): 349-355.

Topkaya, C., J. A. Yura and E. B. Williamson (2004). "Composite shear stud strength at early concrete ages." *Journal of Structural Engineering* **130**: 952-960.

VITAE

NAME	ALA'A HUSAM AHMAD GHAITH
PLACE OF BIRTH	Dammam, Saudi Arabia
ADDRESS	Al Khobar Saudi Arabia
PHONE NUMBER	+966 58 114 3117
E-mail	alaa.h.ghaith90@gmail.com
EDUCATIONAL QUALIFICATION	MS (Structural Civil Engineering) King Fahd University of Petroleum and Minerals, Dhahran, Saudi Arabia
	BS (Civil Engineering) King Fahd University of Petroleum and Minerals, Dhahran, Saudi Arabia